



TECHNICAL REPORT
NATICK/TR-91/046

AD _____

EXPLORATORY DEVELOPMENT OF ADVANCED COMPOSITE GENERIC AIRDROP PLATFORM CONCEPTS

By
E.D. Brewer
W.R. Hendrich
G.M. Wood

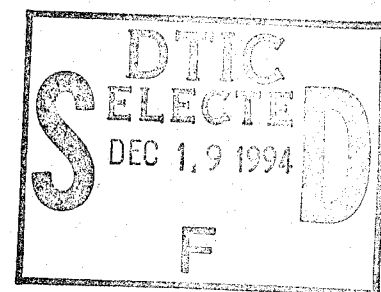
Oak Ridge National Laboratory
Oak Ridge, TN 37830

and

J.C. Brewer
U.S. Army Natick RD&E Center

August 1991

Final Report
January 1990 - December 1990



APPROVED FOR PUBLIC RELEASE
DISTRIBUTION UNLIMITED

Prepared for

19941214 068

UNITED STATES ARMY NATICK
RESEARCH, DEVELOPMENT AND ENGINEERING CENTER
NATICK, MASSACHUSETTS 01760-5000

AERO-MECHANICAL ENGINEERING DIRECTORATE

DISCLAIMERS

The findings contained in this report are not to be construed as an official Department of the Army position unless so designated by other authorized documents.

Citation of trade names in this report does not constitute an official endorsement or approval of the use of such items.

DESTRUCTION NOTICE

For Classified Documents:

Follow the procedures in DoD 5200.22-M, Industrial Security Manual, Section II-19 or DoD 5200.1-R, Information Security Program Regulation, Chapter IX.

For Unclassified/Limited Distribution Documents:

Destroy by any method that prevents disclosure of contents or reconstruction of the document.

REPORT DOCUMENTATION PAGE			Form Approved OMB No. 0704-0188	
<small>Published with a report, this document contains the data needed to understand the report. It is not intended for use as a source of information. The data needed to understand the report is contained in the report. The data needed to understand the report is contained in the report. The data needed to understand the report is contained in the report.</small>				
1. AGENCY USE ONLY (Leave blank)		2. REPORT DATE August 1991		3. REPORT TYPE AND DATES COVERED FINAL Jan 1990 - Dec 1990
4. TITLE AND SUBTITLE EXPLORATORY DEVELOPMENT OF ADVANCED COMPOSITE GENERIC AIRDROP PLATFORM CONCEPTS			5. FUNDING NUMBERS PE 62786 PR 1L162786D283 AG TB1345	
6. AUTHOR(S) E.D. Brewer, W.R. Hendrich, G. M. Wood J.C. Brewer*				
7. PERFORMING ORGANIZATION NAME(S) AND ADDRESS(ES) Oak Ridge National Laboratory Oak Ridge, TN 37830			8. PERFORMING ORGANIZATION REPORT NUMBER	
9. SPONSORING MONITORING AGENCY NAME(S) AND ADDRESS(ES) U.S. Army Natick Research, Development and Engineering Center Kansas St. ATTN: STRNC- Natick, MA 01760-5017			10. SPONSORING MONITORING AGENCY REPORT NUMBER NATICK/TR-91/046	
11. SUPPLEMENTARY NOTES *Professional affiliation: U.S. Army Natick RD&E Center				
12a. DISTRIBUTION AVAILABILITY STATEMENT Approved for Public Release, Distribution Unlimited			12b. DISTRIBUTION CODE	
13. ABSTRACT (Maximum 200 words) This research investigated improvements in weight and performance of generic airdrop platform concepts by the use of advanced composite materials. Several concepts were generated and analyzed for the parachute opening load case. The three most promising concepts were also analyzed for the roller load, extraction load, cresting load, and landing impact cases. Although several concepts performed quite well, the most promising concept had S-glass/epoxy face sheets bonded to pultruded E-glass/epoxy I-beams. It was determined that advanced composite airdrop platforms potentially offer lower weight and better performance than the present platform at a lower life-cycle cost.				
14. SUBJECT TERMS AIRDROP AERIAL DELIVERY COMPOSITE MATERIALS			15. NUMBER OF PAGES 110	
16. PRICE CODE			17. SECURITY CLASSIFICATION OF REPORT UNCLASSIFIED	
18. SECURITY CLASSIFICATION OF THIS PAGE UNCLASSIFIED			19. SECURITY CLASSIFICATION OF ABSTRACT UNCLASSIFIED	
20. LIMITATION OF ABSTRACT SAR				

TABLE OF CONTENTS

	<u>Page</u>
List of Figures	iv
List of Tables	vii
Preface and Acknowledgements	ix
Nomenclature	x
1. Introduction	1
2. Summary of Phase I	2
2.1 Introduction	2
2.2 Review of Natick Analysis	2
2.3 Materials and Methods Evaluation	3
2.4 Design Concepts	6
2.5 Concept Analysis	8
2.6 Concept Selection Discussion	16
2.7 Conclusion	25
3. Phase II, Tasks 1 & 2	27
3.1 Introduction	27
3.2 Concept Modification	27
3.3 Face Sheet Hybridization	29
3.4 Task 1: Detailed Analysis of the Parachute Opening Load Case	29
3.5 Task 2: Final Concept Selection	45
4. Phase II, Task 3	58
4.1 Task 3: Analysis of Other Important Load Cases	58
4.2 Landing Impact Load Case	58
4.3 Roller Load Case	59
4.4 Cresting Load Case	59
4.5 Extraction Load Case	64
5. Phase II, Task 4	
5.1 Task 4: Dynamic Analysis	84
5.2 Analysis Results	84
6. Conclusions and Recommendations	98
6.1 Conclusions	98
6.2 Recommendations	98
7. References	99

[illegible]

LIST OF FIGURES

<u>Figure</u>	<u>Page</u>
2.1 Rib stiffened foam core design	7
2.2 Web braced core design	9
2.3 Sandwich design	10
2.4 Beam and plate design	11
2.5 Beam and plate design using I-beams as stiffeners	12
2.6 A platform with energy absorbing material and tension braces	13
2.7 Platform concept with a continuous corrugated stiffener	14
2.8 End and side closures	18
2.9 Concept weight comparison	19
2.10 Overall concept comparison	26
3.1 Quarter model of E-glass/epoxy I-beam core	30
3.2 Quarter model of S-glass/epoxy face sheets	31
3.3 Isotropic face sheet case deflection results	32
3.4 Composite face sheet deflection results	33
3.5 Improved end closeout model	34
3.6 Displacement results with end closeout improvement	36
3.7 I-beam major principal stresses (bottom flanges)	37
3.8 I-beam major principal stresses (top flanges)	38
3.9 I-beam in-plane shear stresses (webs)	39
3.10 Lower face sheet strains, x-axis	40
3.11 Lower face sheet strains, y-axis	41
3.12 Face sheet ply nomenclature	42
3.13 Ply axes nomenclature	43
3.14 Lower face sheet stress critical area of ply 3, 122	44

LIST OF FIGURES (Cont'd)

<u>Figure</u>		<u>Page</u>
3.15	Lower face sheet stresses in ply 3, f11	46
3.16	Lower face sheet stresses in ply 1, f22	47
3.17	Lower face sheet stresses in ply 1, f11	48
3.18	Lower face sheet stresses in ply 2, f22	49
3.19	Lower face sheet stresses in ply 2, f11	50
3.20	Top face sheet stresses in ply 26, f22	51
3.21	Top face sheet stresses in ply 26, f11	52
3.22	Overall concept comparison	57
4.1	Roller load case model configuration	60
4.2	I-beam web shear stresses, roller load case	61
4.3	Deflection results, roller load case	62
4.4	I-beam web shear stresses, cresting load case	63
4.5	X-axis strains in the top face sheet, cresting load case	65
4.6	X-axis strains in the lower face sheet, cresting load case	66
4.7	Aluminum side rail and end closeout stresses, cresting load case	67
4.8	Deflection results, cresting load case	68
4.9	Extraction load case model	69
4.10	End view of the extraction load case model	70
4.11	X-axis strain in the top face sheet	71
4.12	Critical area, x-axis strain in the top face sheet	72
4.13	Y-axis strain in the top face sheet	73
4.14	Critical area, y-axis strain in the top face sheet	74
4.15	I-beam web shear stresses	76
4.16	I-beam web Von Mises stresses	77
4.17	I-beam flange shear stresses	78
4.18	I-beam flange Von Mises stresses	79
4.19	Aluminum end closeout Von Mises shear stresses	80
4.20	Critical area, Von Mises stresses aluminum end closeout	81
4.21	Deflection results, extraction load case with roller loads	82
4.22	Deflection results, showing x-axis deflections	83
5.1	Mode 1, loaded platform	86
5.2	Mode 2, loaded platform	87
5.3	Mode 3, loaded platform	88
5.4	Mode 4, loaded platform	89
5.5	Mode 5, loaded platform	90
5.6	Mode 1, unloaded platform	92
5.7	Mode 2, unloaded platform	93
5.8	Mode 3, unloaded platform	94
5.9	Mode 4, unloaded platform	95
5.10	Mode 5, unloaded platform	96

LIST OF TABLES

<u>Table</u>		<u>Page</u>
2.1	Pertinent composite manufacturing processes	5
2.2	Platform concepts performance	17
2.3	Performance comparison parameters	21
2.4	Survivability comparison parameters	23
2.5	Overall comparison parameters and ratings	24
3.1	Concept configuration summary	28
3.2	Analyses results	53
3.3	Ratings comparison	54
5.1	Frequency values for pinned corner conditions	85

PREFACE

The research described in this report was conducted by the Engineering Technology Division at Oak Ridge National Laboratory in Oak Ridge, TN during the period 1 January 1990 to 31 December 1990. This work was the second phase of an exploratory development project funded by the Aero-Mechanical Engineering Directorate of the U.S. Army Natick Research, Development and Engineering Center under Interagency Agreement 1909, Proposal No. 1909-C016-A1. Natick personnel provided technical support to the project and contributed to this report.

This report presents findings regarding the advisability of using composite airdrop platforms to replace existing aluminum platforms. Both economic and engineering factors were considered.

Citation of trade names in this report does not constitute an official endorsement or approval of the use of such items.

ACKNOWLEDGEMENTS

The authors wish to thank the following individuals: Richard Davis and Uri Gat of Oak Ridge and John Calligeros of Natick for facilitating the interagency agreement and for technical input; Walter Krainski of Natick and John Clinard of Oak Ridge for their earlier work on the project; and Andreas Blanas, Peter Van Buren, Gary Thibault, and Louis Piscitelle, all of Natick, for their technical review of the work.

NOMENCLATURE

EI	bending stiffness, product of modulus of elasticity, E, and the cross-sectional moment of inertia, I units: pound force inch ² ($2.87 \times 10^{-3} \text{ N m}^2$)
FPF	first ply failure, dimensionless measure for a factor of safety, ratio of allowable stress to calculated or actual stress
ft	feet (0.3048 m)
h	overall platform height units: inches (2.54 cm)
hc	platform core height units: inches (2.54 cm)
Hz	Hertz, cycles per second
inch/inch	units given for strain, equal values in cm/cm or m/m
ksi	thousands of pounds force per square inch ($6.895 \times 10^6 \text{ N/m}^2$)
lb	pound force (4.448 N)
psi	pounds force per square inch ($6.895 \times 10^3 \text{ N/m}^2$)
R	factor of safety, ratio allowable stress or strain to actual or calculated stress or strain units: dimensionless
tb	thickness of side rail box beam units: inches (2.54 cm)
tc	platform core thickness units: inches (2.54 cm)
tfs	platform face sheet thickness units: inches (2.54 cm)
tt	thickness of side rail overlapping tab to face sheet units: inches (2.54 cm)
Wu	unsupported face sheet spacing; distance between core beams or sections units: inches (2.54 cm)
ZDISPL	platform displacement units: inches (2.54 cm)
σ_{calc}	stress calculated (usually via the finite element method) for the loading case considered units: pounds force per square inch ($6.895 \times 10^3 \text{ N/m}^2$)

NOMENCLATURE (cont'd)

- $\bar{\sigma}_{ult}$ ultimate stress for a given platform element and material
units: pounds force per square inch (6.895 X 103 N/m²)
- $\bar{\sigma}_{crit}$ critical stress used with regard to buckling resistance for
a given platform element and material
units: pounds force per square inch (6.895 X 103 N/m²)
- $\bar{\sigma}_{11}$ in-plane ply stress along the ply's fiber direction
units: pounds force per square inch (6.895 X 103 N/m²)
- $\bar{\sigma}_{22}$ in-plane ply stress transverse to the ply's fiber direction
units: pounds force per square inch (6.895 X 103 N/m²)
- $\bar{\theta}$ 1. fiber angle of a single ply relative to longitudinal axis
of the platform 2. (in Table 3.1 only) designated corrugation
section angle with face sheet
- " inch

EXPLORATORY DEVELOPMENTS OF ADVANCED COMPOSITE GENERIC AIRDROP PLATFORM CONCEPTS

1. INTRODUCTION

The Advanced Composites in Airdrop Program was performed to study generic airdrop platform concepts incorporating advanced composite materials. The program was an exploratory development program, with emphasis on analysis and optimization of basic platform elements. The objective of this program was to reduce platform weight and maintain or improve platform performance at the same or lower cost. This program was performed by the Oak Ridge National Laboratory (ORNL), for the US Army Natick Research, Development and Engineering Center (Natick).

The program was conducted in a two-phase effort. Phase I was performed from April through December of 1989. The Phase II effort was from February through December of 1990. All work performed by the ORNL is covered in this report. The Phase I effort is summarized in Section 2, and more information can be found on the Phase I work in an unpublished ORNL report (ORNL staff, Final Report: Phase I of the Advanced Composites in Airdrop Program, January 1990.) Sections 3, 4 and 5 contain information on Phase II, for different analysis tasks covered during this effort. Final conclusions and recommendations resulting from the Advanced Composites in Airdrop Program are given in the last report section.

All work performed in this effort was done in the English Engineering System of units. This is shown in the Nomenclature section in which conversion factors to SI units are given.

2. SUMMARY OF PHASE I

2.1 INTRODUCTION

Phase I of the Advanced Composites in Airdrop Program was performed by the Oak Ridge National Laboratory (ORNL) from April through December of 1989. The Phase I effort included several tasks, which are listed below:

1. A review of previous Natick work.
2. A review of available composite materials and manufacturing processes.
3. The generation of several advanced composite platform concepts.
4. Analysis of these concepts under a static equivalent case of the parachute opening load on the platform.
5. Comparison of these concepts (performance, weight, cost, etc.) and recommendation for three concepts to be further considered in Phase II.

At the conclusion of Phase I, a report was prepared which covered these tasks in detail (Final Report: Phase I of the Advanced Composites in Airdrop Program, ORNL Staff, January 1990, unpublished.) For the purposes of both brevity and completeness, the Phase I task efforts are summarized in the following report sections, rather than including the entire Phase I report.

2.2 REVIEW OF NATICK ANALYSIS

At the beginning of Phase I, Natick supplied to ORNL a package of information describing finite-element analytical investigations of platforms similar to the Type V, but based on laminated composite materials. Several stiffening configurations were explored. Some were similar to the box-stiffened web design of the current 2 ft extruded aluminum sections. Natick's investigation centered around the consideration of two materials: S-glass/epoxy and graphite/epoxy. The plate cross-sectional stiffening configurations for these materials were a continuous corrugated (hat-type) web, a continuous box-stiffened web, and a filament-wound box-stiffened web. All laminates in Natick's work were quasi-isotropic with plies in the D/4 family. That is, the laminates were symmetric about the mid-plane and contained equal quantities of 0°, 90°, 45°, and -45° plies. Cases both with and without the aluminum side rails were analyzed. Twenty-five variations of material and stiffening configuration were evaluated by Natick. This analysis was done for a single static load case representative of the parachute opening shock and using the NISA II finite element composite layered shell and plate program.

The principal conclusions drawn from the Natick work were:

1. Platform configurations using composite materials exhibited considerable weight savings potential, 50 to 60% relative to the modular aluminum platform, with greater weight savings offered by graphite/epoxy.

2. For all the stiffening configurations analyzed, graphite/epoxy configurations were stiffer than the S-glass/epoxy configurations. Greater differences between the two materials were noted for the cases of lengthwise stiffener spanning than for crosswise stiffener spanning.
3. Lengthwise stiffener spanning provided better platform stiffness.
4. The filament wound configurations were similar in stiffness to the continuous box stiffened designs.

2.3 MATERIALS AND METHODS EVALUATION

Composite materials applicable to an airdrop platform were reviewed. Materials were examined for applicability to the platform system requirements. Fiber reinforced polymeric composites and core materials for sandwich panel design were examined with emphasis on material properties, processing, and design factors relevant to an airdrop platform.

Applicable manufacturing processes were reviewed for general suitability and relative cost. All methods thought to be potentially useful were included, although the actual manufacturing would be highly design dependent.

2.3.1 Fibers

Materials with a combination of high specific strength and stiffness are required for optimum platform design. Impact resistance may also be important in some locations of the platform.

Both unidirectional fiber and woven fabrics are potential reinforcement forms.

Three-dimensional braided forms are more expensive than other forms. Short fiber reinforcements were eliminated from consideration because of the loss in properties resulting from the random orientation in the matrix.

2.3.2 Matrices

Composite matrices considered included both thermosets and thermoplastics. At present, most continuous fiber composites are manufactured with thermoset resins, with thermoplastic composite technology still in the developmental stage. However, thermoplastics may eventually provide reduced fabrication costs and more impact resistant structures. The primary thermoset resins considered included epoxies, polyesters, and vinyl esters.

2.3.3 Fiber reinforced laminates

The properties of fiber reinforced laminates are dependent on:

1. the fiber and resin properties,
2. the volume percent fiber content,
3. the fiber orientation, and
4. the stacking sequence.

2.3.4 Core Materials

Sandwich construction using foam or honeycomb core has the potential for weight savings over the present aluminum platform without sacrificing flexural strength and stiffness. A representative design would consist of face sheets made of fiber reinforced laminates bonded or cocured to a suitable core material.

2.3.5 Manufacturing Processes

Final process selection for full scale platform production will be highly design dependent, and may vary with manufacturers' preferences and cost factors. Composite manufacturing processes considered are summarized in Table 2.1.

Resin transfer molding is not suitable for hollow sections. However, this process may be applicable for small, complex sections such as parachute attachments. The major benefit of this process is in the good dimensional tolerance. Filament winding is primarily useful for box beam stiffeners with high fiber loading. The major drawback is the expense penalty incurred when incorporating 0° fibers. This process has low material and production costs and is good for limited production runs.

The pultrusion process shows the most potential for modular and beam components. If tailored reinforcement is used, this process may be the lowest cost for material and production requirements. Zero degree fibers can easily be incorporated. Hollow sections can be produced using this method. Mold costs for new items appear reasonable.

The viability of die molding is design dependent. Simple tooling and the ability to process large plates of fiber reinforced thermoplastics favor using this process. Unfortunately, die molding is relatively expensive. The bag molding process has potential. Using an autoclave, this process provides the most flexibility in part design and selective reinforcement. However, this is a relatively expensive process. Part size for non-modular construction is not a problem, but does limit available manufacturers because of autoclave size.

Vacuum bag molding is more cost competitive than autoclaving for limited production runs. This process uses lower cost materials and has lower plant overhead. Sheet forming via thermoset pultrusion or thermoplastic consolidation followed by co-molding to a core material may eventually provide a semi-continuous method of panel fabrication. However, advances in sheet forming must occur first.

Table 2.1: Pertinent Composite Manufacturing Processes

Manufacturing Process	Matrix	Fibers	Material Form	Cores	Anticipated Components	Estimated Relative Cost	Fiber Volume Fraction
Resin transfer molding	Epoxy Vinylester Polyester	All	Cloth, knit and mat fibers. Wet resin only.	Some Balsa and foams. No honeycombs.	Parachute attachment; section joiners; joiners; tie downs.	2	50
Filament winding	Epoxy Vinylester Polyester	All except boron	Mainly roving with wet resin. Some prepreg.	Not suggested.	Beams and simple rail shapes.	1	65
Pultrusion	Vinylester Polyester	All	Roving mat and cloths. Prepreg and wet resin.	Limited, but possible with foam.	Plates; beams; rails; stiffeners.	1	65
Die molding	Thermosets Thermoplastics	All	All	All	Cored panels; beams; rails; stiffeners; composite-metal hybrids.	4	60
Bag molding (autoclave)	All	All	All, but typically prepreg	All	All, with some design limitations; composite-metal hybrids.	3	65
Bag molding (vacuum)	Mainly thermosets	All	Knits, cloths, mat. Wet resin. Film adhesive.	All	Panels; beams; rails; fasteners; hybrid.	2	55

2.3.6 Materials and Processes Summary

Material selection for new designs must be made carefully. For example, most composite materials exhibit higher specific tensile strength in the fiber direction than metals. However, only exotic and expensive composites tend to have higher absolute moduli or strengths. The best weight savings for a platform might well be achieved using a combination of boron, carbon, and polyethylene fibers. This would in all likelihood be prohibitively expensive. When considering both cost and performance, the best fiber candidates are graphite and S-glass. For optimum use of composite materials, designs cannot be simply constructed using quasi-isotropic materials to replace metals. Designs should have most fibers oriented in the directions of principal stresses, and should exploit material anisotropy.

Selection of materials and manufacturing processes, individual design of the various components, and overall design of the platform are integrated tasks in the development of a composite airdrop platform. A particular manufacturing process cannot be flatly recommended, as final design (materials and geometry) will affect the process selection, and vice versa. However, three processes appear to have the most opportunity for usage. These are pultrusion, vacuum bag molding, and resin transfer molding (for small, attachment-type parts only).

2.4 DESIGN CONCEPTS

In the portion of Phase I concerned with creation and evaluation of different platform concepts, several constraints were used. These were kept as general as possible. The concept constraints used were:

1. limited platform height (3.5" or less);
2. field usage requirements such as environmental exposure, load distributions, etc.,
3. side rails were acceptable,
4. nominal dimensions for this project of 9 ft wide by 20 ft long, and
5. a non-modular concept preferred.

Seven basic concept configurations, with variations included for some of these configurations, were evaluated.

A rib stiffened configuration is shown in Figure 2.1. This concept included a foam core for compression resistance. However, the ability of such foams to resist crushing is questionable. By avoiding the connection of each stiffener to both face sheets, the stress concentrations that arise at the interface between face sheets and stiffeners are reduced and the resistance to delamination is therefore enhanced. Material considerations include the face sheet impact resistance for graphite/thermoset, delamination of the face sheet from the core for graphite/thermoplastic, and a weight penalty for S-glass/thermoset. Graphite/thermoset is a good candidate for the rib material in this concept. The complexity of this concept is a concern.

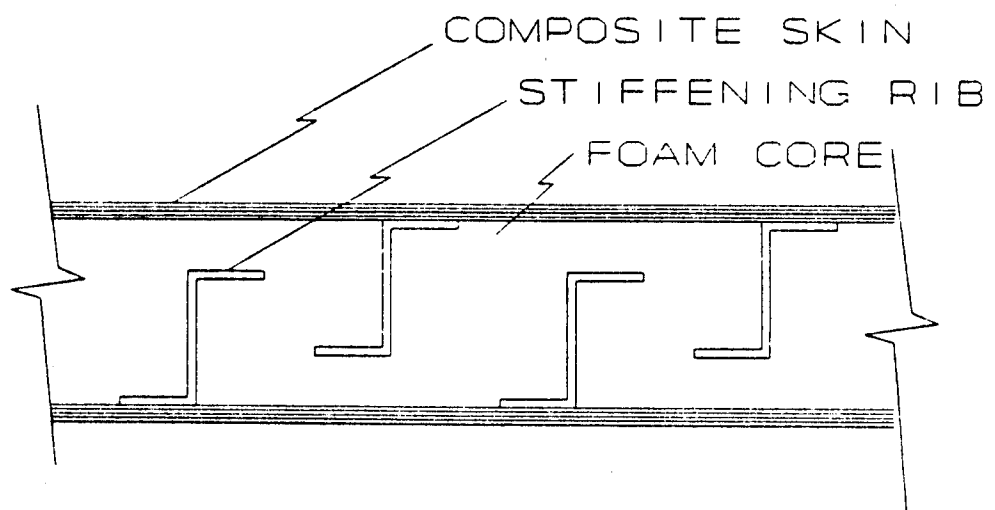


Figure 2.1 Rib stiffened foam core design

Continuous web stiffeners combined with a foam core are shown in Figure 2.2. The web stiffeners provide shear and bending resistance. Material considerations are similar to those for the previous concept. Local stress concentrations at the interface between the webs and the face sheets are a concern for this concept.

A simple sandwich structure with a foam core between two face sheets is illustrated in Figure 2.3. Built up areas could provide selective reinforcement in highly stressed areas. (Face sheet reinforcement could be incorporated into any concept.) A wide variety of core materials is available.

Another concept consisted of a composite skin with beam supports. Longitudinal platform stiffness would be provided by the beams, which would act as roller plate and ground supports. This configuration is shown in Figure 2.4. Details such as the attachment method and the single laminate skin are not necessarily design recommendations. Material considerations indicate graphite/thermoset for the skin and pultruded S- or E-glass for the beams.

In the next concept, composite skins are used with beam stiffeners, as shown in Figure 2.5. Natick had specifically investigated filament wound box stiffened platforms. Joining of the face sheets and beams is a design consideration for this concept. S-glass/thermoset is a leading candidate for face sheets and stiffeners. Graphite/thermoset is a possibility for the beams.

A novel configuration is shown in Figure 2.6. The chief design features are an elastomeric or gel type material for energy absorption, stiffening side rails, a floating top sheet, and possibly internal cross bracing. A stiff yet light material would be best for the face sheets, indicating graphite in thermoset or thermoplastic. A possible design variation for any concept would be the incorporation of elastomer in selected locations for local energy absorption with a minimal weight increase.

A more conventional configuration considered is shown in Figure 2.7. It consists of a corrugated (continuous or separate sections are possible) reinforcement between face sheets. Natick had evaluated continuous web stiffened designs. Different materials are possible for this concept, with similar considerations as for previous concepts such as the I-beam core concept.

Other concepts can be created by combining features of these configurations. The final design can benefit from different aspects of several concepts. An iterative procedure in terms of materials, component design, manufacturing and production design, and cost tradeoffs is recommended.

2.5 CONCEPT ANALYSIS

The analysis effort during Phase I consisted of modelling a static approximation of the parachute opening shock. The main analysis

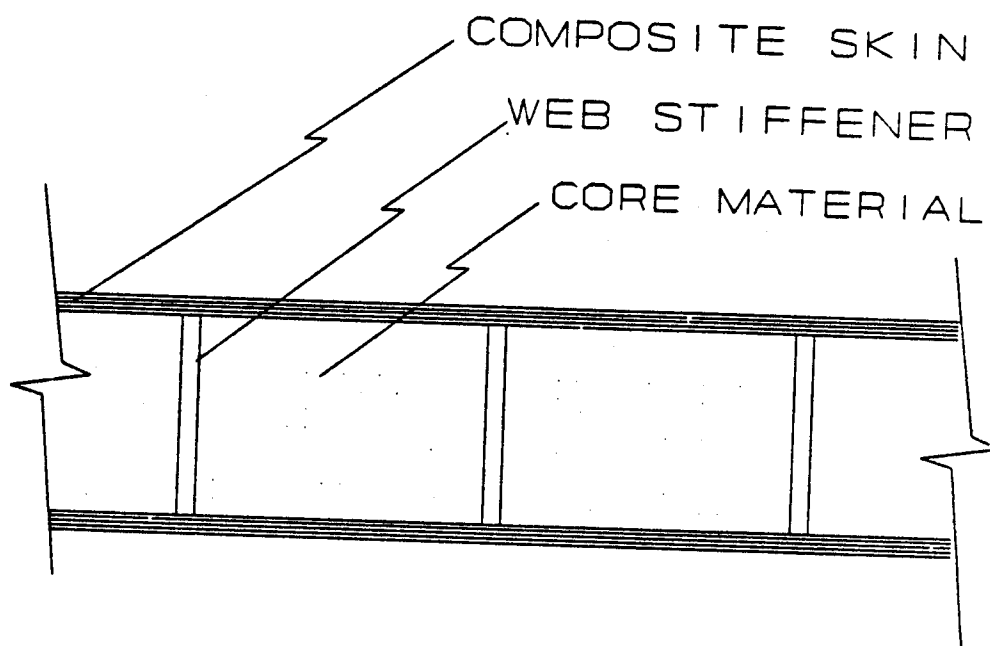


Figure 2.2 Web braced core design

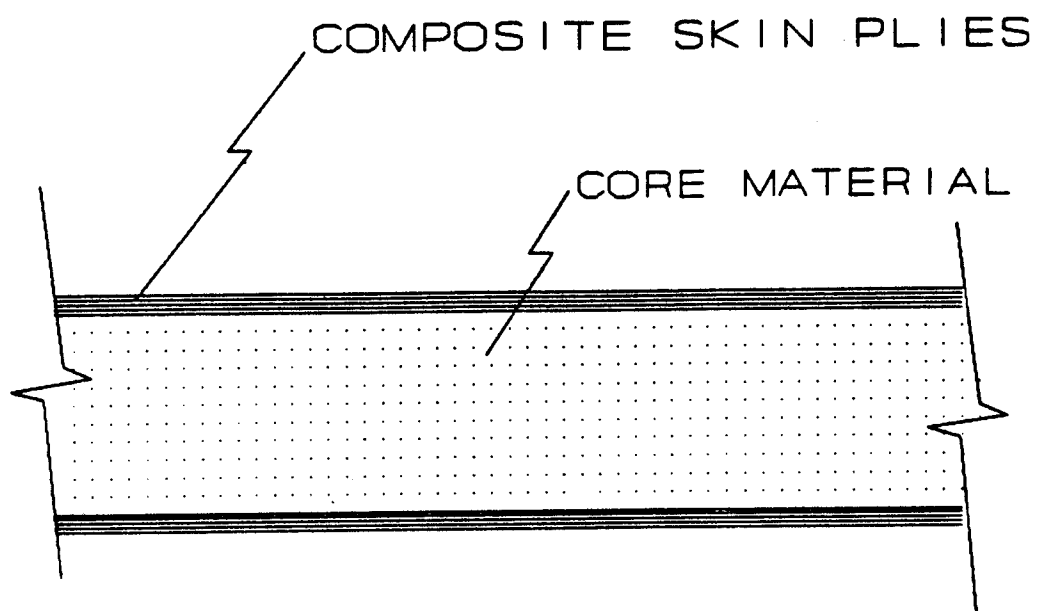


Figure 2.3 Sandwich design

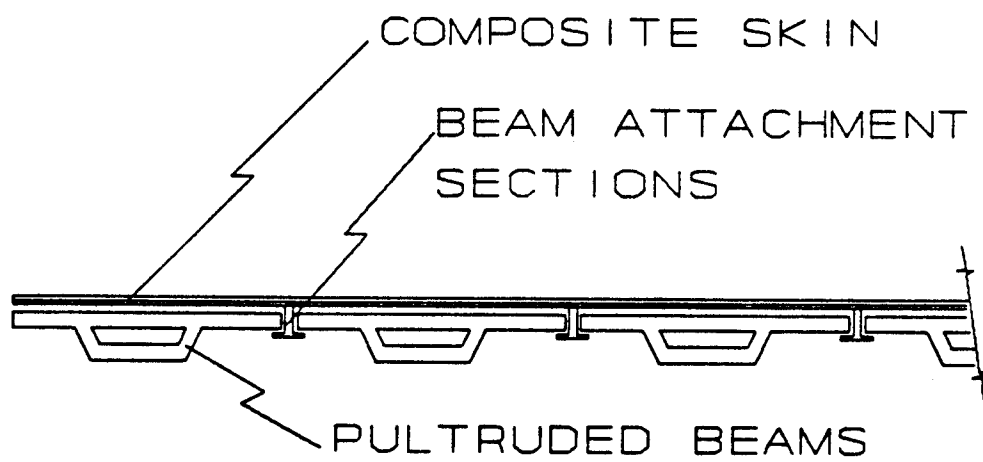


Figure 2.4 Beam and plate design

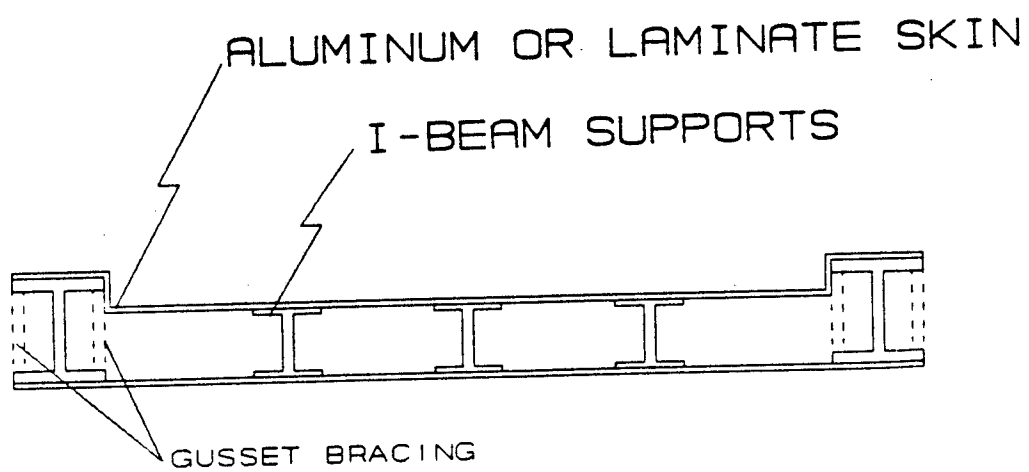


Figure 2.5 Beam and plate design using I-beams as stiffeners

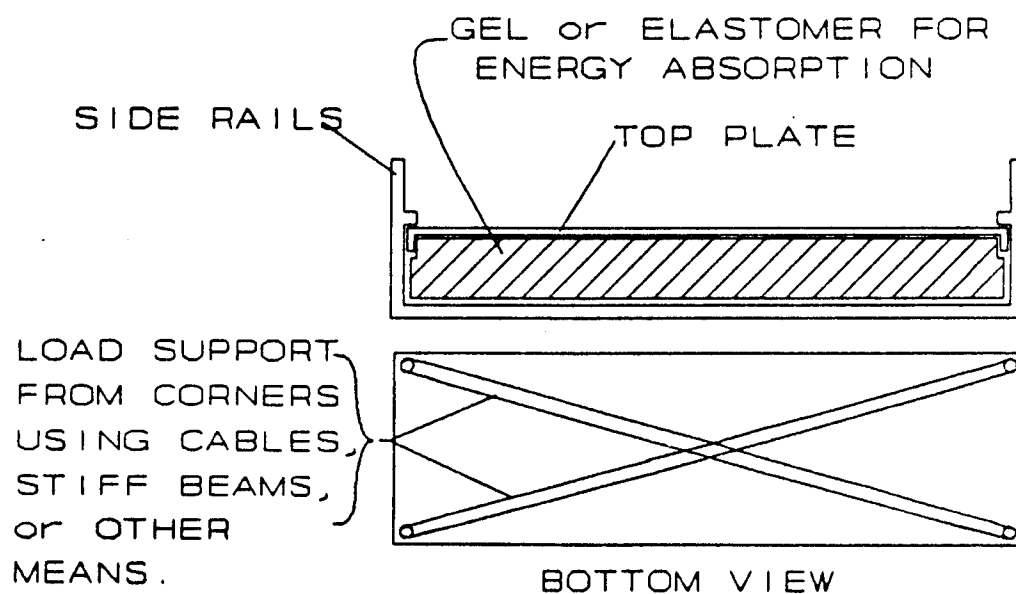
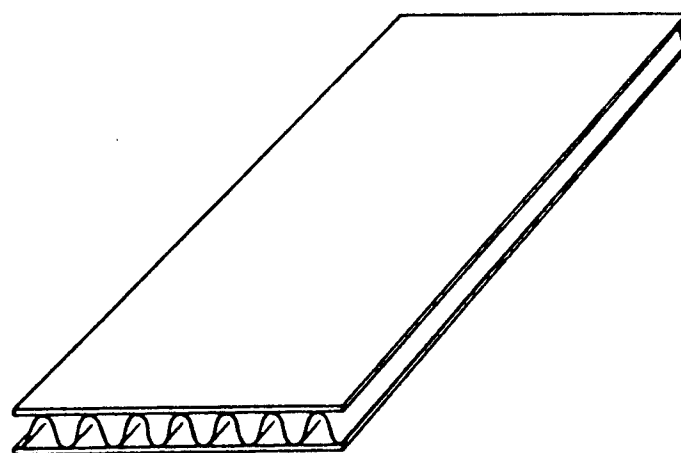


Figure 2.6 A platform with energy absorbing material and tension braces



SINGLE ROW OF CORRUGATIONS

Figure 2.7 Platform concept with a continuous corrugated stiffener

assumptions are summarized below:

1. platform size is 9 ft by 20 ft,
2. equivalent static case of the parachute opening load condition,
3. 23300 lb uniformly distributed load,
4. dynamic magnification factor of two,
5. cables at 60° to the platform,
6. non-modular configuration preferred,
7. external side rails are acceptable, and
8. maximum thickness of the platform is 3.5"

A finite element model was made of the platform using quarter model symmetry. The model had 60 plate elements and 78 nodes. The problem was modelled using these plate elements on the SAP86 personal computer code and checked using the ADINA program on a CRAY computer.

A face sheet scoping study was performed. Different composite materials with different lamination sequences were analyzed under the parachute opening load. (Further details on these calculations are given in the Phase I Final Report, ORNL Staff, 1989.) The lightest weight face sheets with acceptable deflection levels were seen to be composed of graphite/epoxy.

Analysis was performed on versions of each concept. In some cases, different variations of the same concept using the same materials were evaluated in an attempt to quantify the tradeoff between face sheet thickness and number of stiffeners. A full finite element analysis was not always performed. Wherever applicable, a brief "order of magnitude" analysis was used to show sufficient reason for elimination of a concept.

The rib stiffened concept shown in Figure 2.1 contains a complex core structure that is not easily analyzed. However, rough calculations indicate that shear stresses in the foam between the ribs would exceed the capabilities of any weight competitive foam available.

The web braced core concept shown in Figure 2.2 has face sheet buckling as a primary concern. Closely spaced web braces or thicker face sheets could prevent such buckling, but the weight would be substantially increased.

A variation of the honeycomb sandwich construction using balsa as the core material was studied briefly. The most significant problem in this case is the inadequate stiffness of the balsa. Other problems known were poor durability, tendencies to delaminate and deform, and insufficient material supply.

A variation of the I-beam type core having both shallow and deep beams was briefly studied. The net effect of this configuration was found to be a reduced transverse stiffness, but with a higher weight, when compared the uniform depth I-beam configuration. Another variation of this concept consisted of a truss arrangement of beams. With a minimum of 1500 joints necessary, this configuration was deemed to be too difficult and expensive to fabricate.

The concept which used a gel or elastomer core was calculated to be prohibitively heavy. A variation using elastomeric core sections would provide much greater deflection than allowable because of the low stiffness of such materials.

The honeycomb sandwich concept (Figure 2.3), the basic I-beam core concept (Figure 2.5), the continuous corrugated core concept (Figure 2.7), and a noncontinuous corrugation core (sectional core) concept were more fully analyzed. Using an iterative approach involving GENLAM and SAP86, variations of these basic concepts were studied. During the analysis procedure, buckling failure was considered to be a significant failure mode. The stress state in the adhesive was also checked.

The configurations studied in detail included a range of face sheet materials and layups, and a range of core materials and configurations. For each of the platform concepts analyzed, the configuration included aluminum side beams and closeouts. These are shown in Figure 2.8, with the important parameters labelled. The aluminum used, 2219-T87, is a typical material in the aircraft industry, used for relatively high strength for its weight.

The analysis results are summarized in Table 2.2. In this table, the key performance parameters for the concepts analyzed are given, including weight, overall height, critical stresses, and maximum deflections. The total weights given include closeouts and end beams. The effect of the aluminum side rails is included in the bending analysis.

Several important observations can be made:

1. Cell wall buckling is of more importance than face sheet buckling in the honeycomb sandwich concepts.
2. Face sheet buckling is a critical failure mode for I-beam concepts.
3. Graphite/epoxy components provided a significant weight reduction.
4. Relatively few fiber angles were investigated for the composite components. The performance of these configurations could be enhanced via an optimization analysis. The aluminum parts are less likely to experience significant gains in performance when optimized.

2.6 CONCEPT SELECTION DISCUSSION

The concept configurations considered to warrant serious consideration were evaluated and compared. The parameters considered in the evaluation were weight, performance, survivability, and initial cost. These were combined for overall estimation of the lifetime cost.

2.6.1 Weight

In Figure 2.9, the concept weights are shown, from the heaviest to the lightest, with the Type V included. A significant variation occurs from

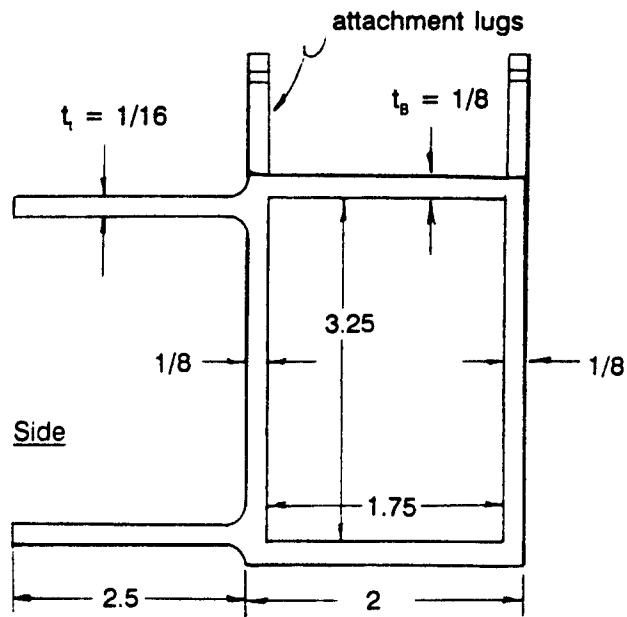
Table 2.2: Platform Concepts Performance

Face/Core Material ^a	# plies	Face Sheet		Core		Total Thickness [in]	Total Weight [lb]	Results		
		thickness t_{fs} [in]	weight [lb]	thickness t_c [in]	weight [lb]			FPF σ_{ult}	Buckling σ_{crit}	Z_{displ} [in]
<u>Honeycomb Cores (Figure 2.3)</u>										
S-glass/Al ^c Graphite/Al Al/Al	17	0.085	317	3.33	600	3.50	1167	2.70	1.70	15.6
	16	0.080	241	2.70	340	2.86	800	1.96	3.00	12.2
	1	0.100	326	3.37	425	3.50	973	1.63	2.29	14.5
<u>I-Beam Cores (Figure 2.5)</u>										
S-glass/E-glass S-glass/E-glass Graphite/graphite S-glass/graphite	18	0.090	335	3.32	546	3.50	1112	1.60	0.89	15.6
	26	0.130	485	3.24	278	3.50	982	2.07	2.10	14.2
	14	0.070	211	3.00	205	3.14	600	1.82	2.03	9.8
	16	0.080	241	3.25	247	3.41	685	2.63	1.88	14.6
<u>Continuous Corrugated Cores (Figure 2.7)</u>										
Al/Al Graphite/graphite	1	0.0885	459	3.02	361	3.20	1025	1.87	2.00	14.2
	15	0.075	225	3.02	208	3.18	599	1.55	2.00	11.3
<u>Noncontinuous Corrugated Cores (Figure 2.7)</u>										
S-glass/Al S-glass/Al	22	0.110	410	3.20	254	3.42	854	2.10	2.22	15.4
	18	0.090	335	3.20	309	3.38	832	1.83	1.94	17.1

^a Graphite and glass composites are designated by fiber type. Epoxy matrix is assumed.

^b Total includes aluminum closeout and adhesive, plus 10 percent contingency.

^c Al= Aluminum



not to scale; dimensions in inches

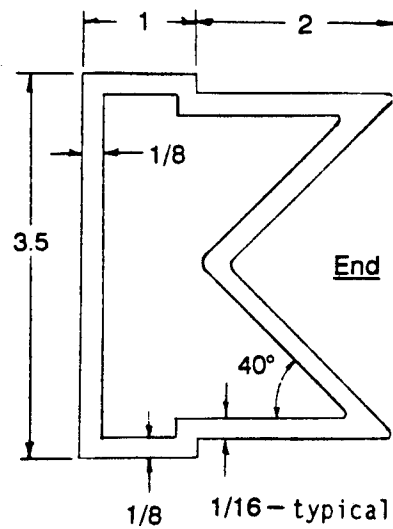


Figure 2.8 End and side closures

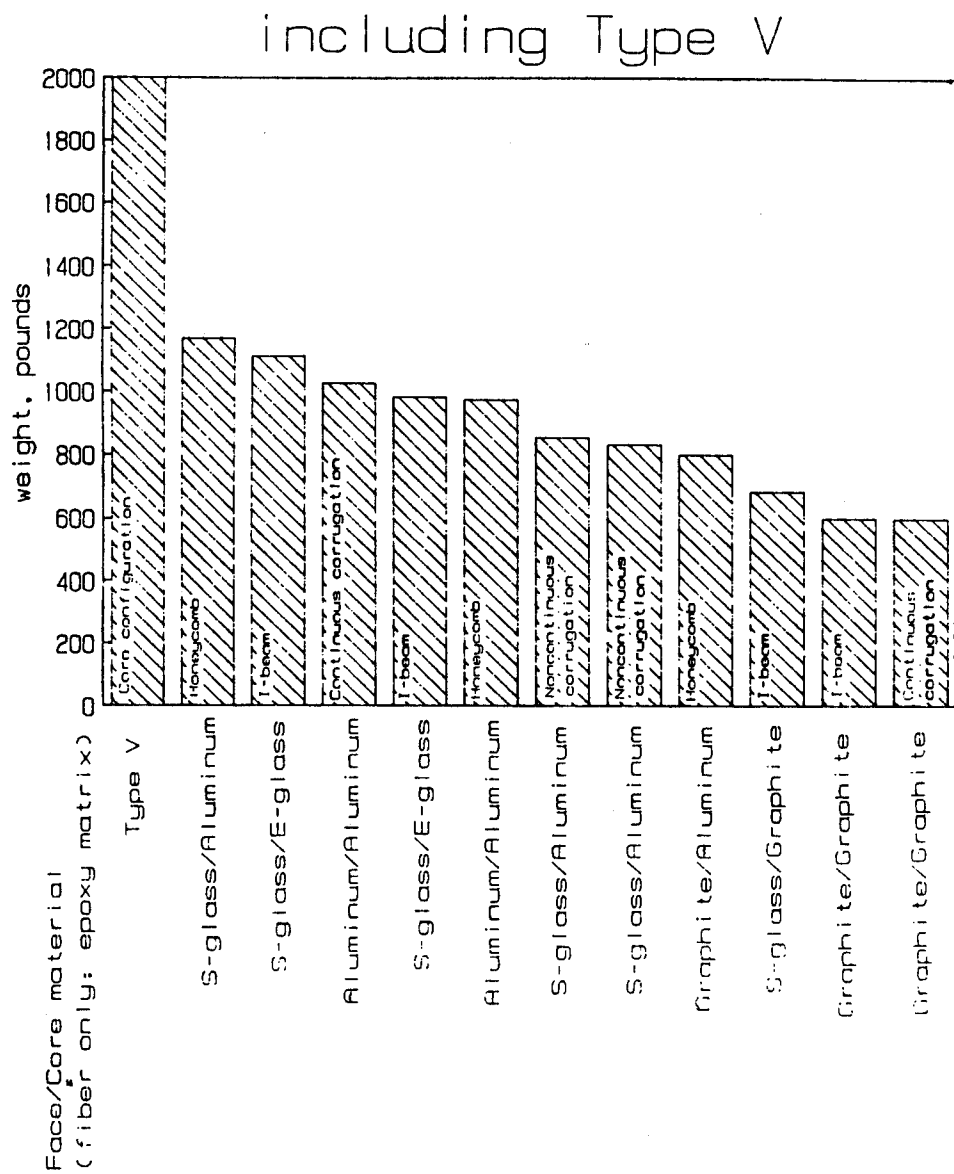


Figure 2.9 Concept weight comparison

the heaviest concept, 1167 lb, to the lightest, 599 lb. All of the composite platform weights are, however, well below the Type V weight. No correlation between basic concept configuration and weight was found to exist. A correlation between material and weight was noted, with the concepts incorporating graphite fibers tending to be lighter, and those incorporating aluminum tending to be heavier.

2.6.2 Performance

The performance parameter was calculated using five factors:

1. the minimum ratio of first ply failure stress to the design stress,
2. the minimum ratio of the critical buckling stress to the design stress,
3. the concept design flexibility (the ease of modifying concept parameters for additional load cases without redesigning from scratch),
4. the transverse shear capability (resistance to face sheet debonding or core collapse resulting from transverse shear), and
5. the bending efficiency (resistance to bending failure modes that might be experienced in other loading cases, e.g. wide column buckling as opposed to face sheet buckling).

For the first two factors, numerical results from the concept analysis were used to calculate normalized parameters. For the last three performance factors, relative comparisons were generated, using the information available from earlier program efforts and past experience. Although unavoidably subjective, these factors are believed important to an adequate calculation of the performance parameter. The performance comparison factors are given in Table 2.3. A rating of 1.0 in an area indicates typical, average performance for that factor. Lower values indicate superior performance. Using these factors, an overall performance parameter was calculated. In this calculation, a weighted average was used, with the design flexibility at a double weight because of its importance. The resulting average ratings are also given in Table 2.3. One effect noted during this comparison is the smoothing out of differences by the averaging, as each concept has strengths and weaknesses. The Type V was assigned a relative ranking number of 1.0, indicating average, acceptable performance.

2.6.3 Survivability

Relative numerical rankings were also estimated for the overall survivability of the platform concepts. This included five factors:

1. resistance to localized damage (the ability to sustain damage to a small area without rendering the entire platform useless),
2. repairability (ease and effectiveness with which localized repairs can be made),
3. environmental resistance (to such factors as extreme heat, humidity or moisture),

Table 2.3: Performance Comparison Parameters

Face/Core Material ^a	FPF	Buckling	Design Flexibility	Transverse Shear	Bending Efficiency	Overall
<u>Honeycomb Cores</u>						
S-Glass/Al ^b	0.7	1.2	1.4	0.4	1.0	1.0
Graphite/Al	1.0	0.7	1.4	0.4	1.0	1.0
Al/Al	1.2	0.9	1.4	0.4	1.0	1.1
<u>I-Beam Cores</u>						
S-Glass/E-Glass	1.2	2.2 ^c	1.0	1.6	0.4	1.2 ^c
S-Glass/E-Glass	0.9	1.3	1.0	1.6	0.4	1.0
Graphite/Graphite	1.1	1.0	1.0	1.6	0.4	1.0
S-Glass/Graphite	0.7	1.0	1.0	1.6	0.4	1.0
<u>Continuous Corrugated Cores</u>						
Al/Al	1.0	0.8	0.8	0.6	0.6	0.8
Graphite/Graphite	1.3	1.0	0.8	0.6	0.6	0.9
<u>Noncontinuous Corrugated Cores</u>						
S-Glass/Al	0.9	0.9	0.4	0.8	0.6	0.7
S-Glass/Al	1.1	1.0	0.4	0.8	0.6	0.7

^a Graphite and glass composites are designated by fiber type. Epoxy matrix is assumed.

^b Al = Aluminum

^c Unacceptable - low critical buckling load.

4. durability (resistance to wear and tear such as roller damage, localized load impact damage, etc.), and
5. overall damage resistance (resistance to permanent deformation after large deflections, ability to absorb impact energy, considerations for other load cases, etc.).

The numerical results generated for concept survivability comparison are given in Table 2.4. The Type V platform was included. Again, low numbers indicate superior performance and a rating of 1.0 indicates average performance. The composite material concepts show an improvement over the aluminum concepts, including the Type V, in the areas of environmental resistance and durability. However, the technology to repair damaged aluminum structures is more advanced than that for repairing composite structures. Thus, all aluminum concepts were judged easier to repair. All concepts had acceptable survivability. The environmental resistance and durability ratings were estimated to be more important to the life-cycle cost of the platform and were therefore weighted double in the overall rating calculation.

2.6.4 Initial Cost

Initial cost estimates were made for the fabrication costs of the most promising concepts. The estimates were based on discussions with manufacturers and included material, production and overhead costs. Several assumptions were made. These assumptions were:

1. Production was assumed to be in the range of 500 to 1000 units per year.
2. Costs included fabrication and assembly, but not shipping.
3. No allowances were made for special treatments such as painting, chemical coating, etc.
4. Machining to accept simple closeouts only was included.

The relative costs thus estimated for the composite platform concepts are shown in Table 2.5. The costs are normalized using the average platform costs. The concepts are far from a final design and the cost estimates are preliminary. Specific dollar figures would therefore show a false level of accuracy. The concepts containing graphite fibers are relatively expensive; the concepts using all S- and E-glass are relatively cheap. Unfortunately, the lightest concepts tend to be more expensive, and vice versa.

2.6.5 Overall Comparison and Concept Selection

Using the survivability, performance, weight, and initial cost ratings, overall concept comparison ratings were calculated. The individual ratings used are given in Table 2.5, along with the overall ratings calculated. Because of the preliminary nature of this project, it was not possible to calculate an accurate dollar/pound value for weight savings. Therefore, three different overall comparison ratings were calculated (see Table 2.5). For rating 1, the initial cost was averaged in at twice the importance of the other three factors. This is essentially rating the

Table 2.4 Survivability Comparison Parameters

Face/Core Material ^a	Local Damage	Repairability	Environmental Resistance	Durability	Overall Damage	Overall
<u>Honeycomb Cores</u>						
S-Glass/Al ^b	0.4	0.6	0.8	0.6	0.6	0.6
Graphite/Al	1.0	1.4	0.8	0.6	0.8	0.9
Al/Al	0.6	0.4	1.4	1.2	0.8	1.0
<u>I-Beam Cores</u>						
S-Glass/E-Glass	0.8	0.8	0.4	0.4	0.6	0.5
S-Glass/E-Glass	0.8	0.8	0.4	0.4	0.6	0.5
Graphite/Graphite	1.4	1.4	0.4	0.4	1.0	0.8
S-Glass/Graphite	0.8	1.0	0.4	0.4	0.8	0.6
<u>Continuous Corrugated Cores</u>						
Al/Al	0.6	0.4	1.4	1.4	1.0	1.1
Graphite/Graphite	1.2	1.4	0.4	0.4	1.2	0.8
<u>Noncontinuous Corrugated Cores</u>						
S-Glass/Al	0.6	0.6	0.8	0.6	0.8	0.7
S-Glass/Al	0.6	0.6	0.8	0.6	0.8	0.7
<u>Type V</u>						
Aluminum (modular)	0.4	0.8	1.0	1.6	1.4	1.1

^a Graphite and glass composites are designated by fiber type. Epoxy matrix is assumed.

^b Al = Aluminum

Table 2.5 Overall Comparison Parameters and Ratings

Face/Core Material ^a	Weight	Initial Cost	Survivability	Performance	1 ^b	2 ^c	3 ^d
<u>Honeycomb Cores</u>							
S-Glass/Al ^e	1.3	1.2	0.6	1.0	1.1	1.0	1.1
Graphite/Al	0.9	1.3	0.9	1.0	1.1	1.0	1.0
Al/Al	1.1	0.9	1.0	1.1	1.0	0.9	1.0
<u>I-Beam Cores</u>							
S-Glass/E-Glass	1.3	0.6	0.5	1.2 ^f	0.8 ^f	0.9 ^f	1.0 ^f
S-Glass/E-Glass	1.1	0.6	0.5	1.0	0.8	0.8	0.9
Graphite/Graphite	0.7	1.2	0.8	1.0	1.0	0.9	0.9
S-Glass/Graphite	0.8	1.1	0.6	1.0	0.9	0.9	0.9
<u>Continuous Corrugated Cores</u>							
Al/Al	1.2	0.7	1.1	0.8	0.9	1.0	1.0
Graphite/Graphite	0.7	1.6	0.8	0.9	1.1	1.0	0.9
<u>Noncontinuous Corrugated Cores</u>							
S-Glass/Al	1.0	0.9	0.7	0.7	0.8	0.8	0.9
S-Glass/Al	1.0	0.9	0.7	0.7	0.8	0.8	0.9
<u>Type V</u>							
Aluminum (modular)	2.3	0.5	1.1	1.0	1.1	1.2	1.4

^a Graphite and glass composites are designated by fiber type. Epoxy matrix is assumed.

^b Weighted average: cost 2X, others 1X.

^c Common average: all parameters weighted equally.

^d Weighted average: weight 2X, others 1X.

^e Al = Aluminum

^f Unacceptable - low critical buckling load.

lifetime cost of the concepts based on the assumption that the weight savings benefit is less important in the lifetime cost than the initial platform cost. Rating 2 was calculated based on approximately equal importance of the weight savings and initial cost. This assumes that a 10% weight savings is worth a 10% increase in cost. This tradeoff is on the order of \$5 to \$10/lb. A third case, in which the weight savings were assumed to overcome the initial cost during a platform lifetime, was also calculated (rating 3). The resulting concept ratings, including the Type V, are graphed in Figure 2.10.

Using the three different rating sets, the concepts were compared for concept selection and for competitiveness with the Type V. Three configurations were selected as the most promising concepts for further study.

The three concept configurations are:

1. S-glass/epoxy face sheets and an E-glass/epoxy pultruded I-beam core (3" x 3.25" x 0.125" beams),
2. S-glass/epoxy face sheets and a noncontinuous corrugated aluminum core (27 core sections), and
3. S-glass/epoxy face sheets and a graphite/epoxy pultruded I-beam core (3" x 3.25" x 0.125" beams)

2.7 CONCLUSION

The conclusion of the Phase I effort was that a composite platform configuration can be competitive with the Type V. Since there was no optimization attempted for the composite concepts, they are likely to be superior. This conclusion is based on material, performance, and economic factors. For roughly comparable initial costs, a better performing and lighter weight platform appears possible.

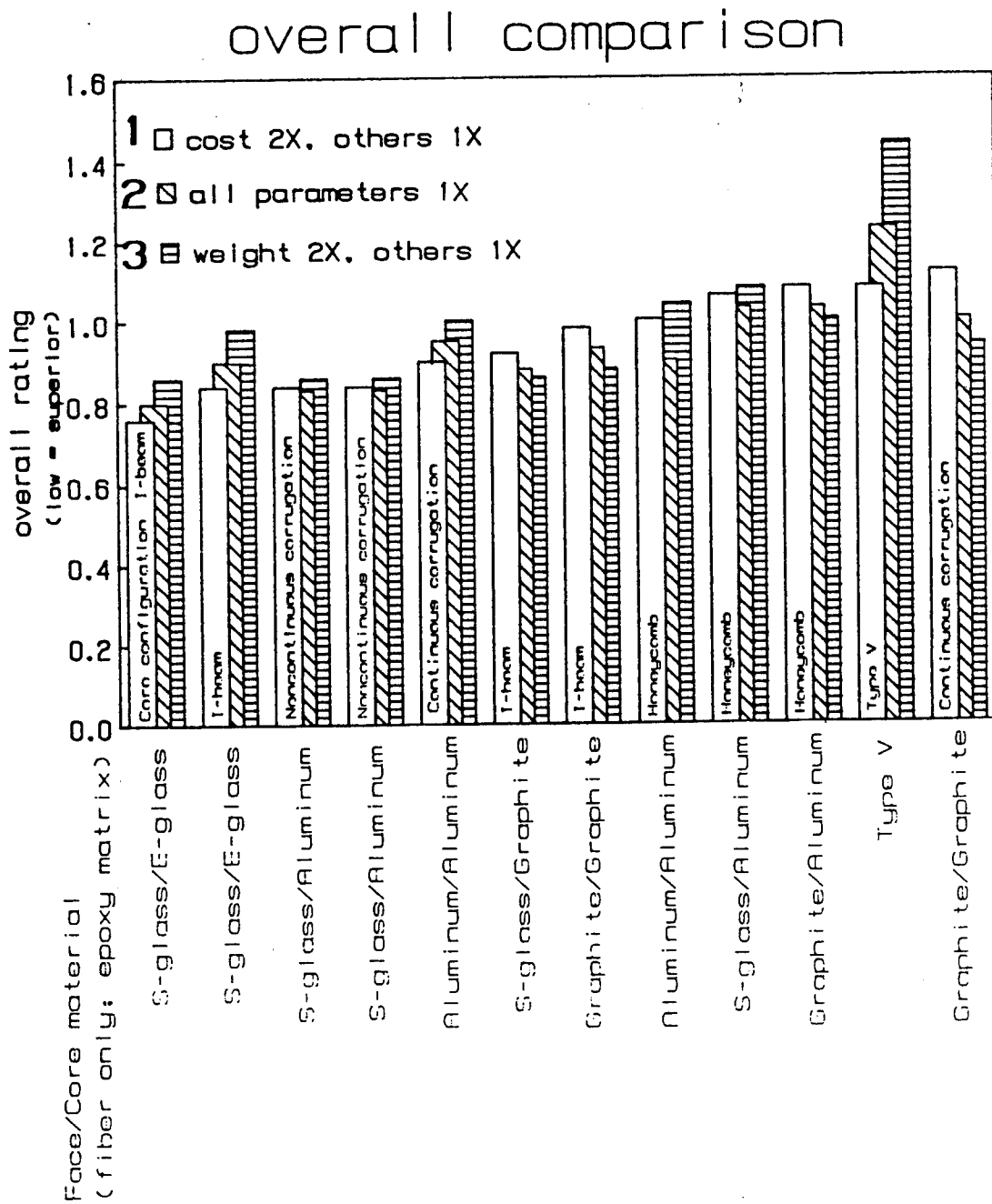


Figure 2.10 Overall concept comparison

3. PHASE II TASKS 1 AND 2

3.1 INTRODUCTION

During Phase II of the Advanced Composites in Airdrop Program, the first task was to perform detailed analysis of the three concepts recommended by Phase I. The Task 1 analysis, as described in the Statement of Work, was to be restricted to the parachute opening load case, but to be more detailed than the previous (Phase I) analysis. Specifically, modelling of individual core elements and more accurate representation of transverse properties were to be included. The added detail in the concept modelling was to provide information concerning such things as specific areas of overstress, failure modes, and the location of first ply failure. Task 2 consisted of selection of one of the three concepts for further study.

This report section is a summary of the work done during the first portion of Phase II. The subtopics covered as part of this work are as follows:

1. modification of the concept having S-glass/epoxy face sheets and a noncontinuous corrugated core,
2. a brief look at face sheet hybridization,
3. Task 1, detailed analysis of the parachute opening load case;
 - a. the detailed model used for the concept having S-glass/epoxy face sheets and an E-glass/epoxy I-beam core,
 - b. results generated using this model,
 - c. a modification to the end cap used in the detailed model,
 - d. results generated with the modified model,
 - e. comparison of these results with the Phase I (SAP86 and GENLAM) results,
4. Task 2, selection of a concept for further analysis, including both performance and cost considerations.

3.2 CONCEPT MODIFICATION

Modification of the concept having a noncontinuous corrugated core consisted of further optimization, as recommended in Phase I. For valid comparison of the different concepts, a wide variance in the degree of optimization of each concept was not desirable. However, it was also not desirable to spend a great deal of time on optimization for the generic platforms being investigated. Several different variations of the non-continuous core concept were briefly analyzed. The most efficient of these was selected to be the final version of one of the three concepts analyzed in detail. The three Phase II, Task 1, concepts are summarized in Table 3.1.

Table 3.1 Concept Description (Material and Configuration)

Face Sheet Construction	Core Construction	Face Sheet Lamination Sequence	Number of Sections or Beams	Core Information
<u>Beam Dimensions</u>				
S-glass/epoxy	Pultruded E-glass/epoxy I-beams	$[\pm 60/0/\pm 60/0_8]_s$	17	3" X 3.2" X 0.25"
S-glass/epoxy	Pultruded graphite/epoxy I-beams	$[\pm 60/0_6]_s$	20	3" X 3.25" X 0.125"
				t θ h_c w_u [in] [°] [in] [in]
S-glass/epoxy	Aluminum sections	$[\pm 45/90/0_{7\frac{1}{2}}]_s$	21	0.060 11 3.29 2.0

3.3 FACE SHEET HYBRIDIZATION

Before generation of complex, detailed models, which are often difficult to modify, the possibility of using hybrid face sheets was examined, using SAP86 and GENLAM as in Phase I. Several different hybrid face sheets were analyzed, using S-glass and graphite fibers in an epoxy matrix. Problems were encountered resulting from the mismatch of the strengths and moduli of the two materials. S-glass fibers have relatively high strength but low stiffness in relation to graphite, especially high modulus graphite. However, a hybrid face sheet was found that provided a weight savings of approximately 100 lb, which is about 10% of the total platform weight. The drawbacks of a hybrid face sheet (increased tendency to delaminate, added cost and complexity, etc.) must be balanced against the benefits (lighter weight, better performance, etc.) in any further study of face sheet hybridization. At this time, it was concluded that, while hybrid face sheets do have potential for weight reduction and performance improvement, further study would be beyond the scope of this project.

3.4 TASK 1: DETAILED ANALYSIS OF PARACHUTE OPENING LOAD CASE

The modelling assumptions (dynamic magnification factor of two, 60° cables, uniform loading of 23300 lb) used in Phase II for the parachute opening load case were identical to those of Phase I. In Phase I, SAP86 and GENLAM were used, as previously discussed. Unless otherwise noted, analysis results in the different Tasks of Phase II were generated using the finite element code NASTRAN and the pre- and post-processor PATRAN. A detailed quarter symmetry model of the concept having an E-glass/epoxy I-beam core was made. The side and end closeouts used were the same as those used previously. In Figure 3.1, the I-beams and closeouts are shown. The I-beams are all 0.125" thick, except for the half beam in the center, while the end and side closeouts and the half beam are 0.0625" thick. The face sheet geometry is shown in Figure 3.2. Areas of concern in the model setup were the cable attachment corner and the accuracy of the boundary conditions. These concerns were checked by first running the model using isotropic aluminum face sheets, then with S-glass/epoxy face sheets. The deflection contours and values obtained in both cases were similar to those determined for the concepts in Phase I, implying the model was valid and running properly. These deflection results for the first two analysis runs are shown in Figure 3.3 (the isotropic face sheet case) and Figure 3.4 (the composite face sheet case). One note of interest in the comparison of the two cases is that the concept with the composite face sheet had a slightly larger displacement along the short side of the platform. This results from the orthotropic nature of the composite face sheets. Since most of the plies are oriented along the long axis of the platform, the transverse bending stiffness was lower than that of the aluminum concept.

A concern was noted in regard to the end cap used, which had originally been configured for use with several different cores, including honeycomb cores. The end cap was modified for more optional configuration with the three concepts to be analyzed. Vertical aluminum plates (0.125" thick) were added along the inner surface of the end close out for the entire 52" length. The improved end close out model is shown in Figure 3.5.

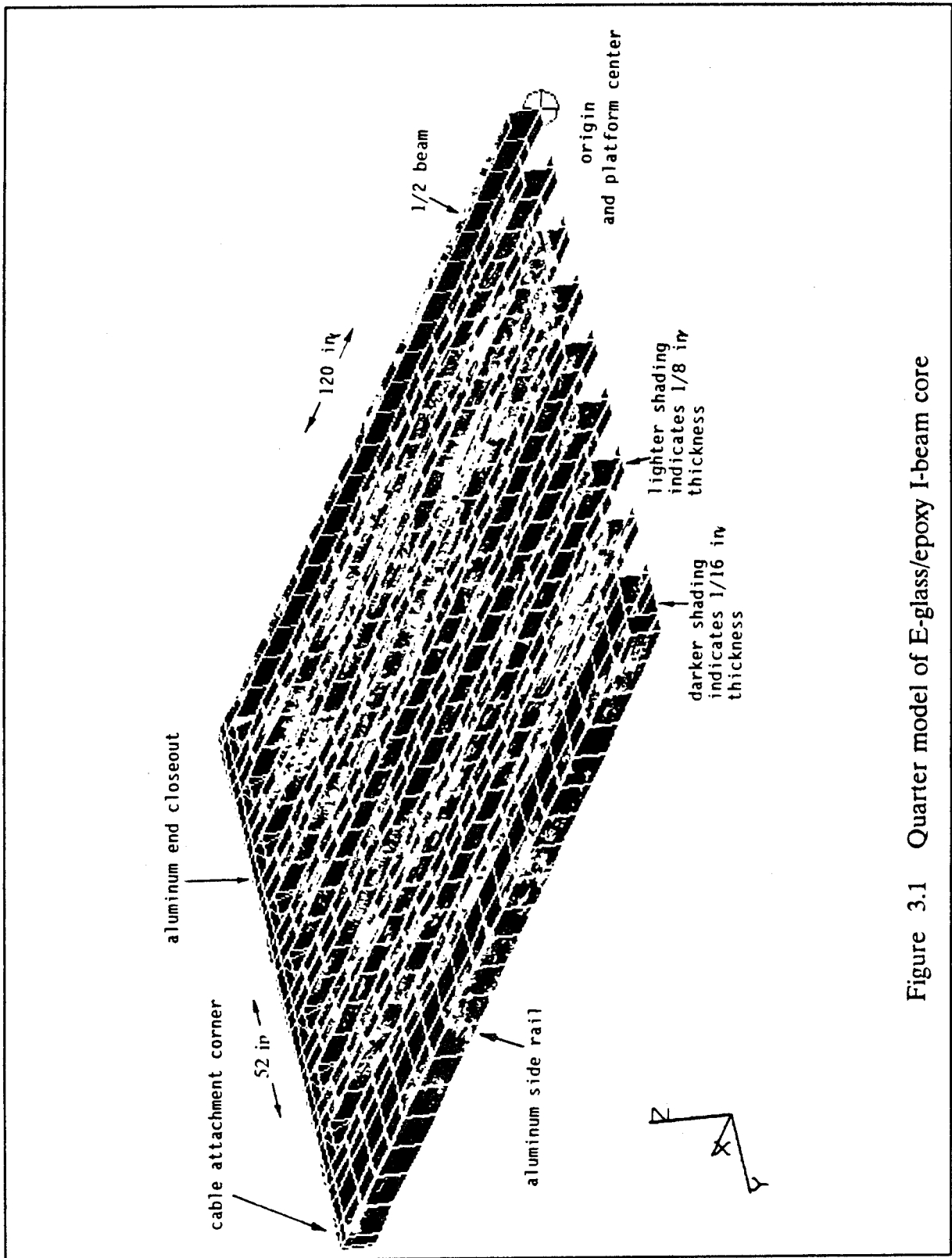


Figure 3.1 Quarter model of E-glass/epoxy I-beam core

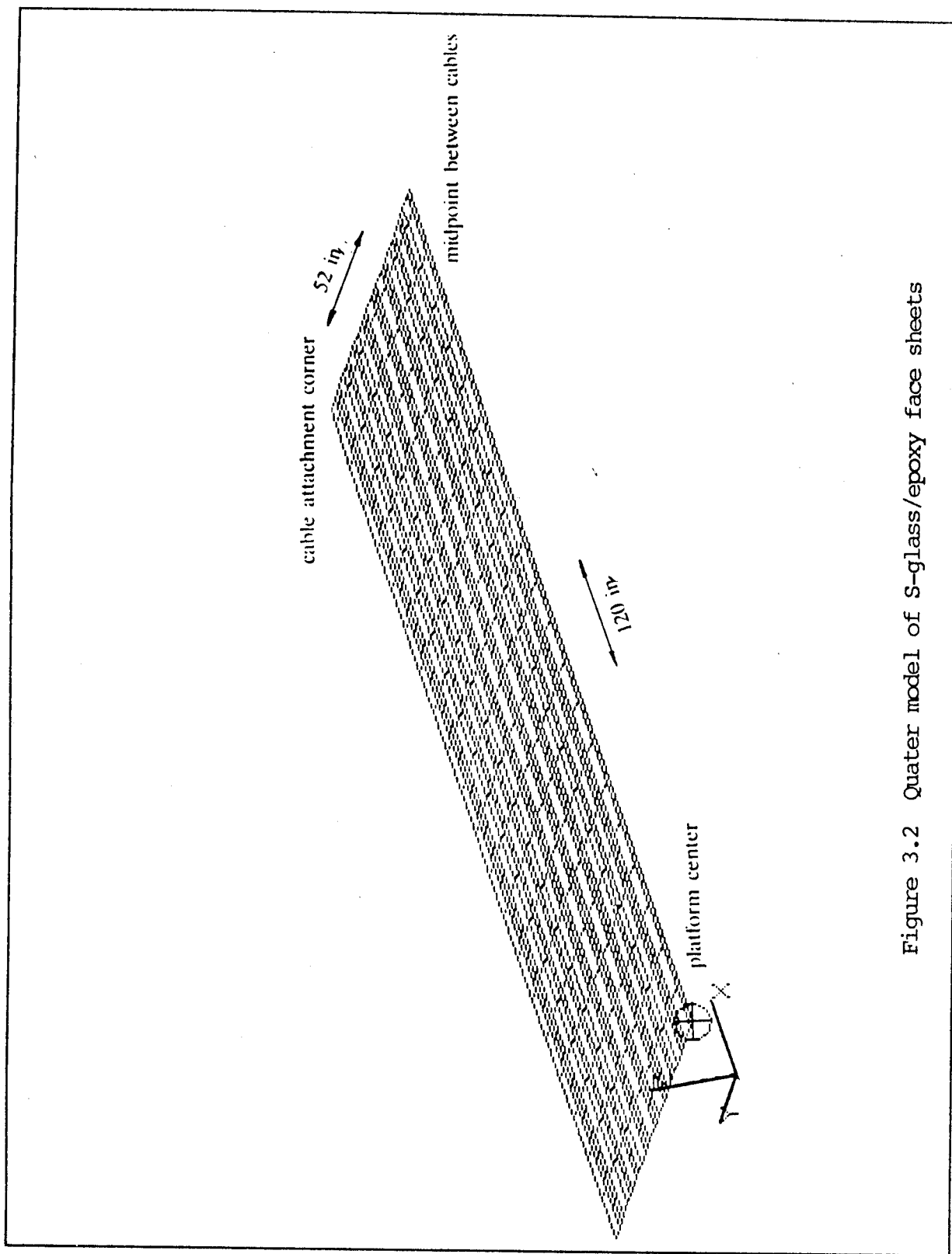
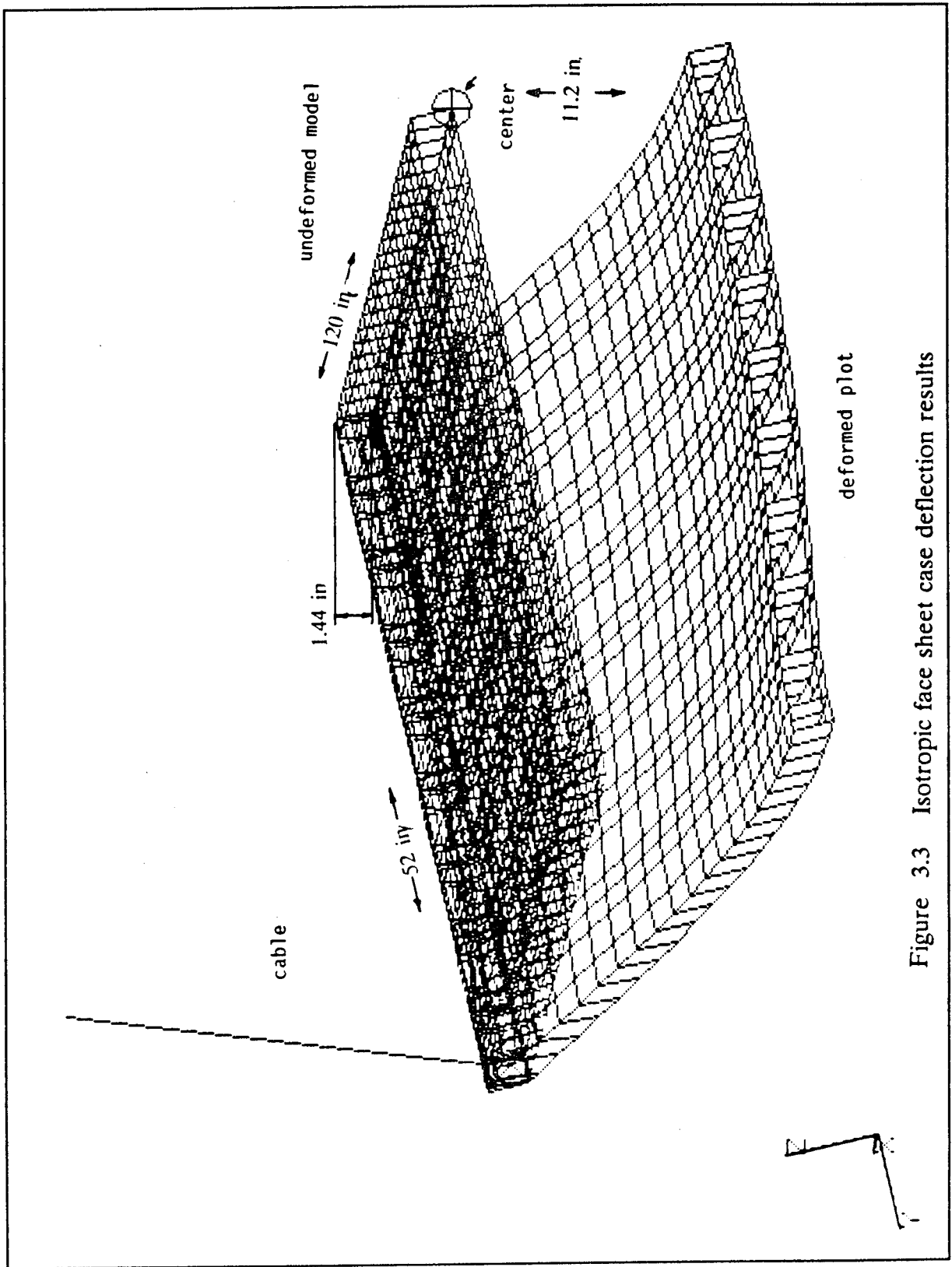


Figure 3.2 Quarter model of S-glass/epoxy face sheets



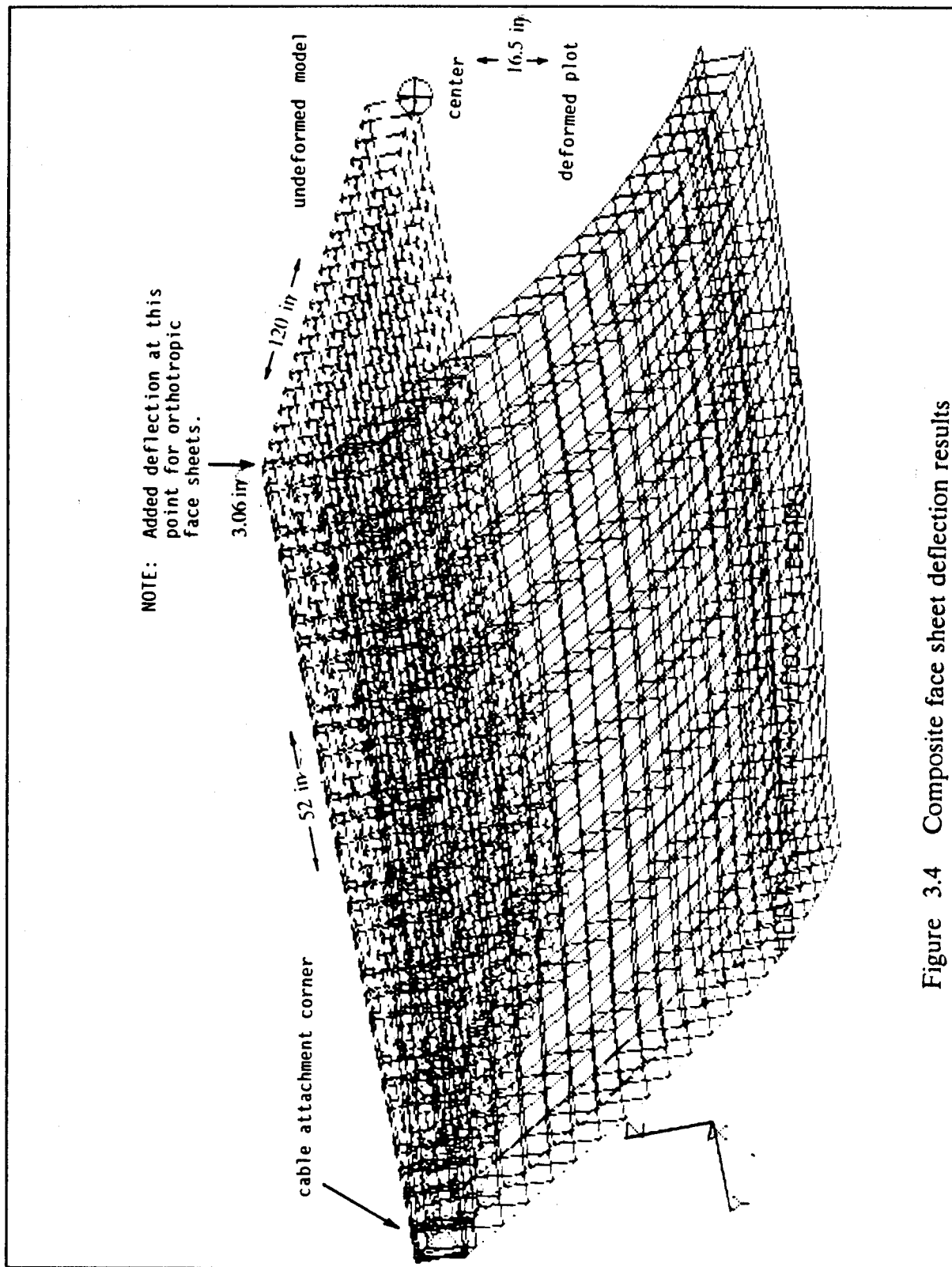


Figure 3.4 Composite face sheet deflection results

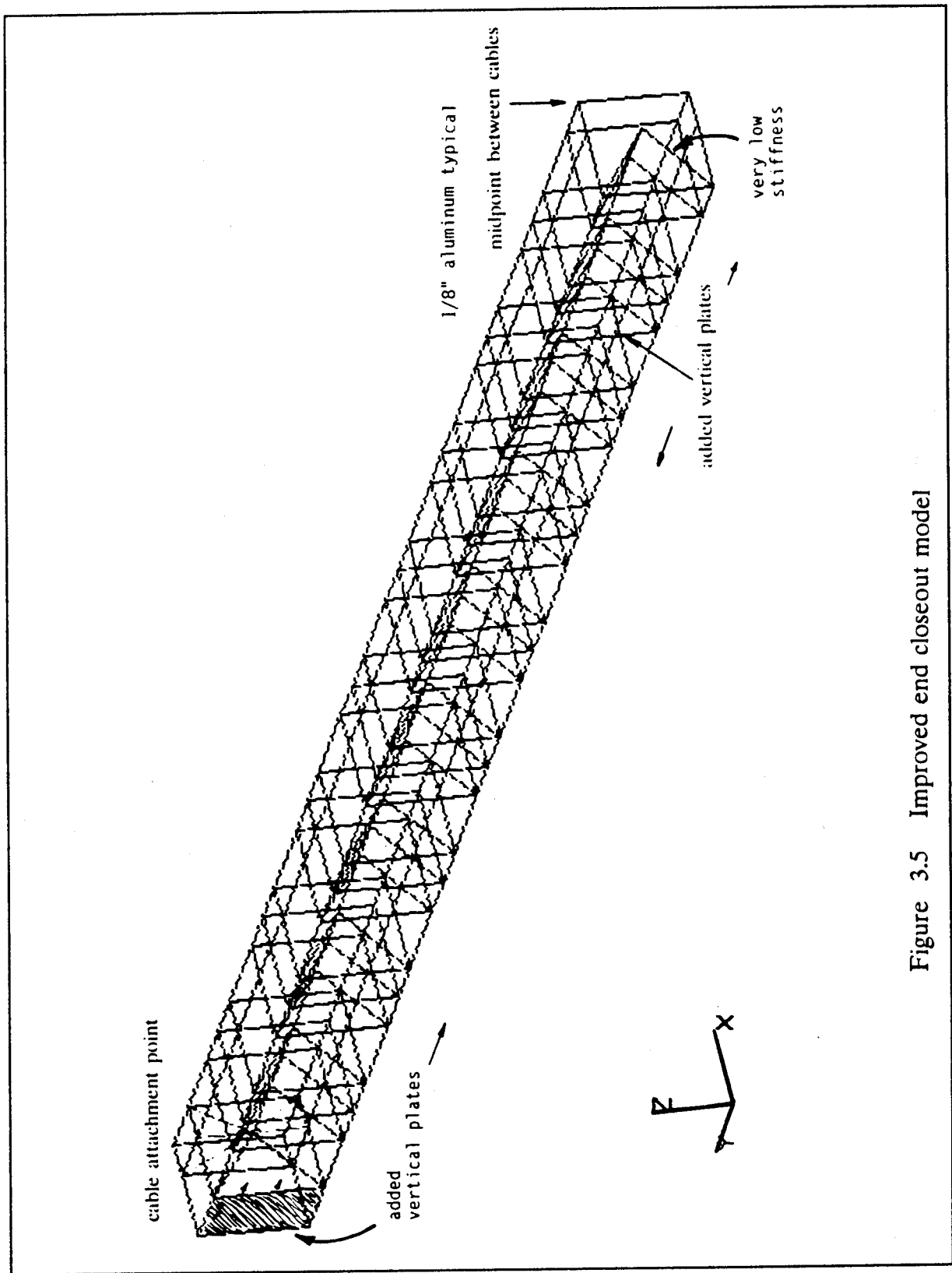


Figure 3.5 Improved end closeout model

The E-glass/epoxy I-beam core concept was then analyzed again. The results thus obtained were only minimally different, with typically a 10% or less change observed. The displacement results for this analysis run are given in Figure 3.6. Any results given later in this report are for the case having the improved end closeout, as the changes were an improvement, even if slight. The end closeout stress was found to be less than 42.7 ksi, with a factor of safety of 1.4. Shear stresses for the end closeout and side rail were less than 16 ksi, giving a factor of safety of greater than 2.3.

In examination of the analysis results, the stresses in the I-beam core were found to be relatively low in comparison with allowable values. Figures 3.7, 3.8, and 3.9 show the stresses in the I-beams, for the bottom flanges, top flanges, and webs, respectively. (Numbers beside shaded areas indicate the maximum value for the plotted variable within the area indicated, for Figures 3.7 to 3.9 and subsequent figures as applicable.) The I-beam flange major principle stresses are bounded by -4.2 ksi and +10.0 ksi ($R > 3.0$). The peak principle stresses can be seen near the center of the platform, as would be expected. The web in-plane shear stresses are low, bounded by -1.2 ksi and 2.5 ksi. Allowable values for the webs are 6.0 ksi to 7.0 ksi.

The critical stress for this load case and concept was found to occur in the lower face sheet. Face sheet results are shown in Figure 3.10 (lower face sheet, x-axis strain) and Figure 3.11 (lower face sheet, y-axis strain). These strains are for the equivalent orthotropic plates used in the NASTRAN solution. These values are used by NASTRAN and PATRAN to compute the stress in each ply for the composite face sheets. The strain in the long direction (x-axis, Figure 3.10) indicated essentially beam bending. The levels of x-axis strain show strips roughly parallel to the y-axis, with the highest level near the platform center. The strain in the y-axis direction (see Figure 3.11) is somewhat different. Strain values are indicated in a circular pattern, with the highest value at the center. This center is located at the midpoint between the cables, along the aluminum end closeout. Also, the I-beam flange effect can be seen. Lower strain values are seen for the I-beam locations, since the flanges are strained in conjunction with the face sheets.

The nomenclature used for ply numbering is shown in Figure 3.12. The nomenclature used for the stresses in ply axes is given in Figure 3.13. The global x and y axes for the overall model, also shown in Figure 3.13, correspond with the individual ply axes for the 0° plies only. As indicated in Figure 3.13, the $\bar{1}11$ axis is along the fibers; the $\bar{1}22$ axis is perpendicular to $\bar{1}11$ and the fiber orientation.

The ply with the lowest safety factor for first ply failure was the third ply of the lower face sheet. This is a 0° ply, indicating the fibers are oriented parallel to the x-axis. High strain values were seen in a circular pattern around the critically stressed area. The peak stress value occurred at the midpoint between the cables, along the end closeout, in the $\bar{1}22$ direction. The critically stressed area of ply 3 is shown in Figure 3.14. The minimum factor of safety for first ply failure occurs in this ply as a result of the high transverse stress loading the matrix rather than the fibers. If enough overload were applied, the failure would result from transverse tension, causing matrix cracking or

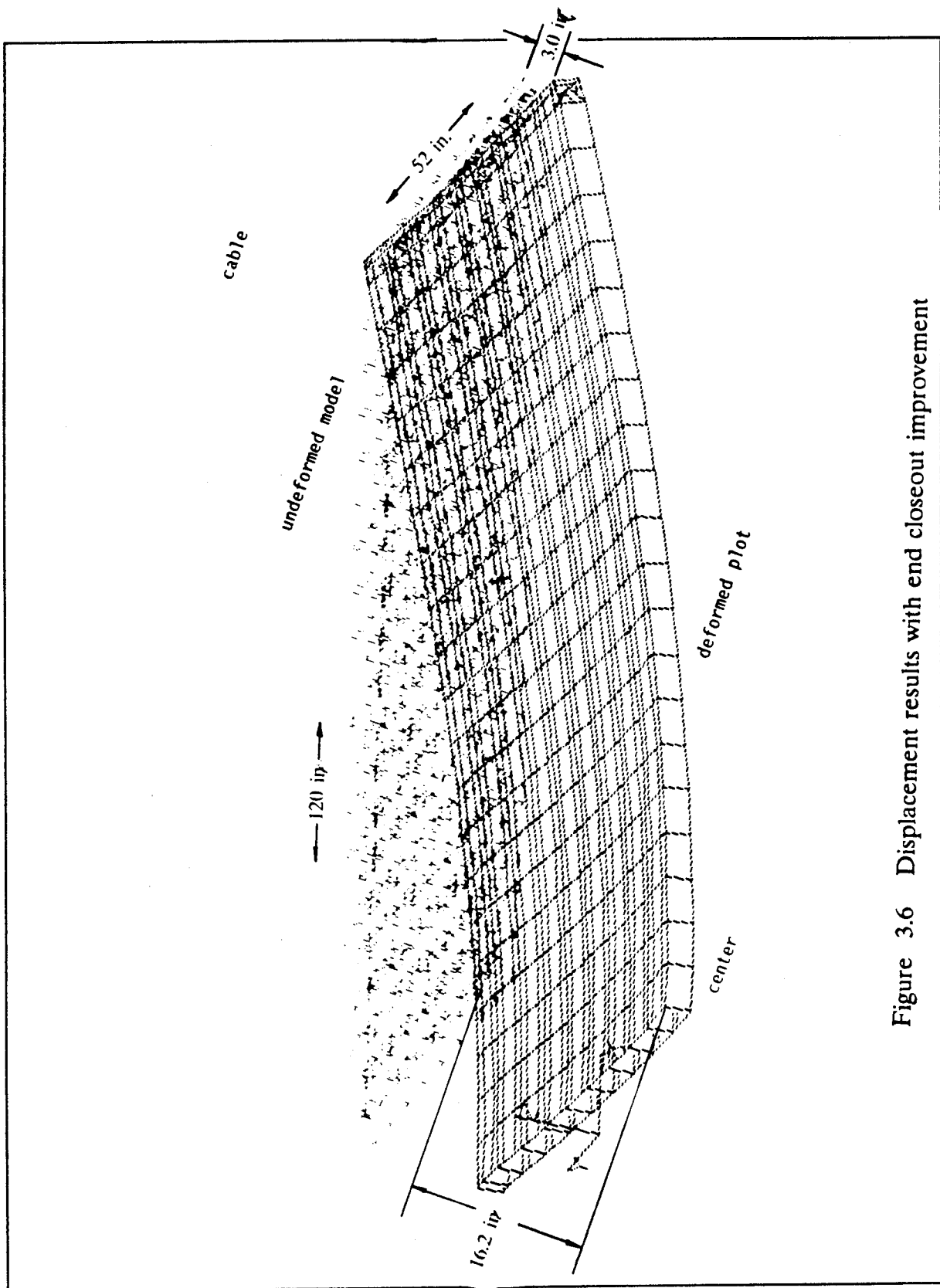


Figure 3.6 Displacement results with end closeout improvement

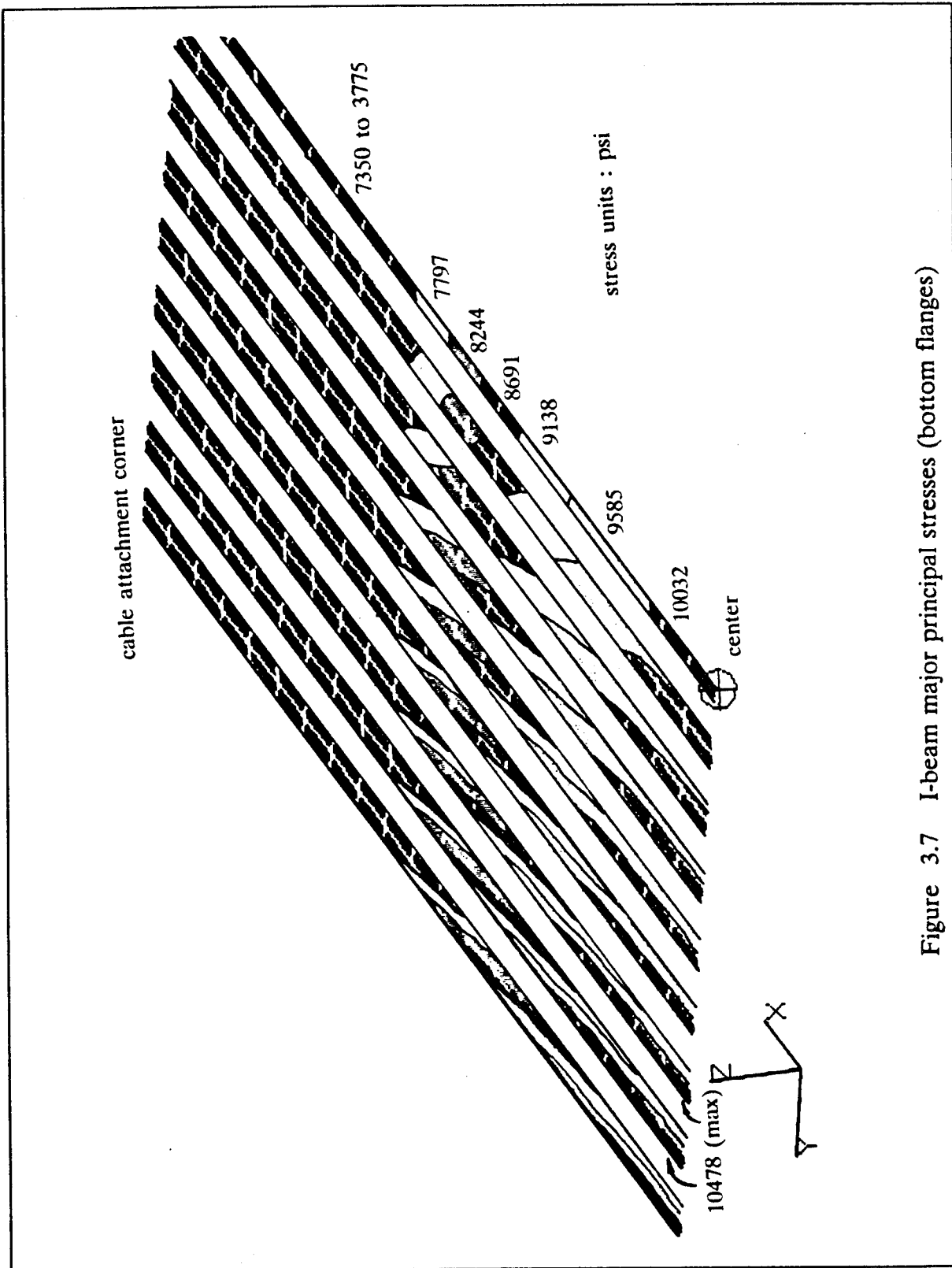


Figure 3.7 I-beam major principal stresses (bottom flanges)

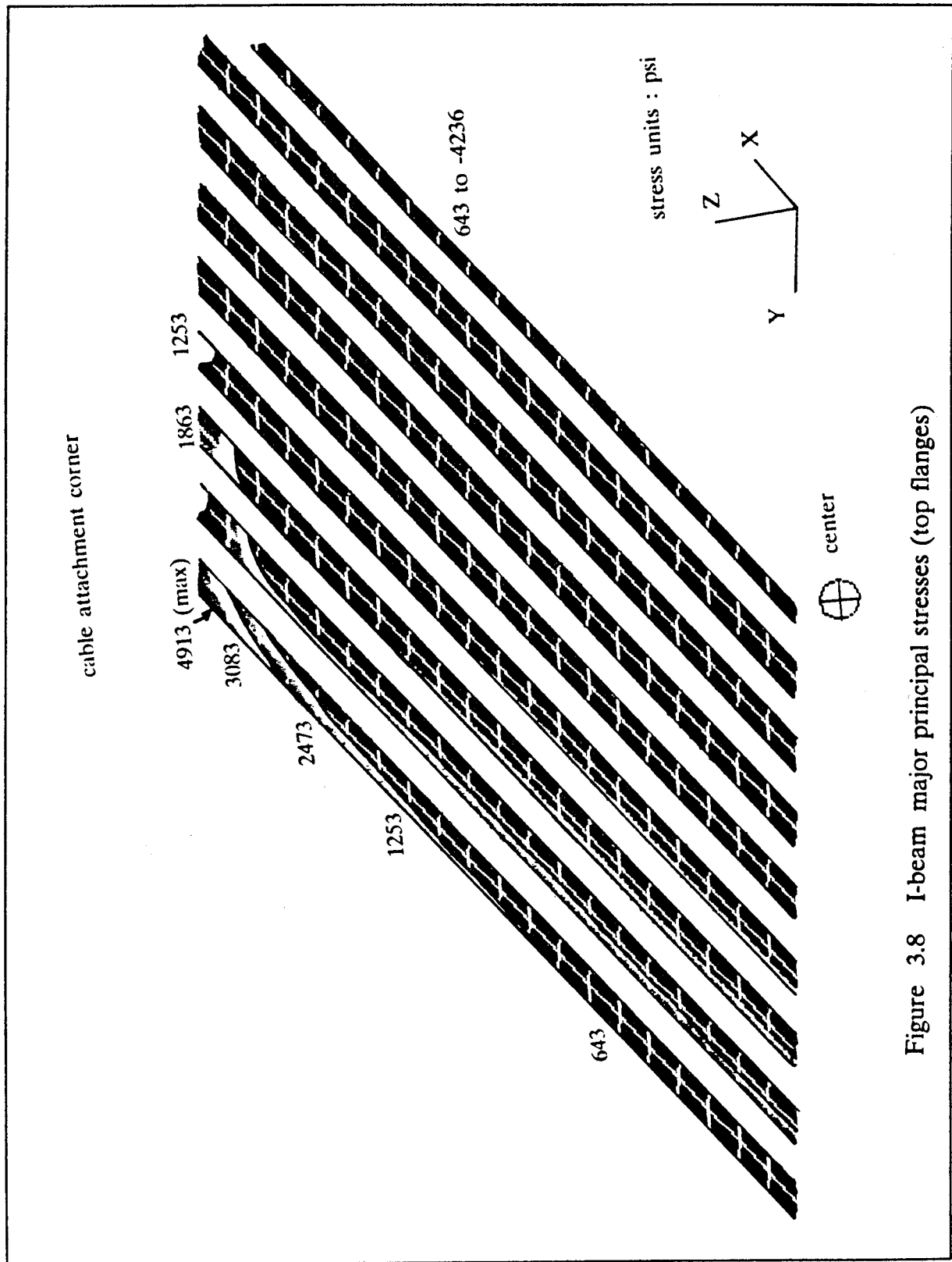


Figure 3.8 I-beam major principal stresses (top flanges)

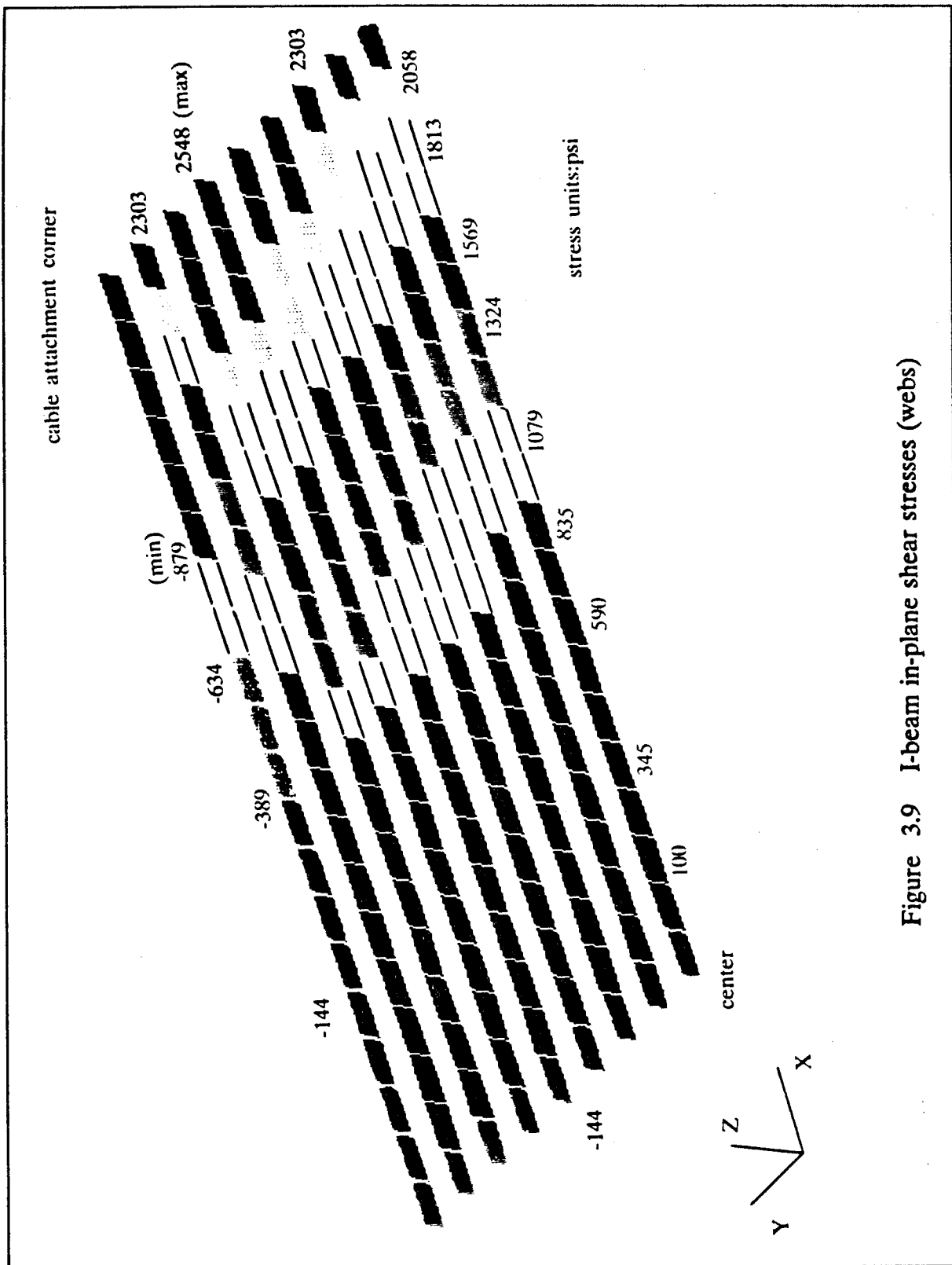


Figure 3.9 I-beam in-plane shear stresses (webs)

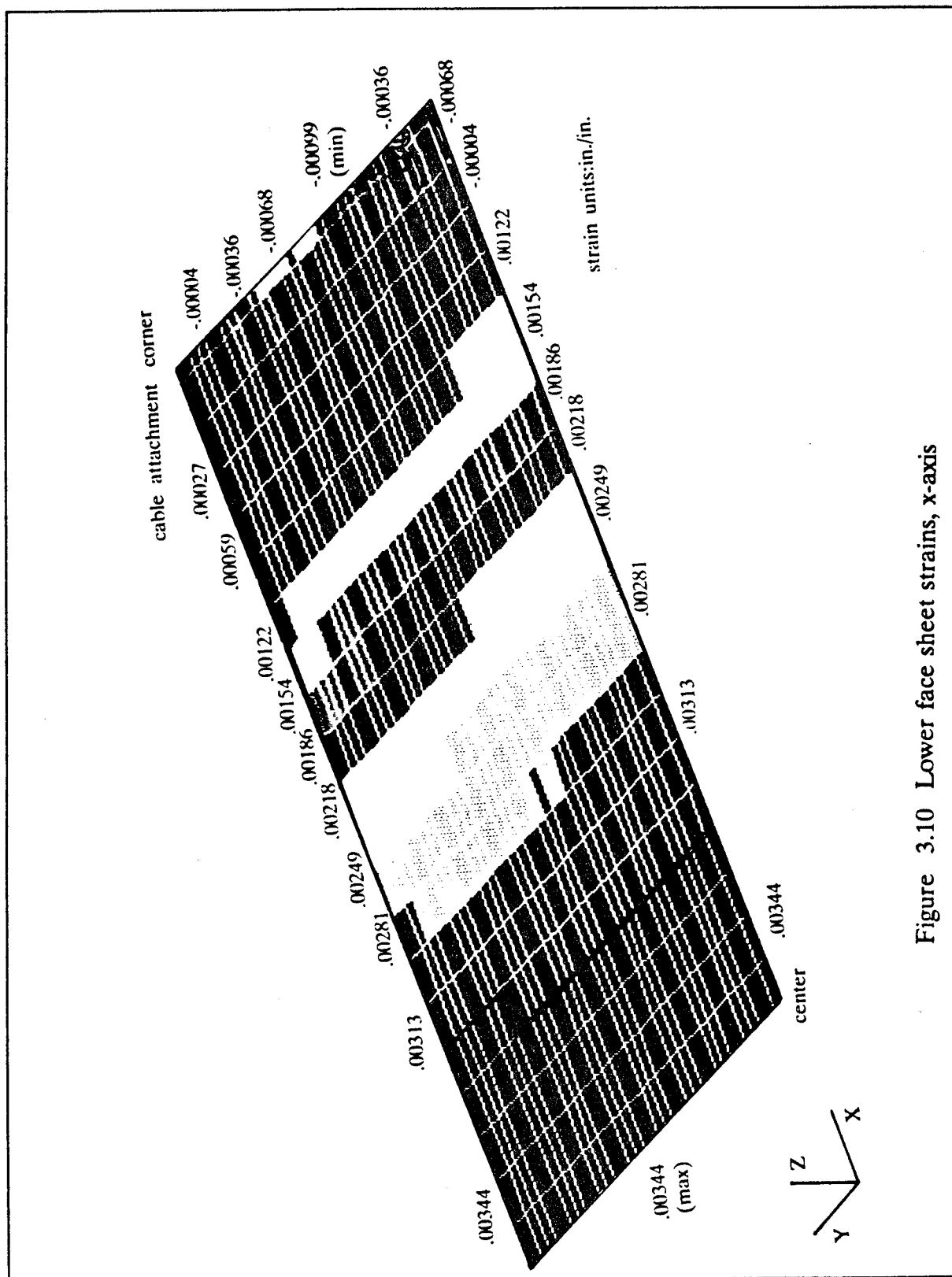
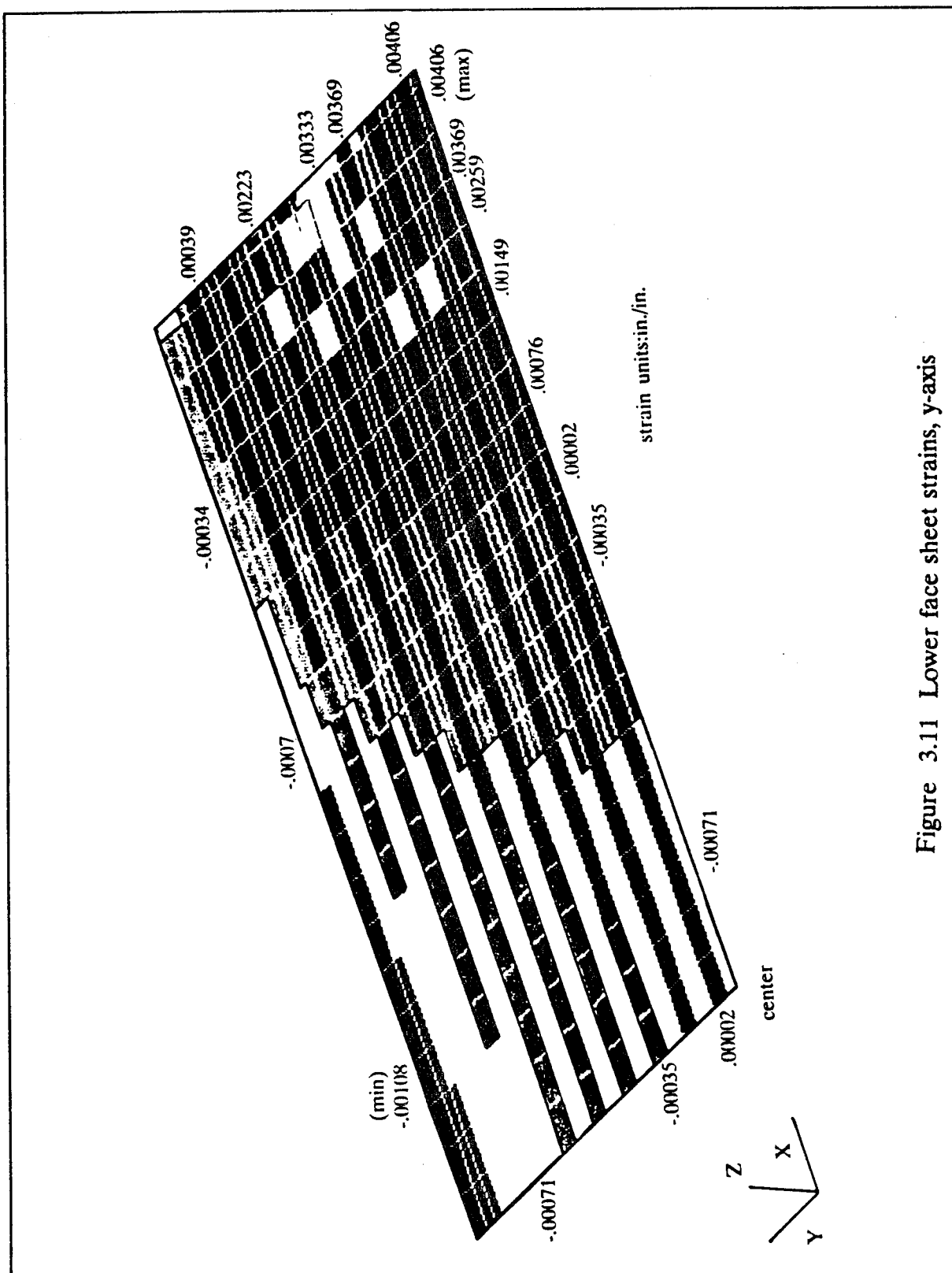


Figure 3.10 Lower face sheet strains, x-axis



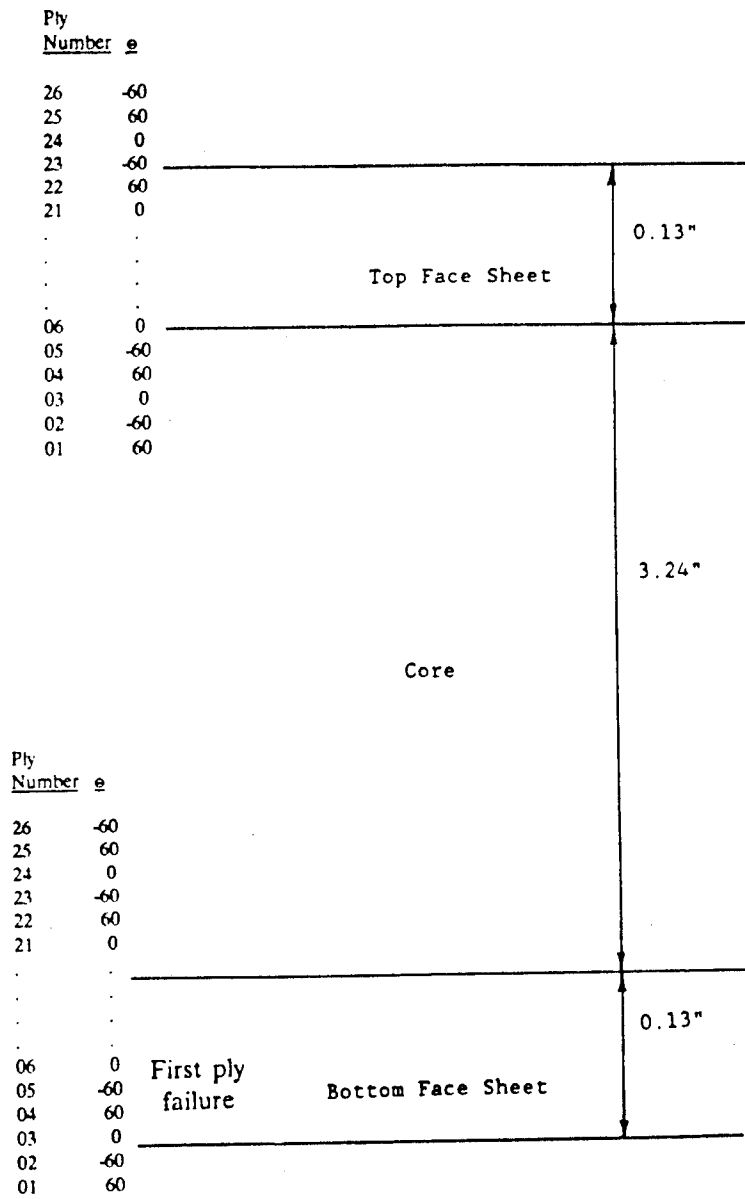


Figure 3.12 Face sheet ply nomenclature

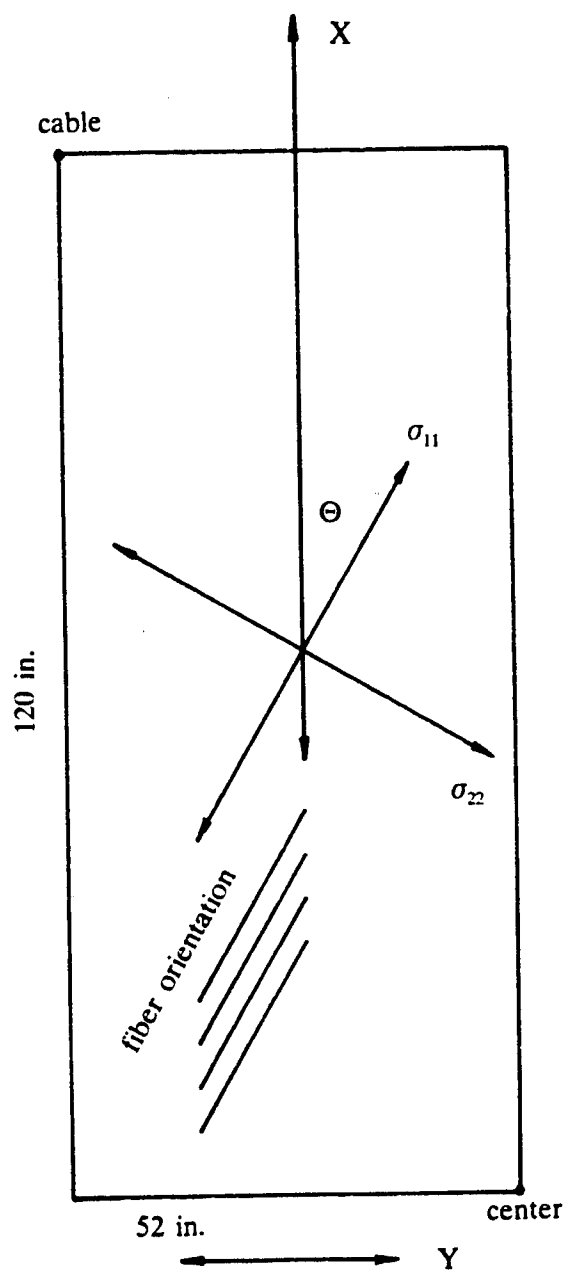


Figure 3.13 Ply axes nomenclature

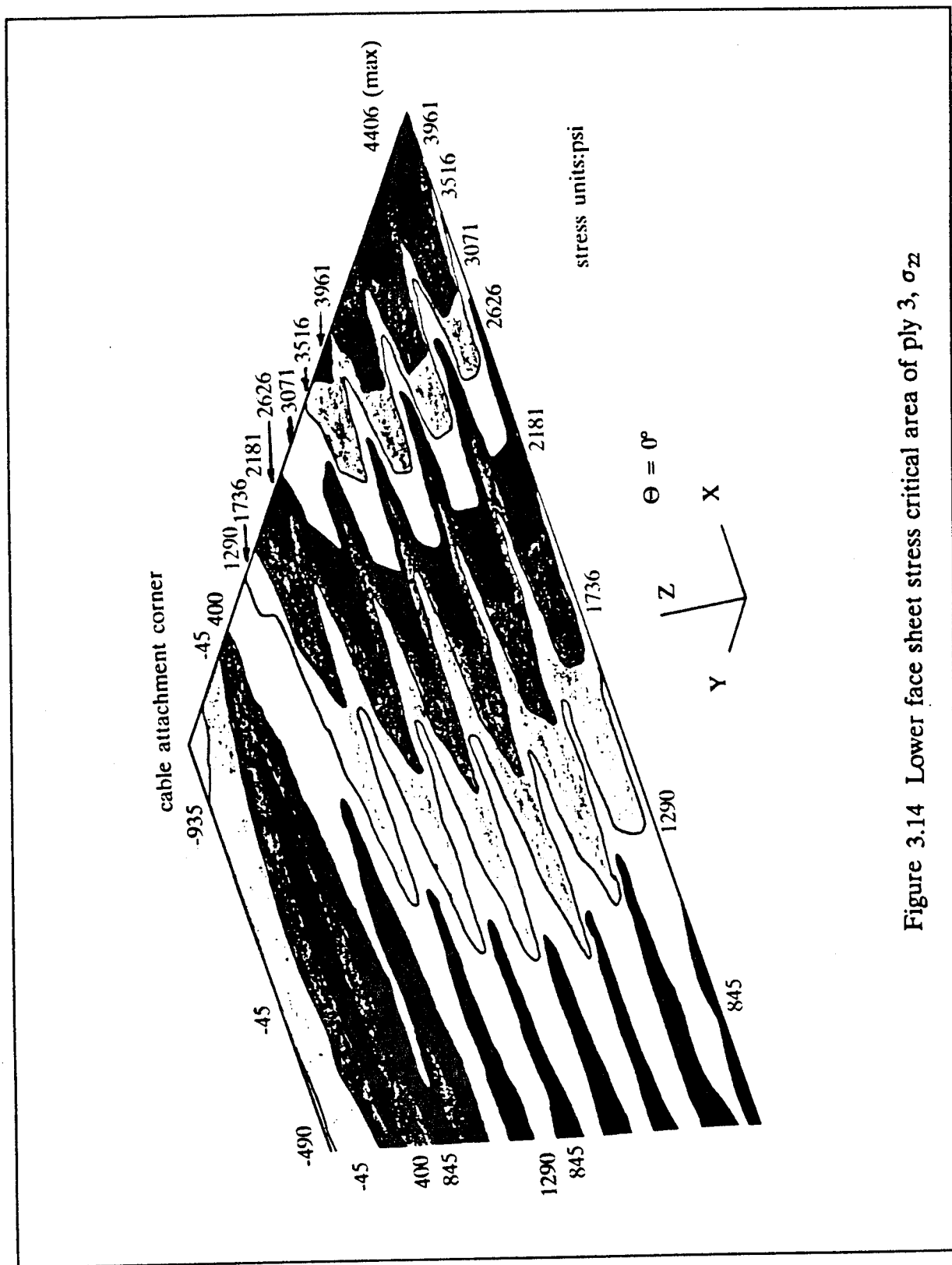


Figure 3.14 Lower face sheet stress critical area of ply 3, σ_{zz}

fiber-matrix interface failure. The stresses in ply 3 for the $\bar{1}11$ direction are shown in Figure 3.15. Note that these stresses are much higher because of the orientation of the fibers with the stress axis allowing much higher stress before failure would occur.

The concept with S-glass/epoxy face sheets and a pultruded E-glass/epoxy I-beam core was compared with one with an aluminum face sheet and the same core. In contrast with the critical stress location found for the composite face sheet, the isotropic aluminum face sheet case analysis indicated that peak stress values were near the center of the platform. The peak transverse stress for the aluminum face sheet case was found along the end closeout, at the midpoint between the cables. However, the transverse stress at this point was lower than the longitudinal stress at the center of the plate, indicating that the isotropic face sheet failure would occur at the center of the platform. Thus, the potential failure location in a composite face sheet can differ from that of an isotropic face sheet because the stresses within a laminate can vary from ply to ply and because composites are anisotropic with regard to strength as well as stiffness.

For a more complete picture of the stresses in the face sheet individual plies, the $\bar{1}11$ and $\bar{1}22$ axis stresses are shown for plies 1 and 2 in the lower face sheet and ply 26 in the upper face sheet in Figures 3.16 through 3.21. Again, the $\bar{1}11$ stresses are consistently higher than the $\bar{1}22$ values, shown by comparison of Figures 3.16, 3.18, and 3.20 with 3.17, 3.19, and 3.21. Another note of interest is the similarities between the stress patterns in similar layers, illustrated by the comparison of ply 1 of the lower face sheet with ply 26 of the top face sheet (Figures 3.16 and 3.17 compared with 3.20 and 3.21, respectively). The anisotropic nature of the composite face sheets is shown by comparison of Figures 3.16 through 3.21, also.

Overall, the performance of the S-glass/epoxy face sheet and E-glass/epoxy I-beam core concept was again found to be satisfactory under the parachute opening load case. No major differences between the detailed analysis and the earlier analysis were found. The critical area was found to be along the end closeout near the center of the platform, with minimum first ply failure indicated in a 0° ply (ply 3 of the lower face sheet) and having a factor of safety of 1.6.

In Table 3.2, the results for the Phase I analysis and the NASTRAN/PATRAN analyses are summarized. This table shows the correlation of results from the Phase I and Phase II analysis methods for the E-glass/epoxy I-beam core concept. During the discussion of final concept selection for Tasks 3 and 4 of Phase II, the similarity of results from the two methods was important.

3.5 TASK 2: FINAL CONCEPT SELECTION

The selection of one concept for further analysis was based on three major factors: performance, weight, and cost. The Phase I ratings for the three concepts are given in Table 3.3, for reference. As discussed in the Summary of Phase I, while considering these ratings, the lower ratings are indicative of relative superiority in a category. This corresponds

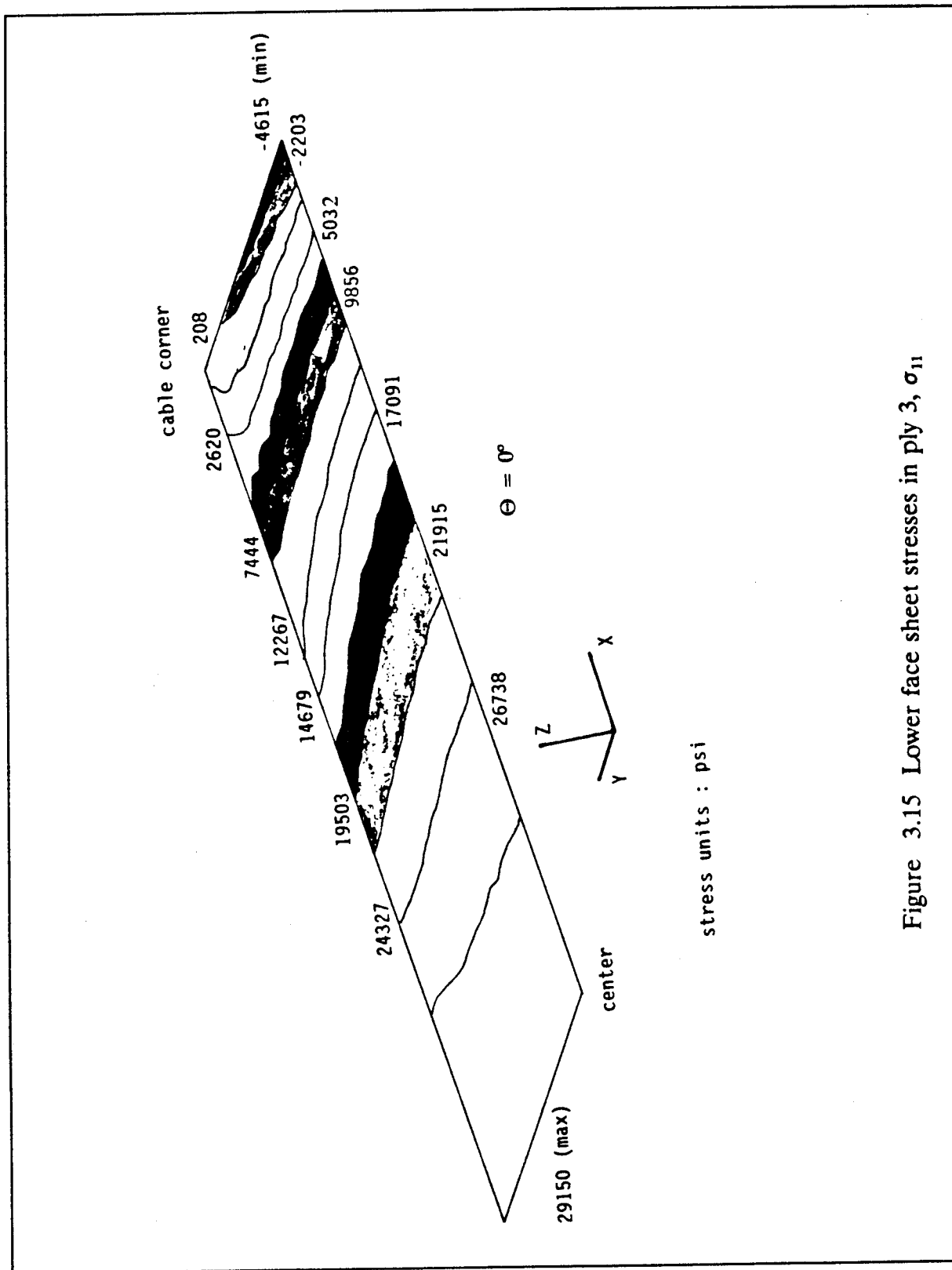


Figure 3.15 Lower face sheet stresses in ply 3, σ_{11}

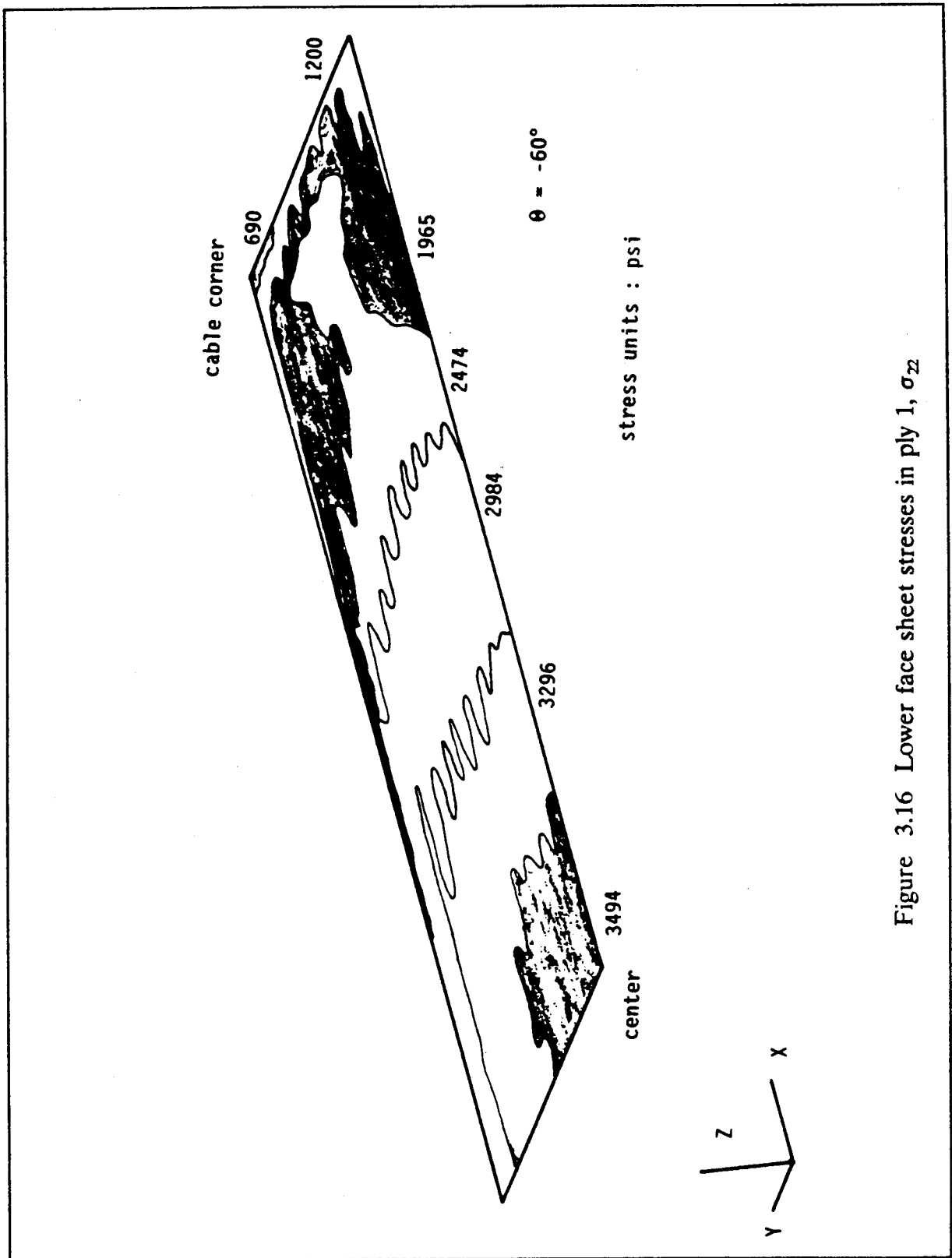


Figure 3.16 Lower face sheet stresses in ply 1, σ_{zz}

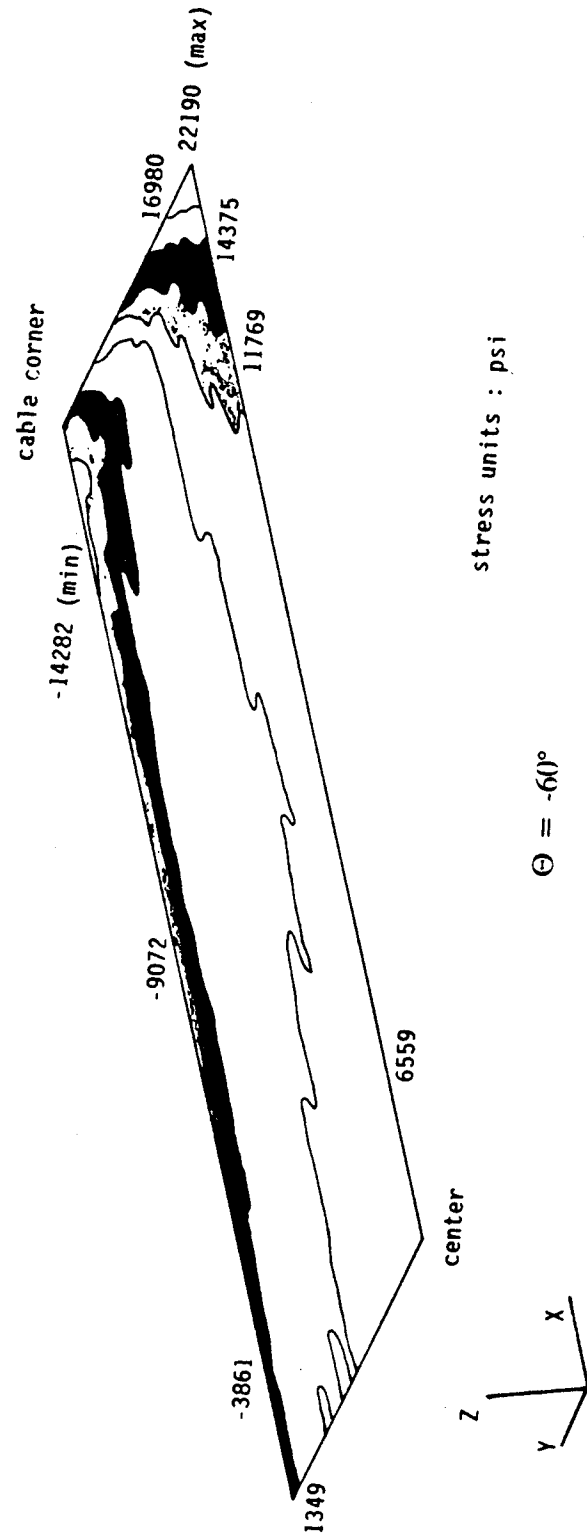


Figure 3.17 Lower face sheet stresses in ply 1, σ_{11}

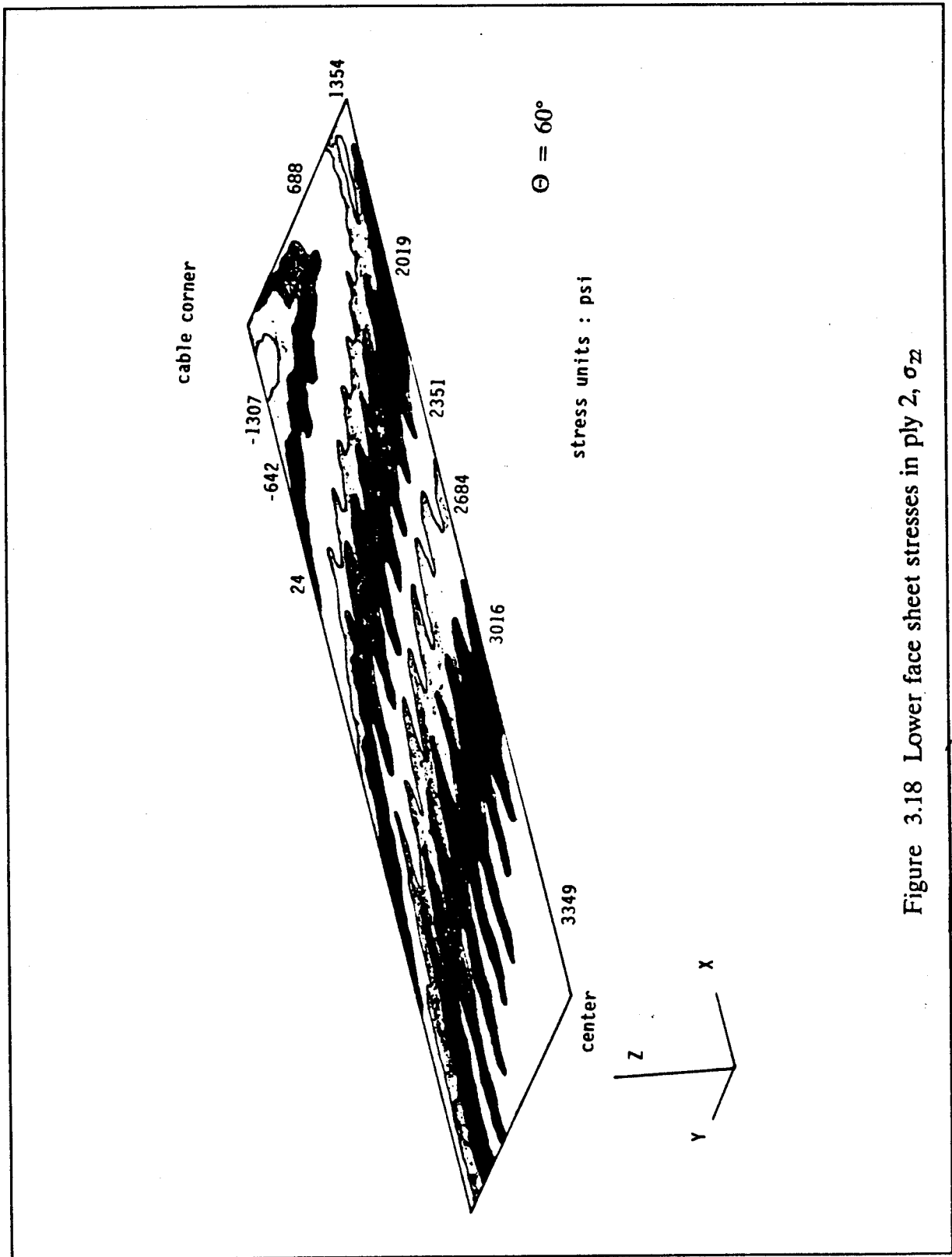


Figure 3.18 Lower face sheet stresses in ply 2, σ_{zz}

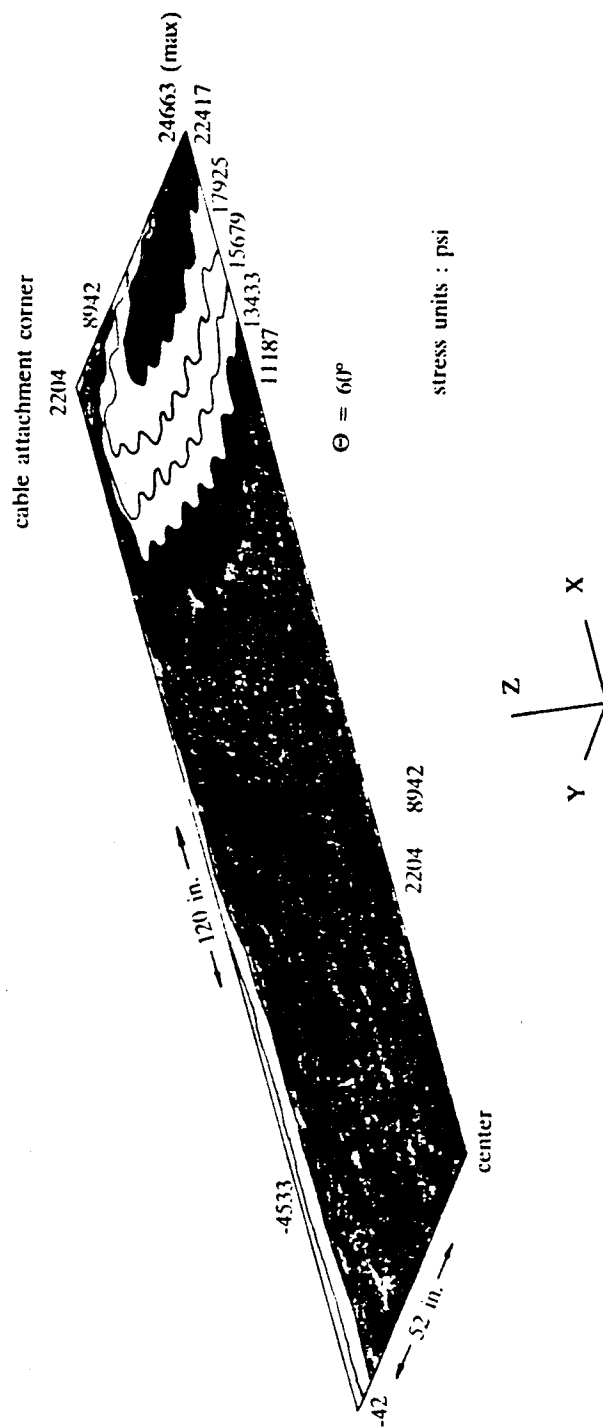


Figure 3.19 Lower face sheet stresses in ply 2, σ_{11}

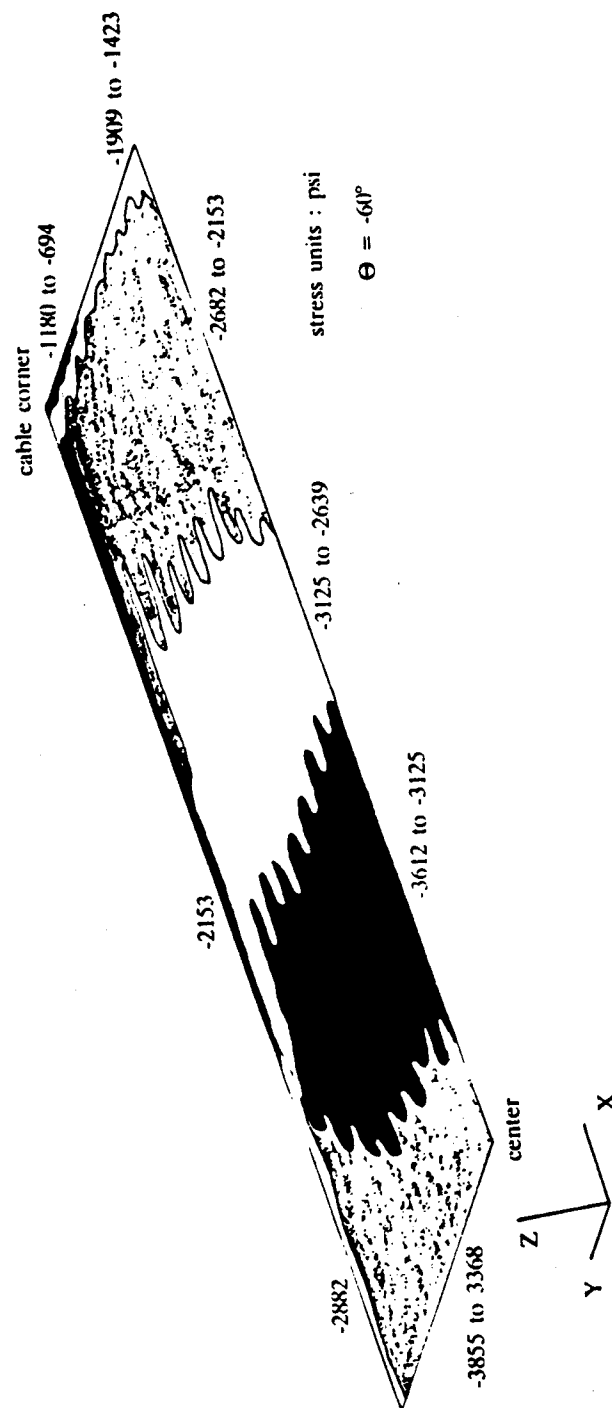


Figure 3.20 Top face sheet stresses in ply 26, σ_{zz}

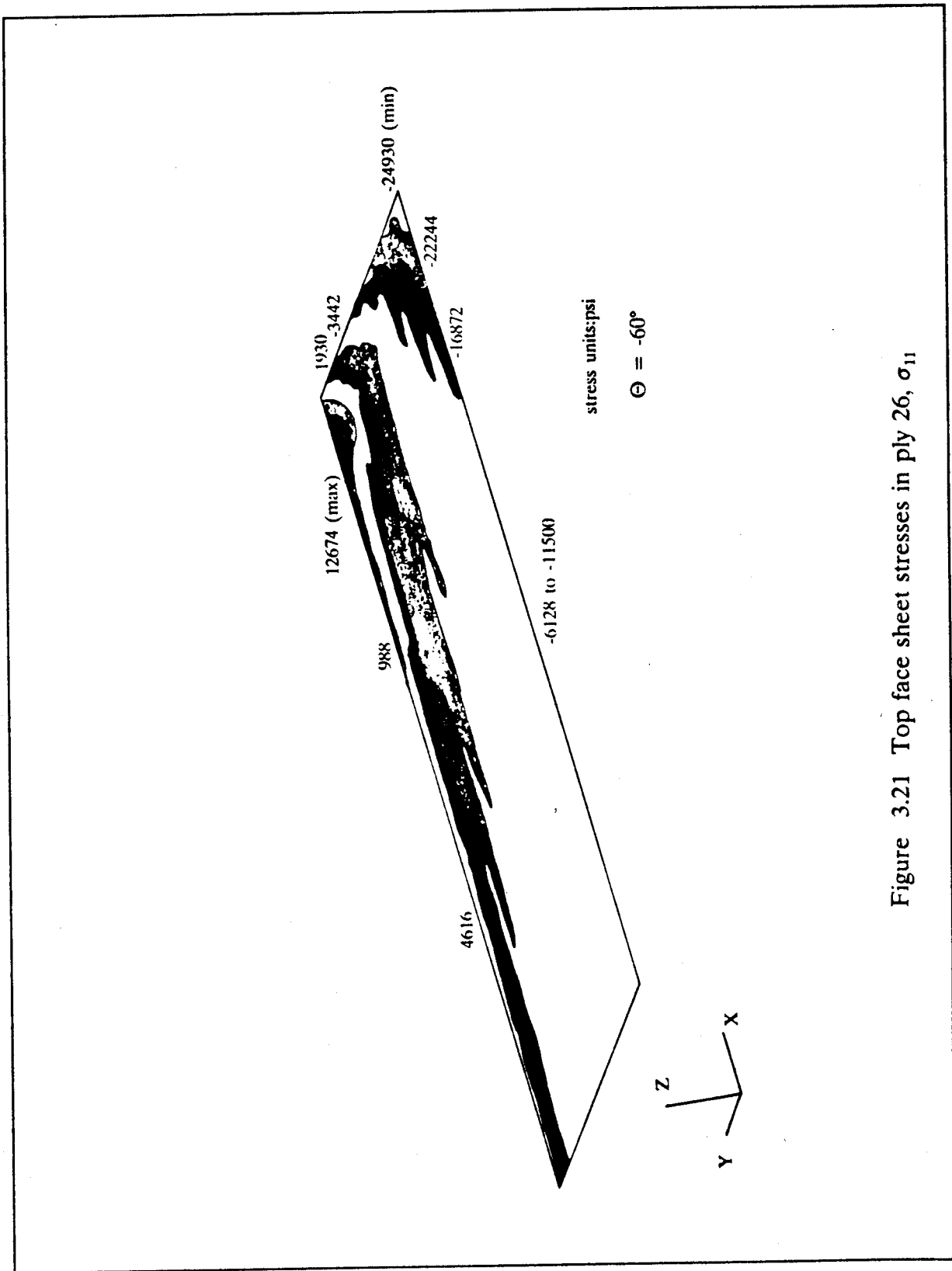


Figure 3.21 Top face sheet stresses in ply 26, σ_{11}

Table 3.2: Analyses Results^a

Face Sheet Construction	Core Construction	SAP86/GENLAM		NASTRAN/PATRAN			
		Minimum Safety Factor	Displacement ^b [in]		Minimum Safety Factor	Displacement ^b [in]	
			midpoint ^c	center ^d		midpoint ^c	center ^d
S-glass/ epoxy	Pultruded E-glass/epoxy I-beams	2.1	2.9	14.2	1.6	3.0	16.2
S-glass/ epoxy	Pultruded graphite/epoxy I-beams	1.3	4.2	14.6	NA ^e	NA ^e	NA ^e
S-glass/ epoxy	Aluminum non-continuous corrugated core	2.0	3.1	15.5	NA ^e	NA ^e	NA ^e

^a Opening load case.

^b Displacements are relative to the corner cable attachment.

^c Midpoint of the short side of the platform.

^d Center of the platform.

^e Not Applicable - this analysis was not done.

Table 3.3: Ratings Comparison^a

Face Sheet Construction	Core Construction	Weight	Cost	Survivability	Performance	1 ^b	2 ^c	3 ^d
S-glass/ epoxy	Pultruded E-glass/epoxy I-beams	1.1	0.6	0.5	1.0	0.8	0.8	0.9
S-glass/ epoxy	Pultruded graphite/epoxy I-beams	0.8	1.1	0.6	1.0	0.9	0.9	0.9
S-glass/ epoxy	Aluminum non-continuous corrugated core	0.8	0.9	0.7	0.7	0.8	0.8	0.9

^a Lower ratings indicate superior values to correspond with cost and weight considerations.

^b Weighted average: cost 2X, others 1X.

^c Common average: all parameters weighted equally.

^d Weighted average: weight 2X, others 1X.

with the fact that low weight and low cost are aims of the project. The survivability and performance factors were generated following a similar trend, with all four factors kept as qualitative measures rather than quantitative values. During Phase II, no further information concerning cost or survivability factors was calculated. Therefore, the concept ratings in these categories were kept constant from Phase I. The weight and performance ratings were reevaluated based on Phase II work.

Weight ratings were reevaluated after some optimization of the concept having the noncontinuous corrugated core. The weight changed from 832 lb to 821 lb. This slight change resulted in no apparent change to the ratings. The weight ratings, therefore, also can be taken from Table 3.3.

The values in Table 3.3 indicate that the concept with the E-glass/epoxy I-beam core is as good as or slightly better than the other two concepts when all factors are weighted evenly. As stated in Chapter 2, equal weighting of the parameters corresponds to a cost to weight tradeoff of between \$5 and \$10 per pound. It is likely that a life-cycle cost analysis would support spending no more than \$2 or \$3 to save a pound of weight. Thus, rating 1, which gives more emphasis to the cost parameter, is more likely to reflect the eventual ranking. In this rating scheme, the concept with the E-glass/epoxy I-beam core scores slightly better than the other two concepts. Nonetheless, the difference in the scores of the three concepts can be considered within the "scatter" of the analysis.

Additional factors became important in the selection of the concept to be analyzed in subsequent tasks. The results from Phase I were compared with those from the more detailed modelling in Phase II for the concept with S-glass/epoxy face sheets and E-glass/epoxy I-beams. The performance was similar for the two models of the concept. The detailed Phase II analysis was not conducted for the other two concepts because it was not believed that the results would alter the performance parameters significantly and because project resources could be more efficiently expended on other tasks.

The detailed Phase II analysis identified concerns about the concept with E-glass/epoxy I-beams. These concerns were evaluated for the other two concepts based on the Phase I results. These included a close look at stresses near the midpoint of the short edge of the platform. Referring to Table 3.1, the concept with the graphite/epoxy I-beam core exhibited a low safety factor for failure at this spot as a result of the thinner face sheets used in this concept. The stiff graphite/epoxy core allowed the use of a thinner face sheet from a bending stiffness standpoint, but failure considerations were found to limit the reduction in thickness and therefore weight and cost. The concept with E-glass/epoxy I-beams could be manufactured with fewer longitudinal stiffeners and a thicker face sheet to achieve an acceptable platform bending stiffness. The thicker face sheet provided both transverse strength and face sheet buckling strength. The tradeoff to thicker face sheets and fewer stiffeners in the other two concepts would have worsened their standing on cost and weight grounds. In reevaluating the performance of the noncontinuous aluminum core concept, the wider spacing of the core sections along the bottom face sheet was considered a weakness when the concept was subjected to loading conditions other than the parachute opening load.

After reevaluation based on the issues identified in Phase II, it appeared likely that performance parameters for the graphite/epoxy I-beam core concept and the noncontinuous aluminum core concept would prove to be inferior rather than superior to their Phase I values. The concept with E-glass/epoxy I-beam stiffeners was therefore chosen for evaluation in following tasks, although all three have considerable merit for the case studied. The three overall ratings for the final three concepts considered are shown in Figure 3.22. This figure illustrates the closeness of the competition. In conclusion, the concept having S-glass/epoxy face sheets and an E-glass/epoxy I-beam core was recommended for further evaluation, under the additional load cases described in Task 3.

overall comparison

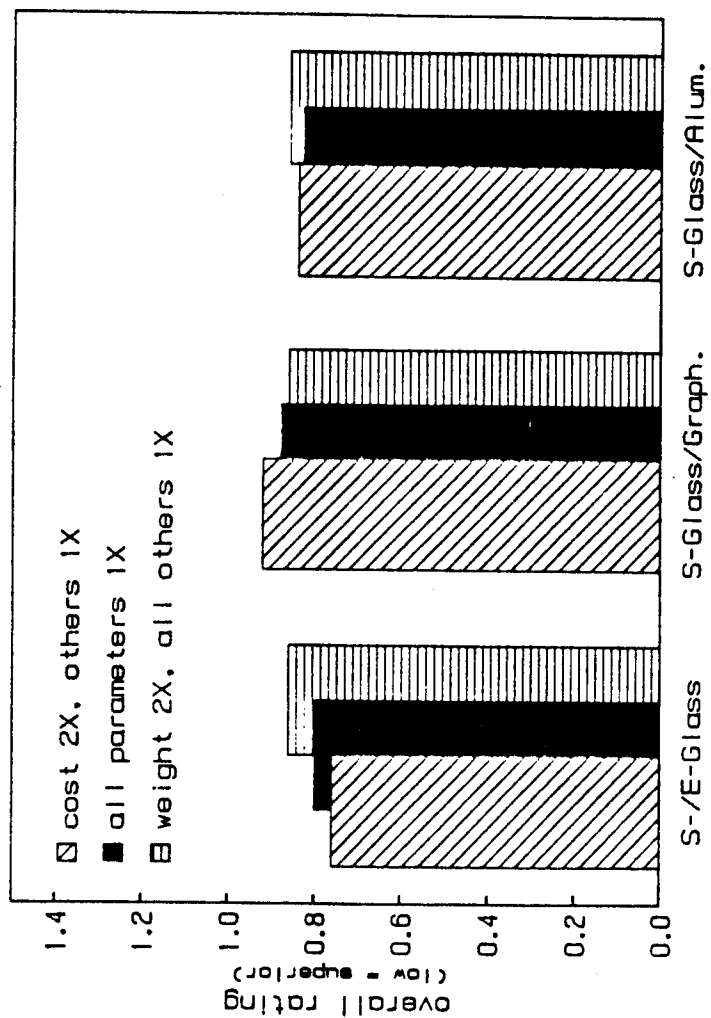


Figure 3.22 Overall concept comparison

4. PHASE II

TASK 3

4.1 Task 3: ANALYSIS OF OTHER IMPORTANT LOAD CASES

In Task 3 of Phase II, important loading conditions other than the parachute opening load were to be analyzed. As described in the Statement of Work, static equivalent cases were to be analyzed, with emphasis on basic platform elements such as face sheets and stiffeners. Detailed design of components and specific design of the overall platform were beyond the scope of Task 3. Analysis was to be directed toward determination of the selected platform concept under different loading conditions, as specified by Natick.

The load cases analyzed were as follows:

1. landing impact,
2. roller load,
3. cresting load, and
4. extraction load.

A description of each loading case, including pertinent assumptions, is given prior to the results generated for that case.

4.2 LANDING IMPACT LOAD CASE

This loading case was included to simulate the compressive loading when the platform, while carrying a payload, impacts the ground. As per Natick test data, during ground impact, intense short duration loading peaks with more than 100 times the acceleration of gravity can be generated. However, these loads are of such short duration that a full state of stress is not experienced by the platform. More realistically, peak loads of approximately 18.5 times the acceleration of gravity can be expected for as long as 75 milliseconds, thus allowing a full stress state to develop. A dynamic multiplication factor of 18.5 was, therefore, used with the payload weight evenly distributed over the surface of the platform. The entire lower surface of the platform was constrained not to displace.

In the analysis of this case, the full finite element analysis (using NASTRAN and PATRAN) was not necessary, as a relatively brief hand calculation indicated the stresses generated were quite low. The simplified analysis indicated a compressive load in the webs of 800 psi. Since the compressive strength of the webs is 20 ksi, the factor of safety is 25. A minimum first ply failure factor of safety of 4.73 was calculated for the top face sheet. Thus, a substantial margin of safety exists for this case. No other landing configurations were studied, although other possible impact cases (i.e. uneven impact; impact onto a rock, etc.) could cause more damaging load cases.

4.3 ROLLER LOAD CASE

The roller load case simulated the load experienced by the platform while stationary on an aircraft ejection roller system. A payload weight of 23300 lb was evenly distributed as a pressure load over the upper face sheet. The roller pad surface area on the lower face sheet was constrained to have zero deflection. Platform mass was assumed to be negligible. Actual roller pad surface areas are 11" wide longitudinal strips running the entire 20 ft length of the platform. The roller pad strips are located from 10.75" to 21.75" and 36.75" to 47.75" from the longitudinal centerline. The roller pad strip location as set up in the model was changed slightly because of the location of the model nodes. Figure 4.1 illustrates the actual location of the rollers as given above, and the modified set of nodes used. This slight modification provided a realistic roller pad setup, while allowing the same detailed model as previously generated to be used without time consuming modification. Symmetry considerations allowed the continued use of one quarter model, resting on two roller pad strips.

In examination of the analysis results for this case, the first platform element to be critically stressed was the center I-beam web element adjacent to the aluminum end closeout. This is shown in Figure 4.2, a plot of the I-beam web shear stresses. As the allowable shear stress in the webs is approximately 6 ksi, the minimum factor of safety in this case is therefore about 8.6. In the face sheets, the critical first ply was found to be ply 24 ($\bar{\sigma} = 0^\circ$) in the top face sheet, with the highest stresses near the platform center. At this point, the first ply failure factor of safety was calculated to be 22.7. In the aluminum side rails and end closeout, the lowest factor of safety was found to be 21.5, in the end closeout near the center.

Displacement results for this case are shown in Figure 4.3. (Note that the scale for this plot is not the same as the displacement plot scales in other previous figures showing displacement.) The peak displacement in this case was 0.15", seen near the center of the platform. Near the end closeout, displacement was negligible, about 0.0035", near the midpoint between the cable attachment corners.

4.4 CRESTING LOAD CASE

The cresting load case simulates the loading on the platform when it is halfway out of the aircraft. At this point, the platform can be considered as balanced on a fulcrum. A payload weight of 23,300 lb was uniformly distributed over the upper face sheet surface. Vertical displacement was allowed everywhere except directly over the one roller at each of the roller pad strips, as the platform was assumed to be balanced on a single roller at each strip. The one quarter model, with the same roller pad configuration and symmetry considerations as in the roller load case, was used. Platform support was modelled only along one edge, using 13 nodes on the yz plane.

For this case, the controlling stress was found to be the shear stress in the I-beam webs near the two roller contact areas. The web shear stresses are shown in Figure 4.4. A factor of safety of 1.64 was calculated for the webs in the localized areas near the two roller contact points. The highly localized nature of the critical stress for this case

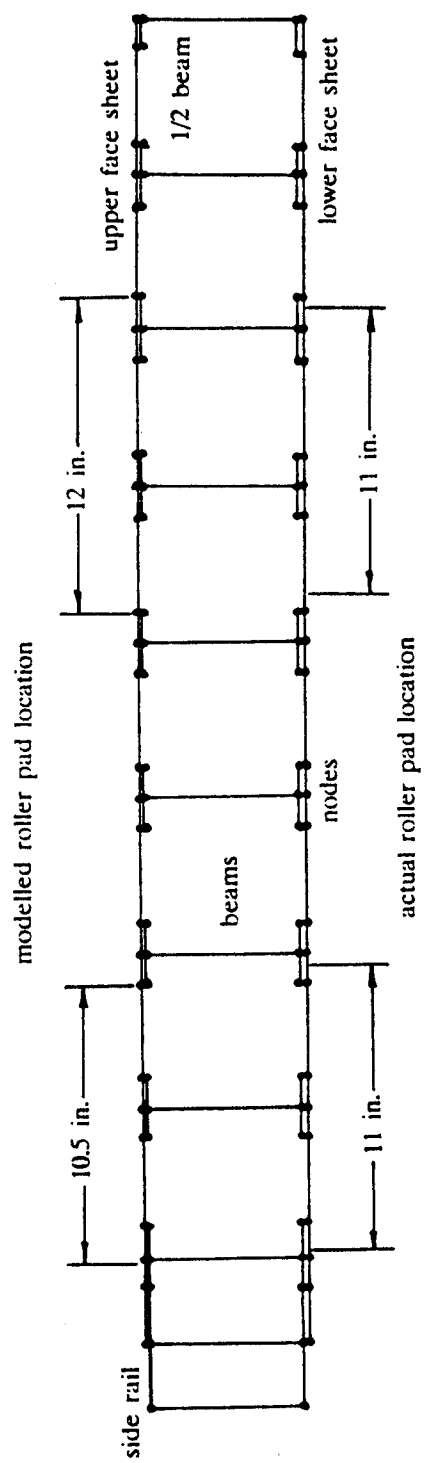


Figure 4.1 Roller load case model configuration

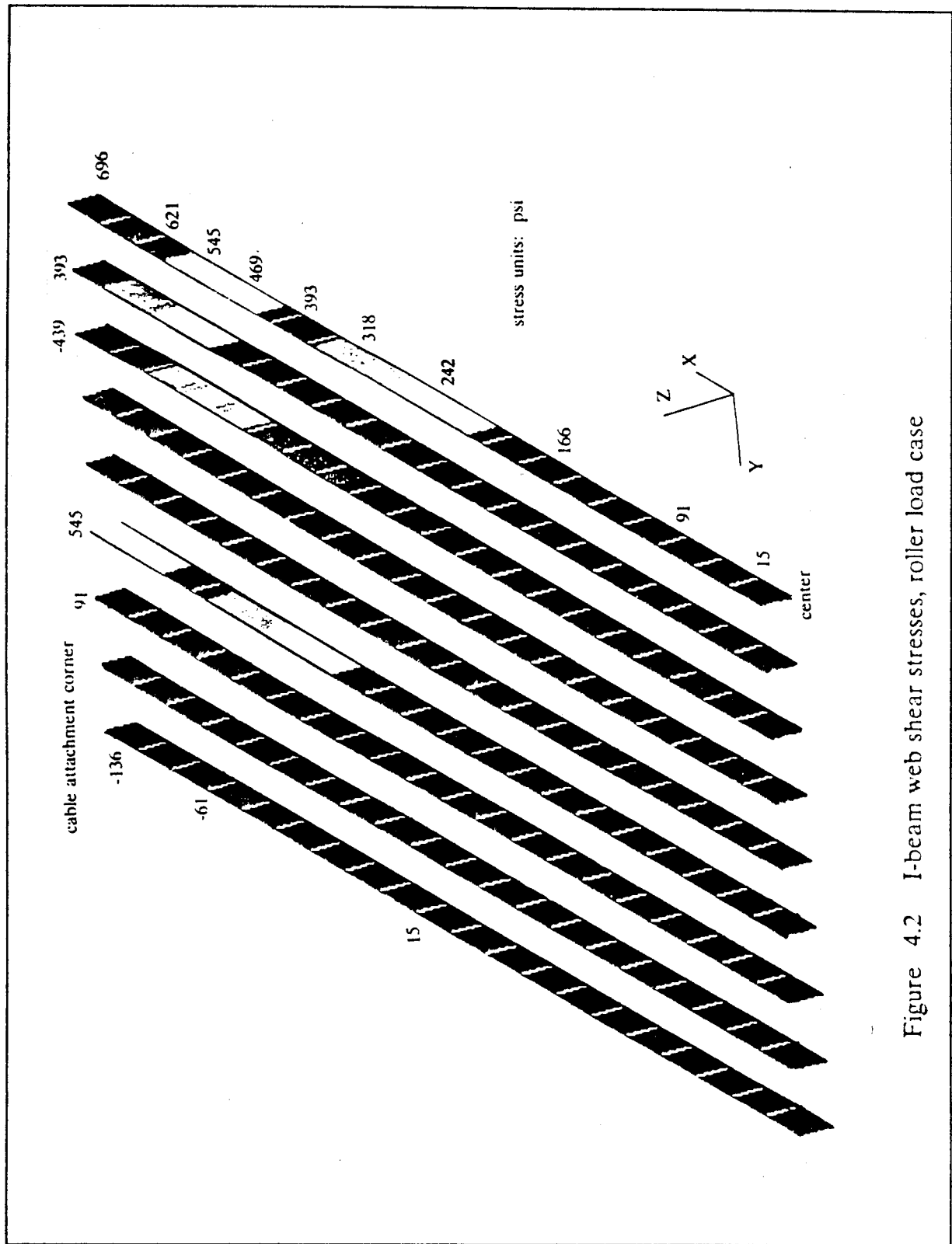


Figure 4.2 I-beam web shear stresses, roller load case

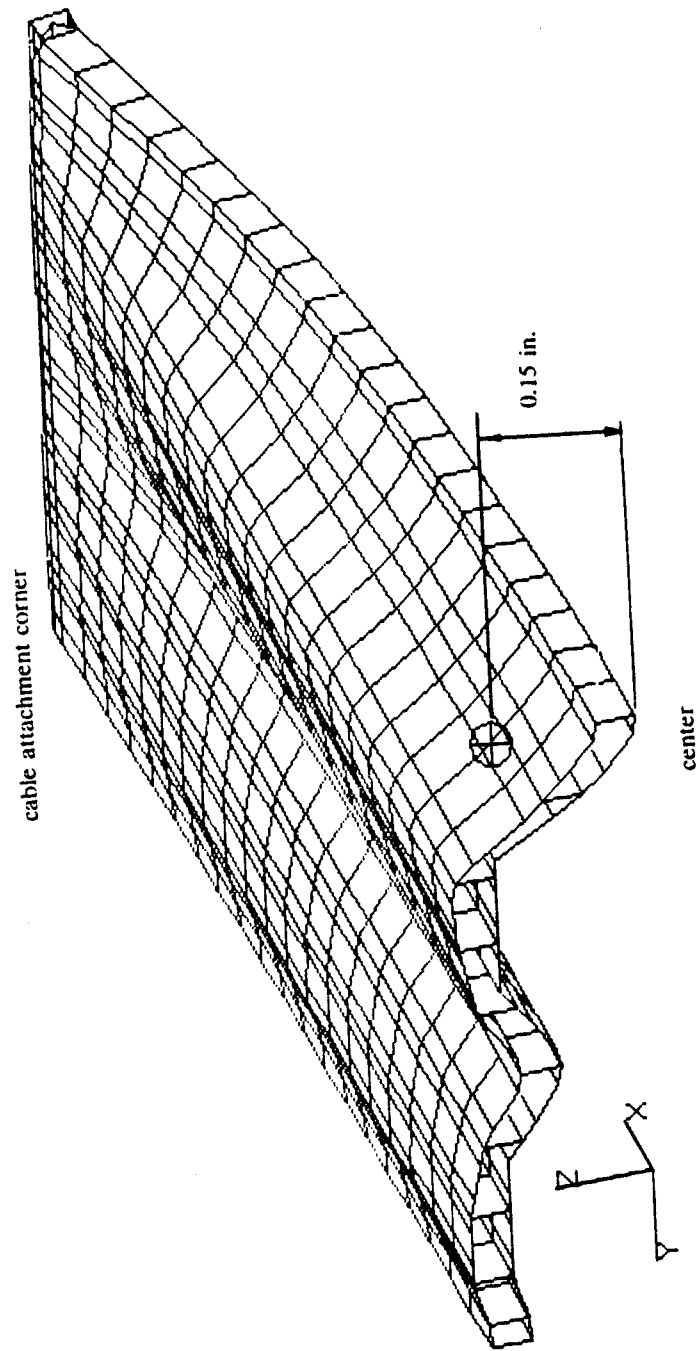


Figure 4.3 Deflection results, roller load case

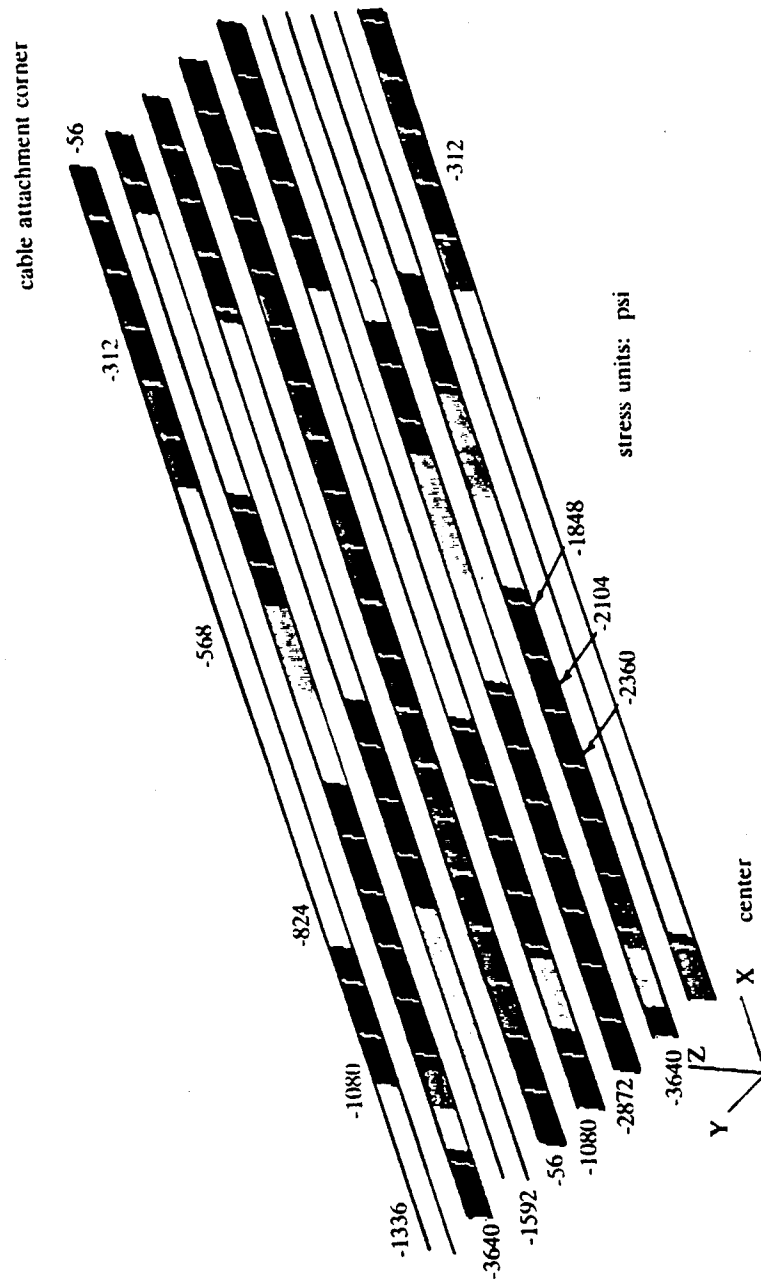


Figure 4.4 I-beam web shear stresses, cresting load case

is intensified by the modelling constraints of no deflection and contact with only one roller bar at each of the roller pads. These constraints are quite conservative, as more realistically the rollers would deflect slightly and more than a single roller at each strip would probably be in contact at all times.

In the face sheets, the minimum first ply failure factor of safety was found to be 3.26, in the top face sheet and, again, near the roller contact points. The localized nature of the high stresses is also seen in the face sheets, as shown in Figures 4.5 and 4.6. Figure 4.5 shows the strains in the x-axis direction for the top face sheet. Figure 4.6 shows the x-axis strains for the lower face sheet.

In the aluminum side rails and end closeout the highest stress state was found to occur at the longitudinal center of the side rail. A factor of safety of 3.75 was calculated for the most highly stressed area. Again, the area of high stress was quite small, as shown in Figure 4.7.

Deflection results for this load case are shown in Figure 4.8. Maximum deflections were along the leading exit edge of the platform. Values ranged from 4.4" at the center to 4.25" at the outside (cable) corner.

4.5 EXTRACTION LOAD CASE

The extraction load case simulates the loading experienced by a platform, with payload, during extraction from the aircraft. Extraction is performed by a drag parachute attached to an extraction bracket, located at the center end of the platform. For the currently used extraction bracket, a static test of 86000 lb is used to verify a 56000 lb dynamic rating.

A simplified and conservative load case was devised to study the stress concentration in the localized area of the platform where the extraction load will be applied. The one quarter model was retained with symmetric boundary conditions, so that reactive loads resulted. This is shown in Figure 4.9. The 86000 lb load was modelled as a pressure over an area covering the webs of three of the 17 I-beams. The entire flanges of the outer I-beams were not covered, causing considerable load to be transmitted by shear of the outer flanges of the outer beams. In Figure 4.10, showing an end view of the local loading, it can be seen that only three plates on the model were loaded with a pressure of 2171 psi.

This loading is equivalent to a 1 ft plate for the total model. The weight of the 0.75" thick, 1 ft wide, 3.3" high aluminum plate is 3.0 lb. This is well within the 10% weight contingency given in the concept weight calculation.

The results of this analysis case for the face sheets are shown in Figures 4.11 through 4.14. (Note: the roller load case results are superimposed on the extraction load case in these results.) The x-axis strains are shown for the entire upper face sheet in Figure 4.11 with an expanded view of the critical area near the extraction load application bracket shown in Figure 4.12. Figures 4.13 and 4.14 are similar, showing the y-axis strains overall and in the critical area. The critical area

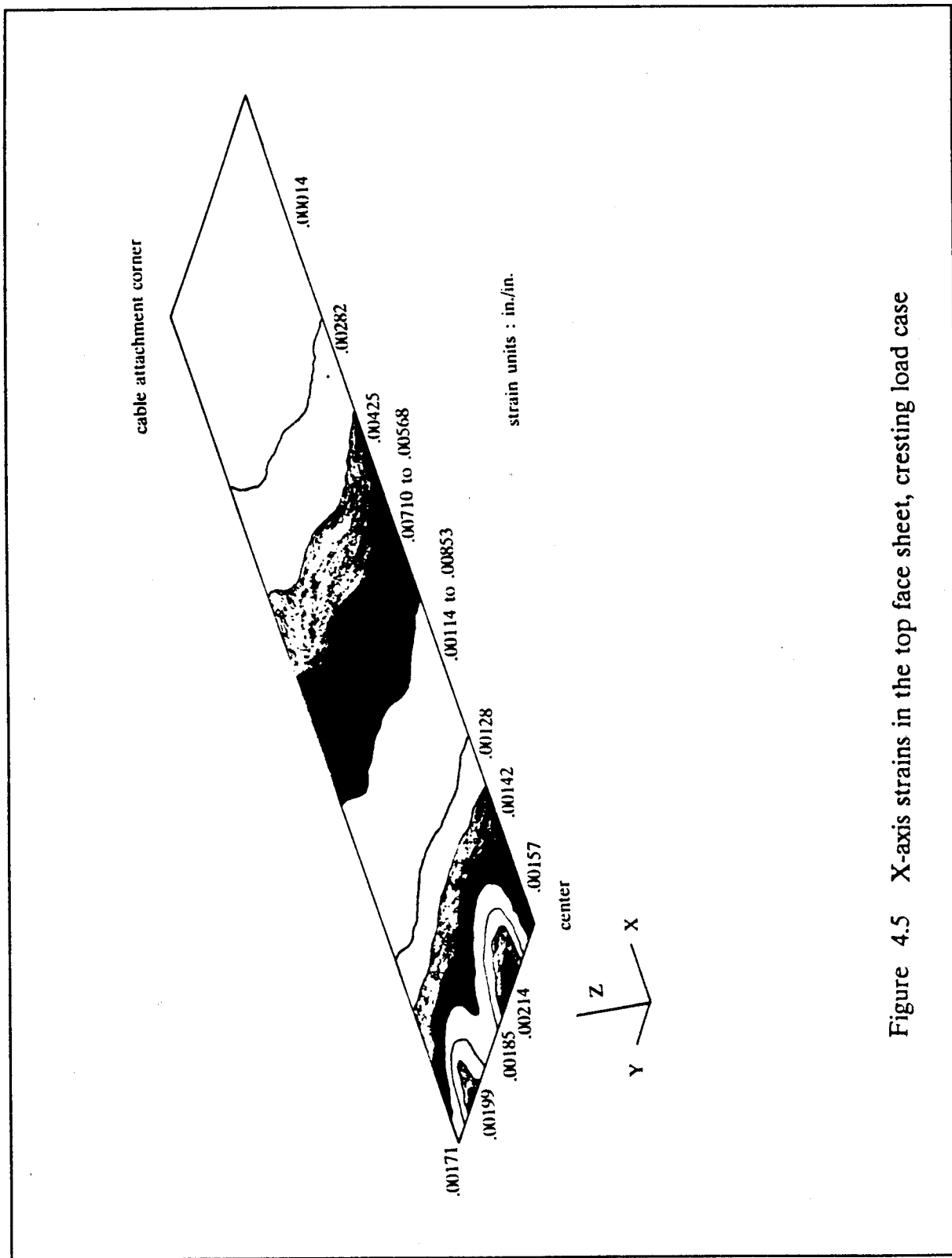


Figure 4.5 X-axis strains in the top face sheet, cresting load case

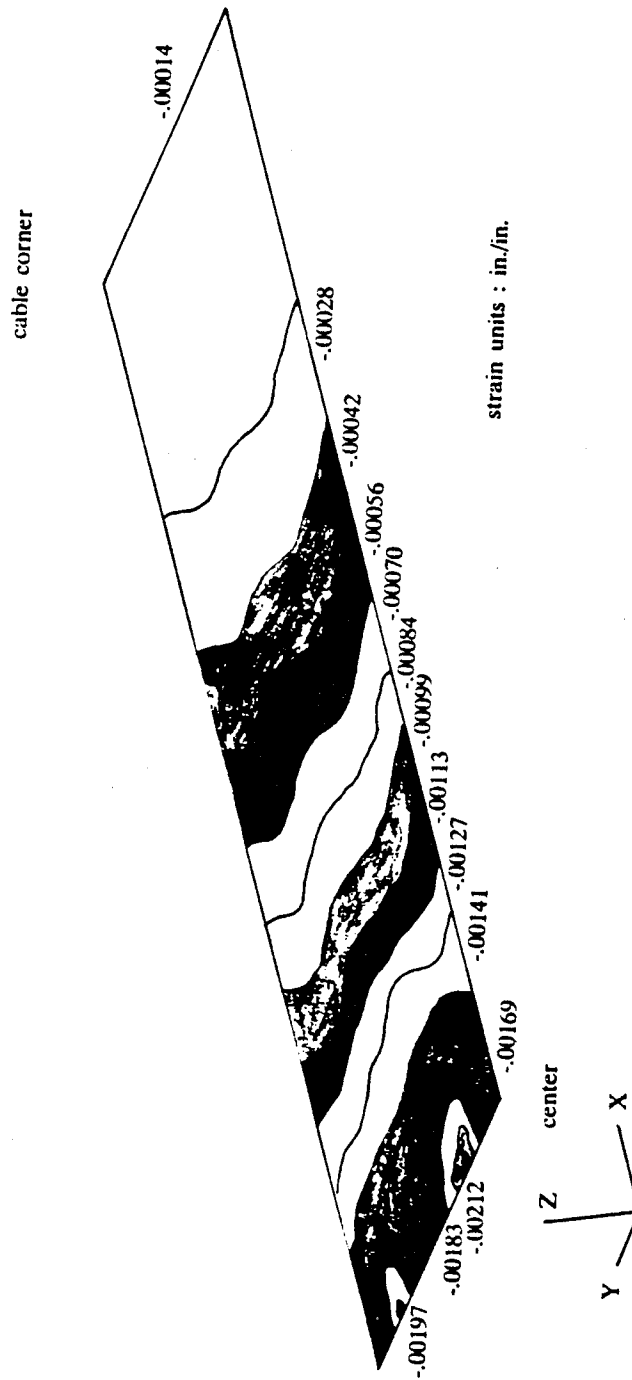


Figure 4.6 X-axis strains in the lower face sheet, cresting load case

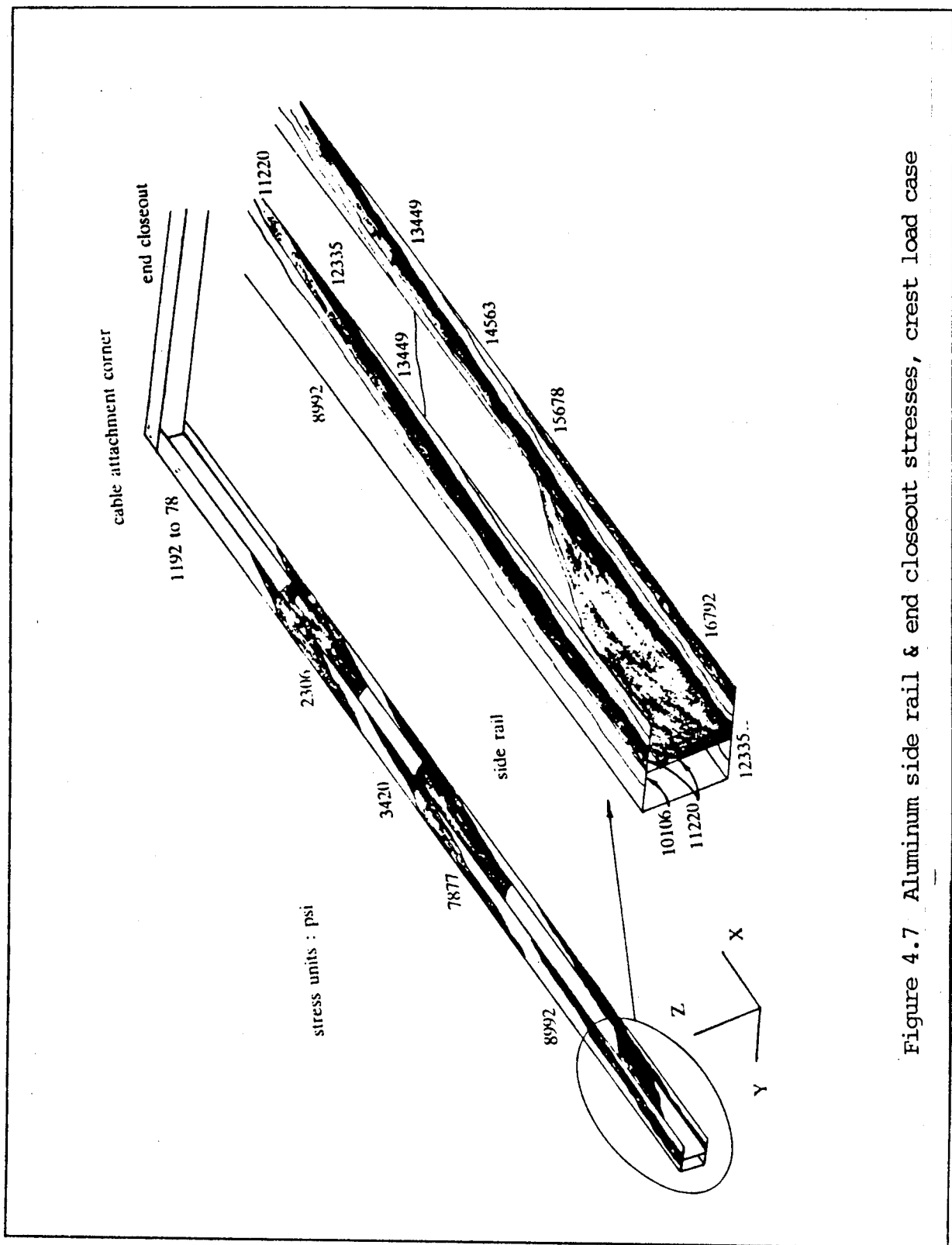


Figure 4.7 Aluminum side rail & end closeout stresses, crest load case

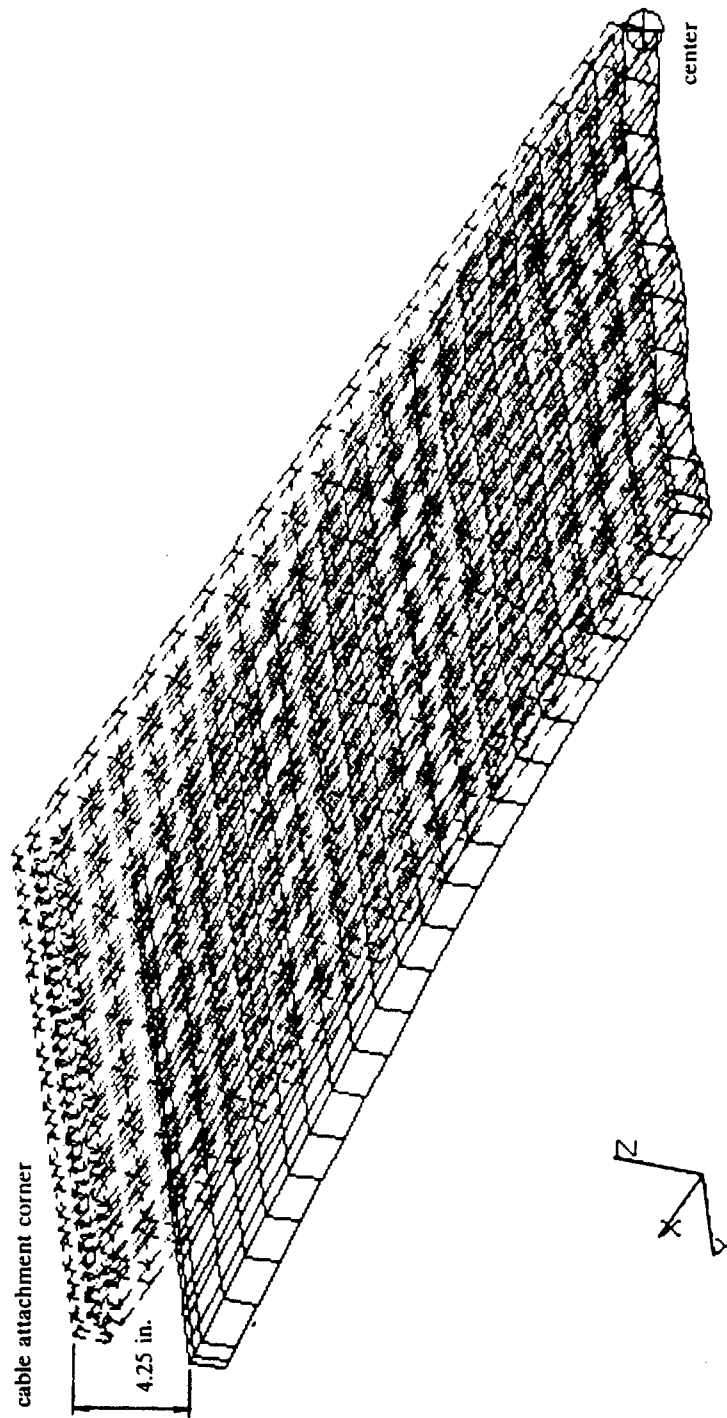


Figure 4.8 Deflection results, cresting load case

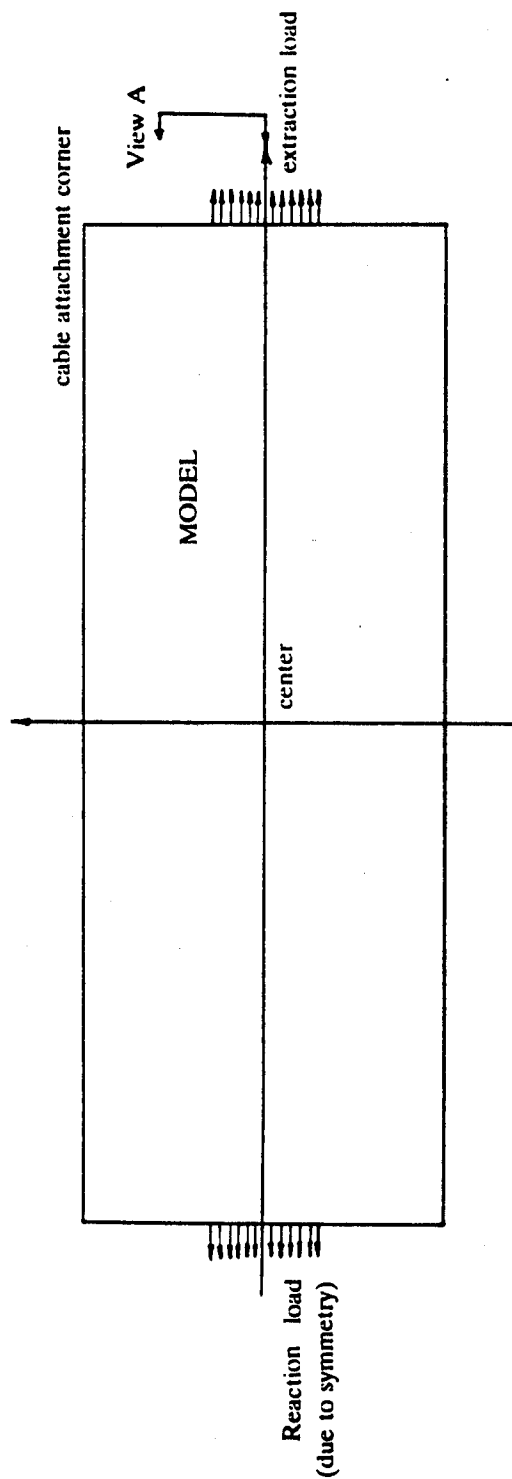


Figure 4.9 Extraction load case model

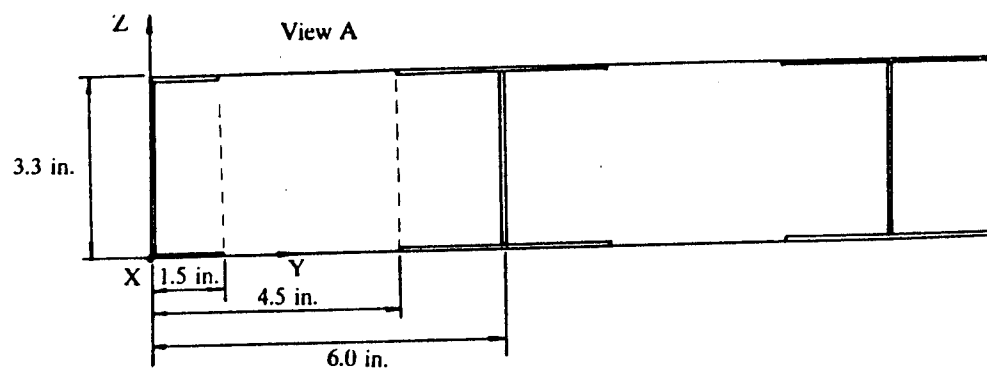


Figure 4.10 End view of the extraction load case model

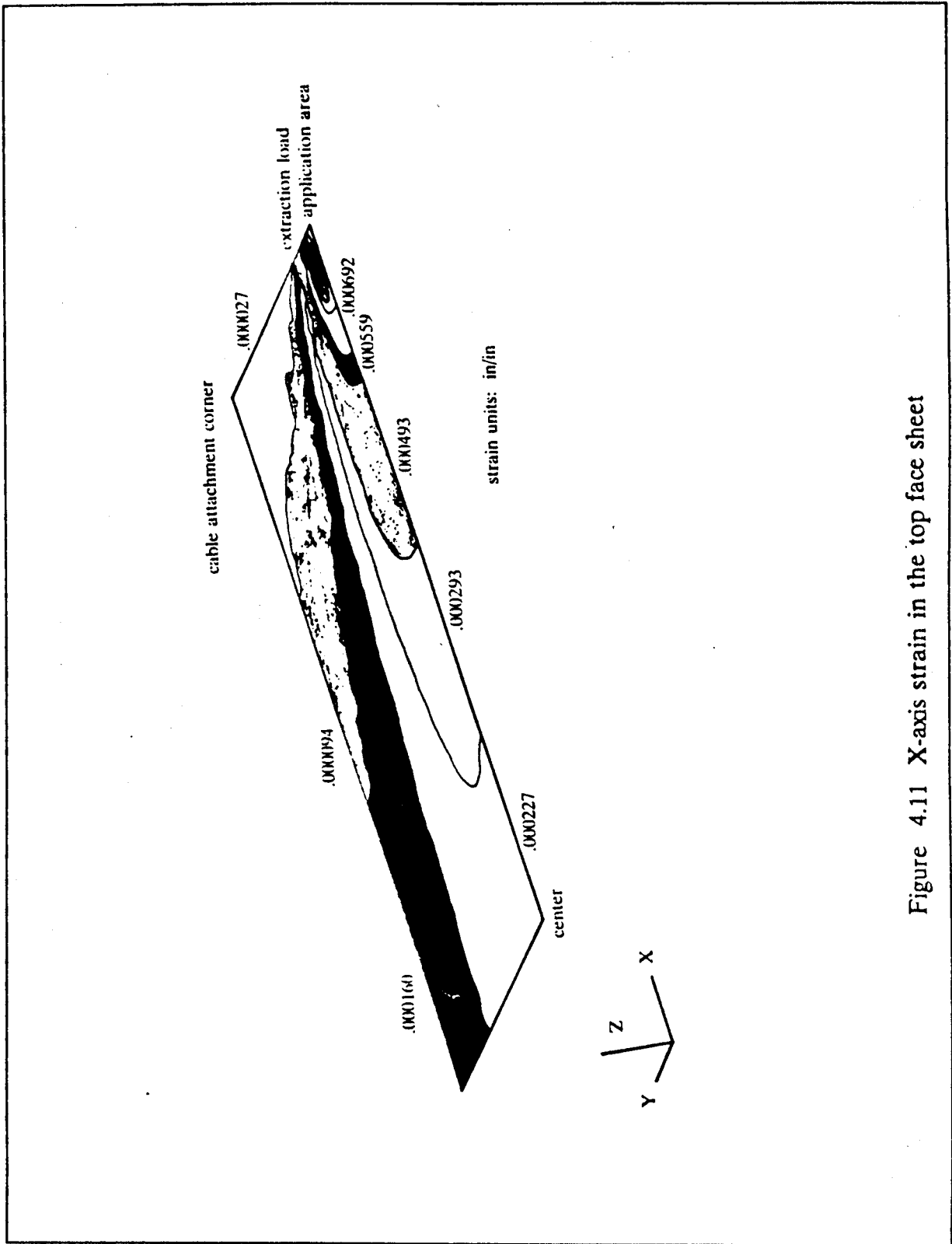


Figure 4.11 X-axis strain in the top face sheet

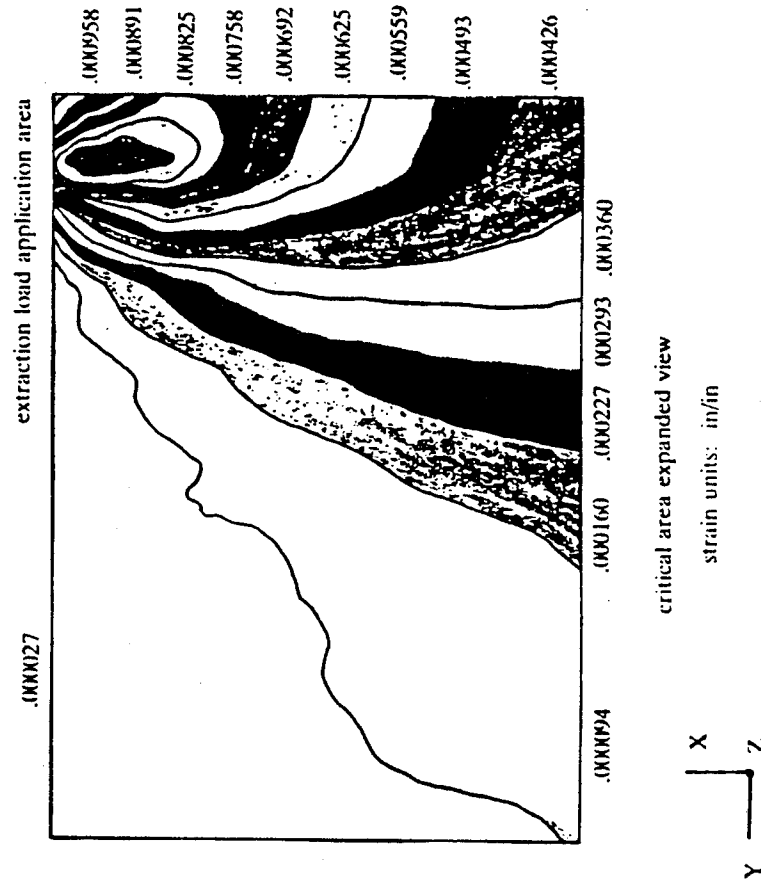


Figure 4.12 Critical area, X-axis strain in the top face sheet

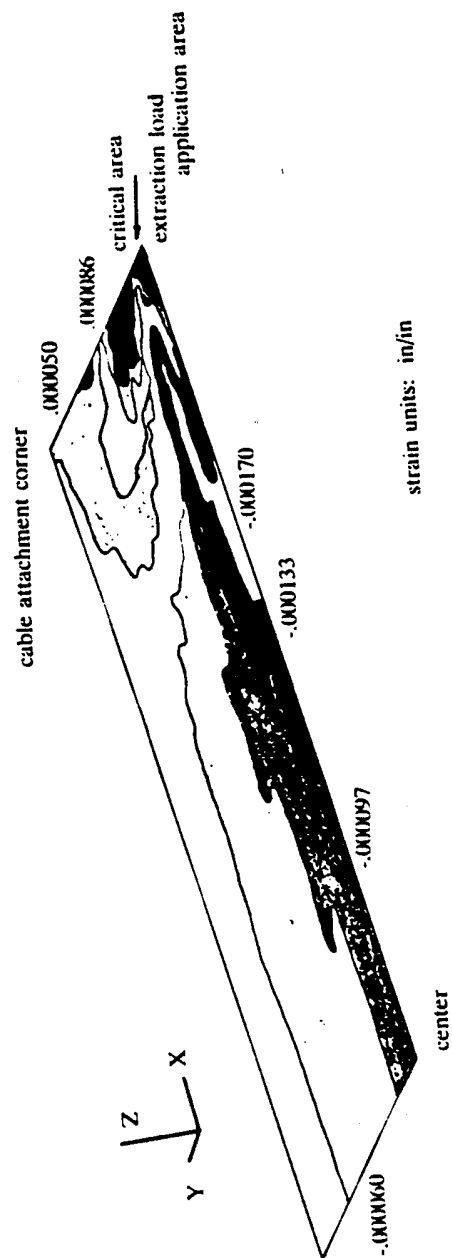


Figure 4.13 Y-axis strain in the top face sheet

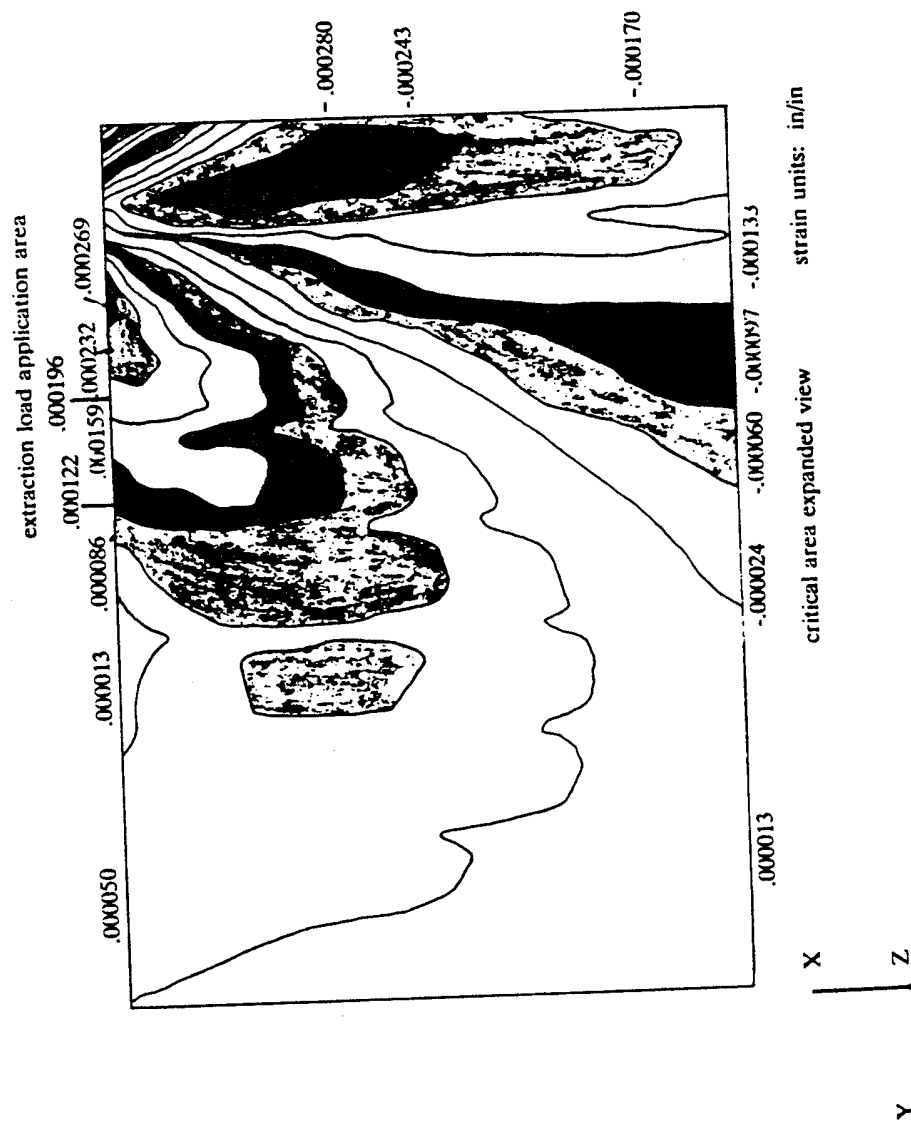


Figure 4.14 Critical area, Y-axis strain in the top face sheet

was near the extraction load application, as shown in the figures. Specifically, the critical area of the face sheets is near the load application area at the interface between the 0.75" bracket and 0.125" closeout. The minimum factor of safety in the face sheets, based on a first ply failure criteria, was found to be 5.39, thus allowing a 3.59 load amplification while retaining a 1.5 factor of safety. The critical ply was ply 2 of the lower face sheet, a +60° ply.

In the roller load case, the I-beams were the critical factor as a result of the web shear stresses. In Figure 4.15, the I-beam web shear stresses for the extraction load case (again, the extraction load case includes the roller load) are shown. The shear stress in the critical beam element increased from 696 psi (for the roller load case) to 707 psi. The extraction load primarily causes an increase in tension in the webs, resulting in this slight increase in the shear stress. Using an ultimate strength for shear in the webs of 6 ksi gives a factor of safety of 8.5. The Von Mises stresses in the webs are shown in Figure 4.16. These stress values were low, peaking at 2.2 ksi.

Shear stresses in the flanges are shown in Figure 4.17. These values are quite low, bounded by +300 psi and -1300 psi. The Von Mises stresses in the flanges, shown in Figure 4.18, were of similar magnitude as those in the webs. Peak stress values were approximately 2.8 ksi, with an ultimate strength of 30 ksi. Thus, the beam flanges were not considered to be a critical component in this load case.

For this load case, the most critical component of the platform concept was the aluminum end closeout. In the roller load case, the central vertical area in the closeout was heavily loaded in shear. With the addition of the 0.75" thick aluminum extraction bracket, this problem disappeared, as the bracket carried most of the load. However, the interface between the 0.125" aluminum closeout and the 0.75" aluminum bracket was a problem area. Figures 4.19 and 4.20 show the Von Mises stresses in the aluminum end closeout, overall and an expanded view of the critical area, respectively. The aluminum in the critical area carried more of the load than the face sheets because of the difference in material moduli. The greatest stress in the aluminum (10.08 ksi), compared to the ultimate strength of 37 ksi, gives a factor of safety of 3.67. With retention of a 1.5 factor of safety, this corresponds to a load amplification factor of 2.45. Thus, the aluminum closeout, at the extraction bracket/closeout interface, is the critically loaded platform component for this load case.

Displacement of this case is nearly identical to the roller load case except for the local deformation around the attachment area in the x direction. The x displacement in this area ranges from 0.040" to 0.054", not an extreme amount. These results are shown in Figure 4.21 and Figure 4.22.

In conclusion, the critically loaded platform component for this load case, based on the simplified conservative analysis performed, is the end closeout, at the interface between the load bracket and the closeout itself. Detailed design of brackets, closeouts, etc. is beyond the scope of this program. However, a higher factor of safety could be achieved by selective reinforcement of critical aluminum plates around the load bracket.

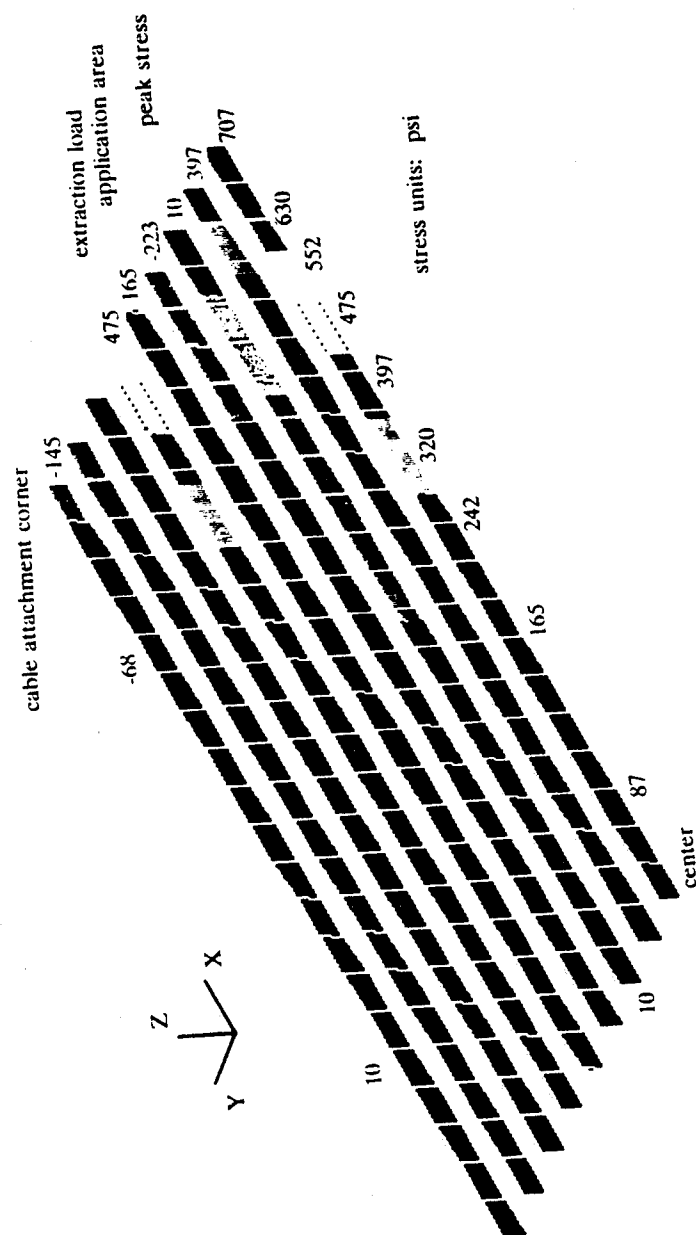


Figure 4.15 I-beam web shear stresses

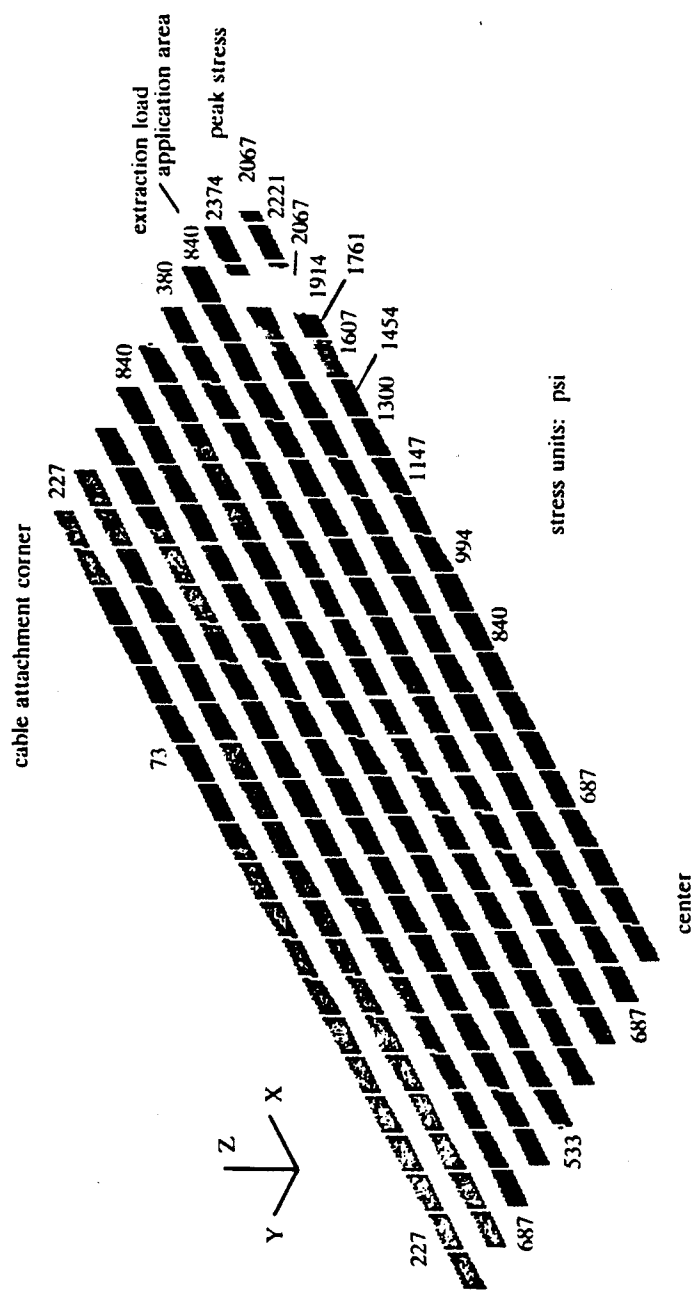


Figure 4.16 I-beam web Von Mises stresses

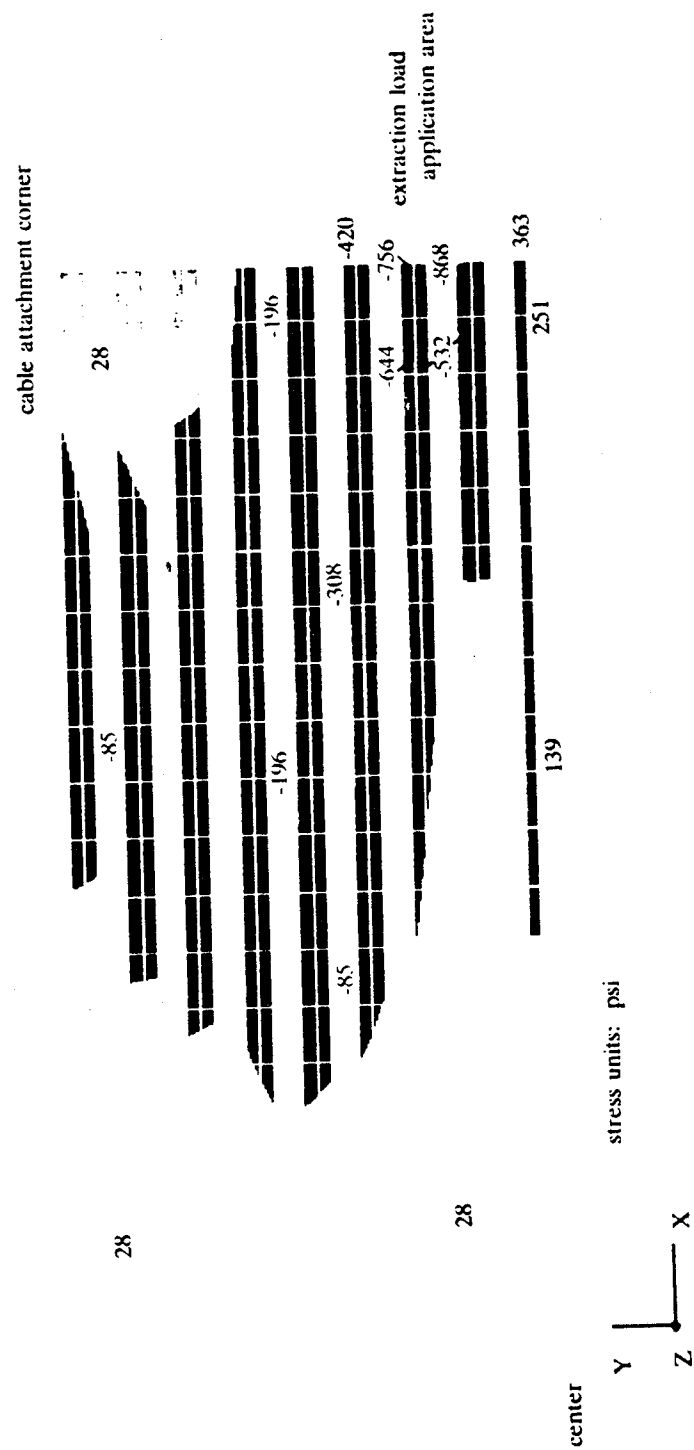


Figure 4.17 I-beam flange shear stresses

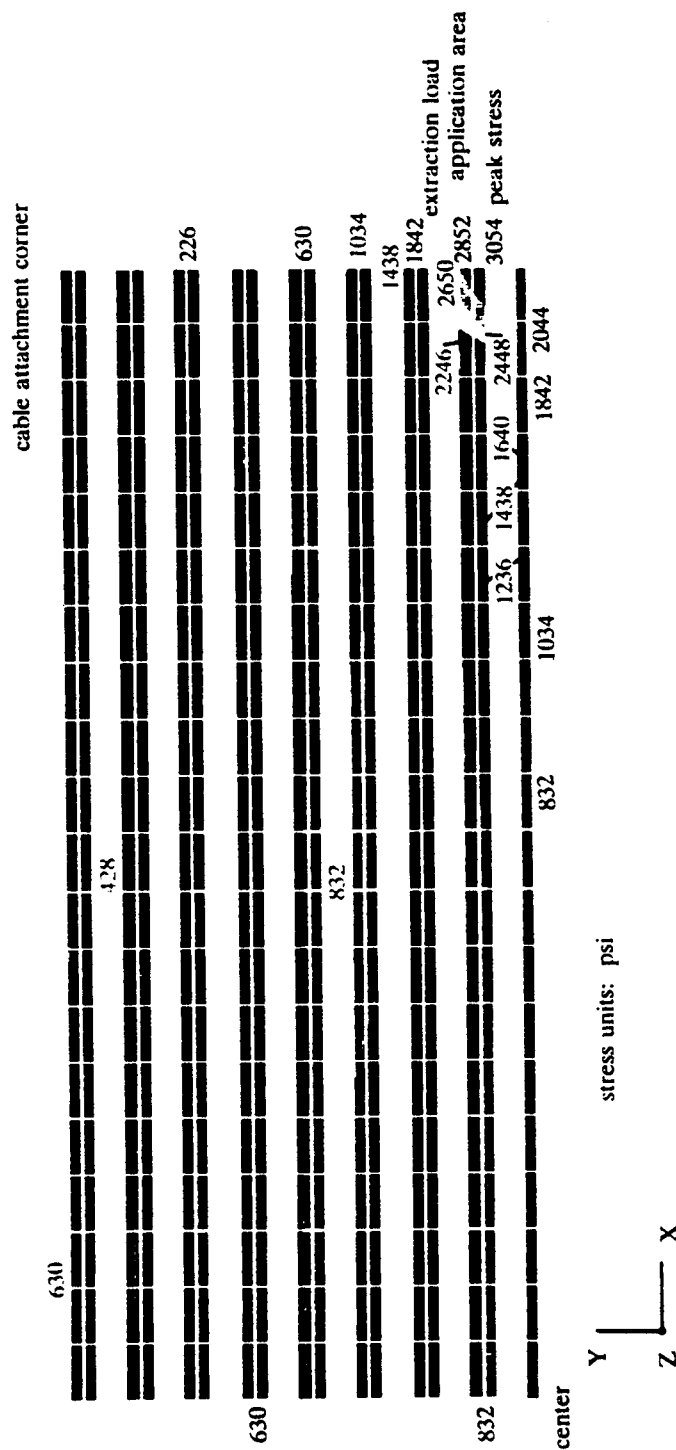


Figure 4.18 I-beam flange Von Mises stresses

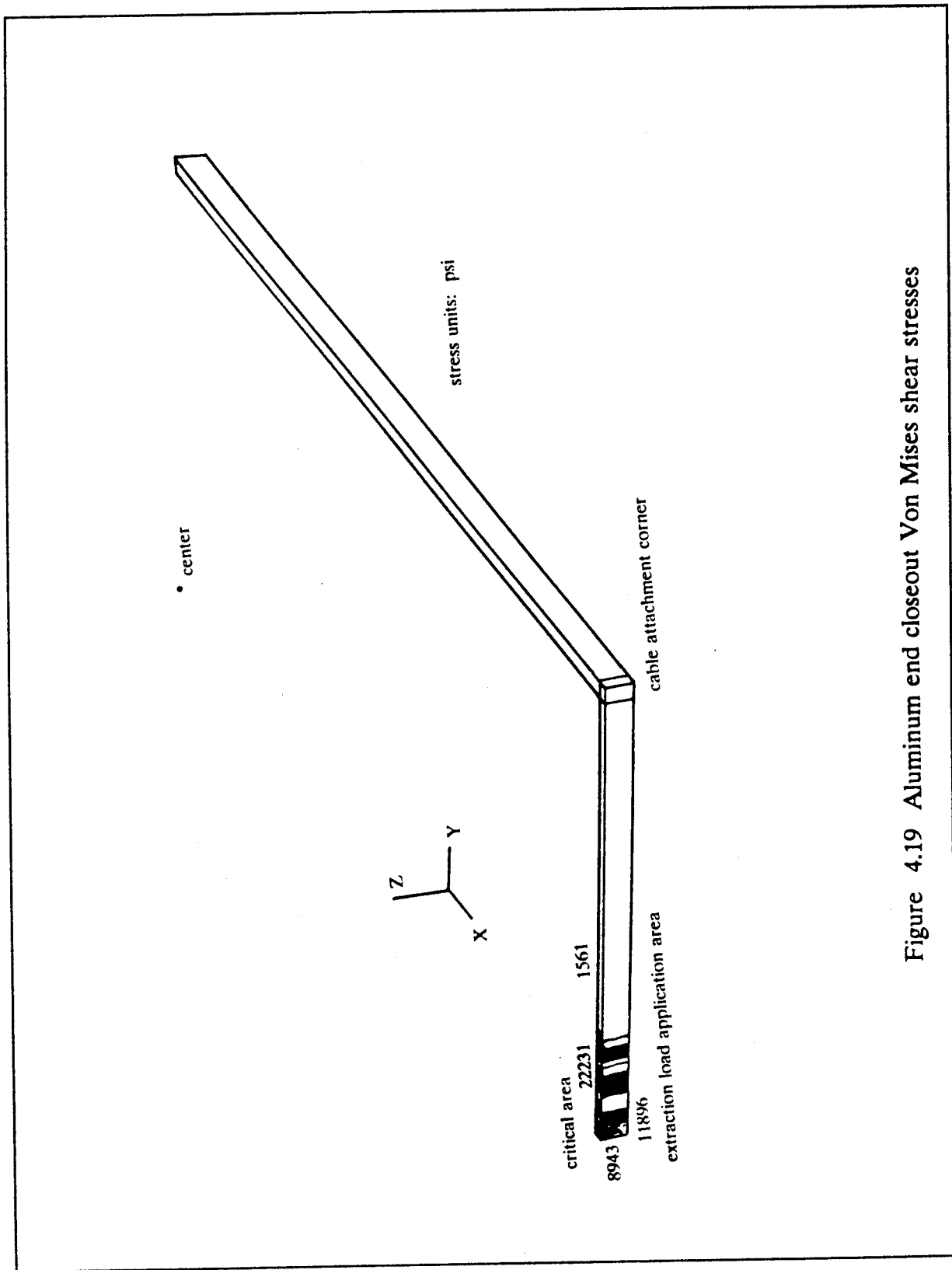


Figure 4.19 Aluminum end closeout Von Mises shear stresses

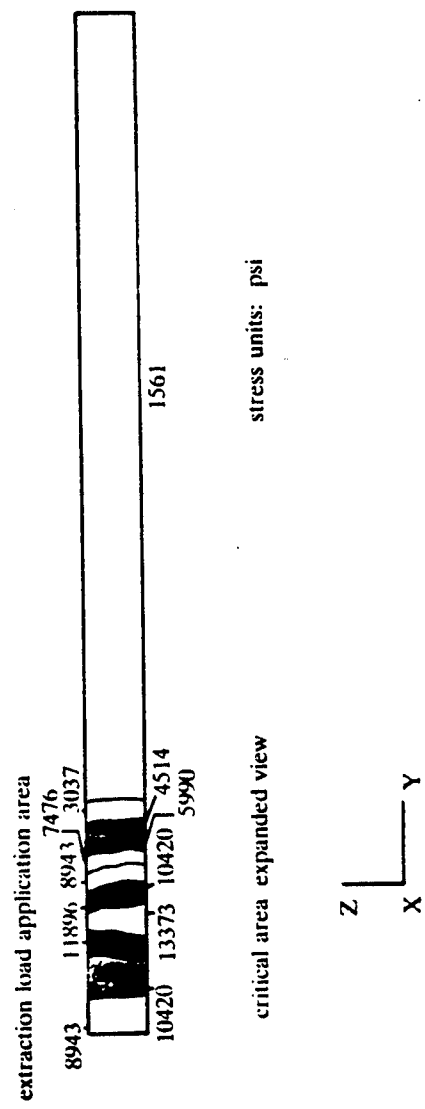


Figure 4.20 Critical area, Von Mises stresses aluminum end closeout

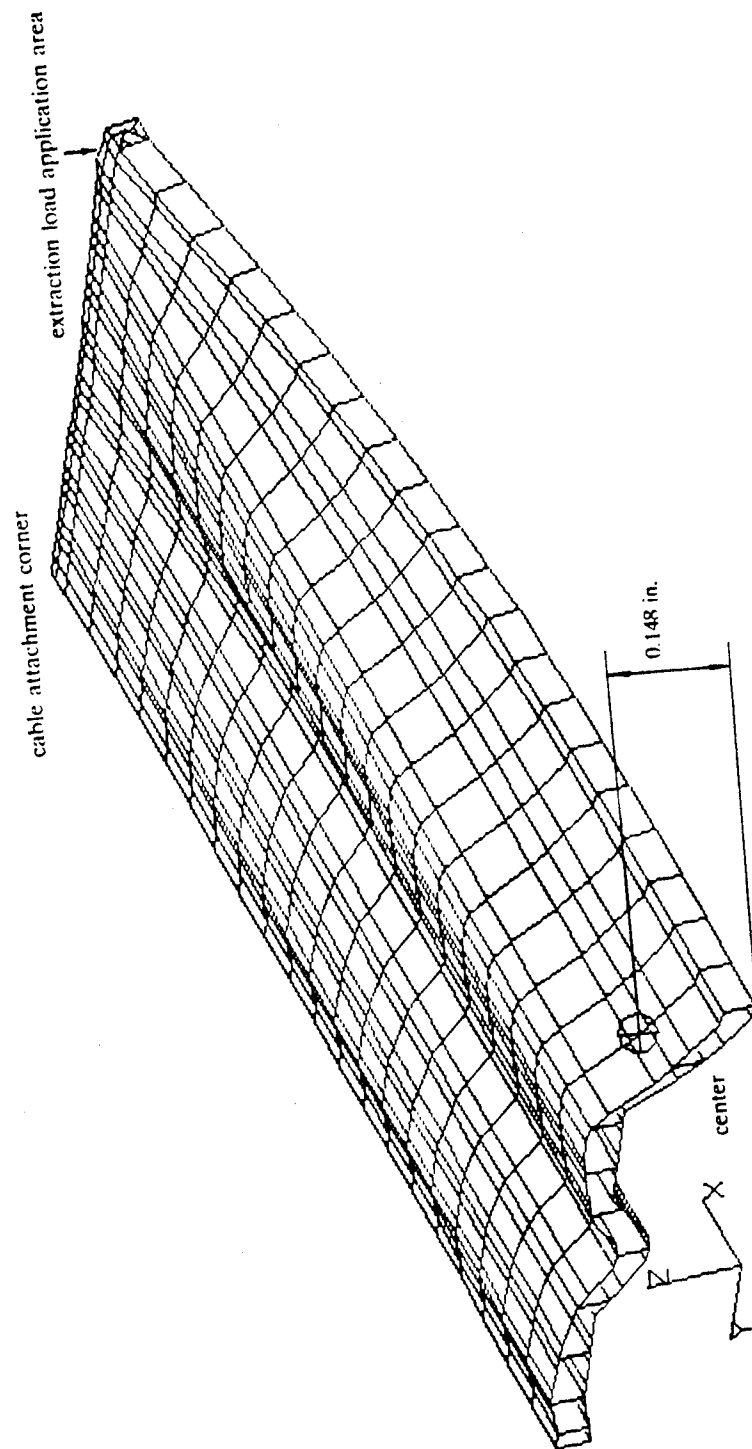


Figure 4.21 Deflection results, extra load case w/roller loads

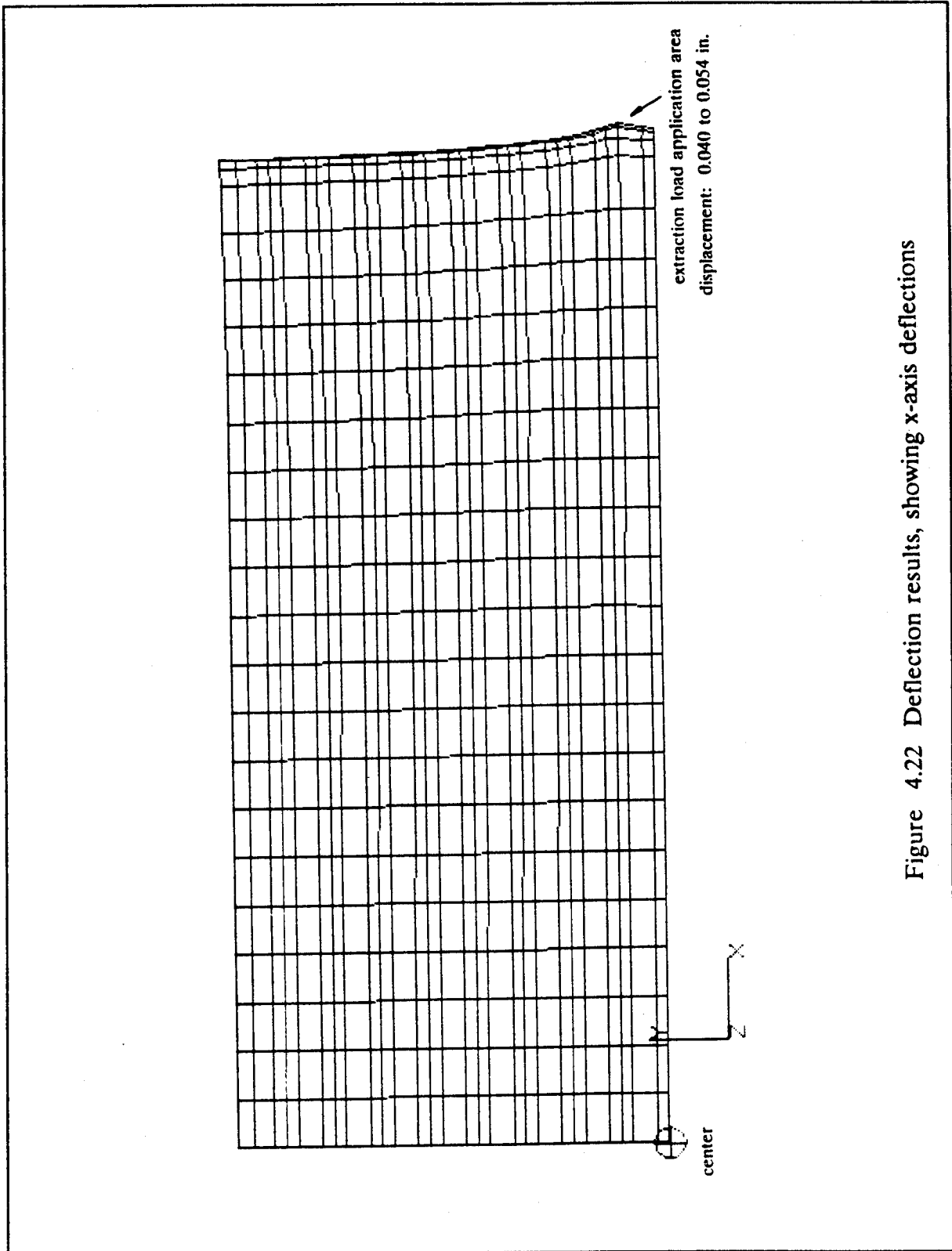


Figure 4.22 Deflection results, showing x-axis deflections

5. PHASE II

TASK 4

5.1 TASK 4: DYNAMIC ANALYSIS

In Task 4, for the same platform concept as analyzed in Task 3, the natural frequencies for platform excitation and the type of mode(s) most likely to be excited were to be evaluated. As given in the Statement of Work, the analysis was to be done for one set of platform boundary conditions, with two payload cases considered. These load cases were specified to be 1) no platform load and 2) concentrated masses as a simple load, and boundary conditions were, for both load cases, pinned at the four corners.

5.2 ANALYSIS RESULTS

For the cases and set of boundary conditions given above, the first five out-of-plane modes and frequencies were computed for the platform. The payload and platform mass were distributed as nonstructural mass over the top face sheet, including all of the S-Glass/Epoxy face sheet, but leaving the side rails and end caps unloaded. A pinned boundary condition was used at the cable attachment point, so that the cable flexibility was not included in the analysis. A gravity load case was run to check that the total mass on the system was within 2% of the targeted 23300 lb for the loaded platform and 1000 lb for the unloaded platform.

The symmetric (with respect to the xz and yz planes) modes were run, because these are the important modes which could potentially couple with the parachute response. The modal participation in the anti-symmetric modes would be zero with the attachment points at the corners.

Frequency values are given in Table 5.1. Earlier closed form solutions for the fundamental frequency of the loaded platform gave a value of 1.3 Hz, which is in excellent agreement with the NASTRAN value of 1.27 Hz. The fundamental mode shape shown in Figure 5.1 shows deformations similar to those that result from gravity loading. Only the top face sheet was plotted in the figures to simplify the plots. The undeformed top face sheet is shown in dashed lines and the deformed values (solid lines) are superimposed.

The first five symmetric modes are shown in Figures 5.1 through 5.5 for the loaded platform. In the more complicated shapes a hidden view plot was made of the deformed shape to simplify the figure, as in the case of mode number 3, Figure 5.3.

The mode shapes for the unloaded platform remained virtually unchanged since the mass distribution is uniform over the entire platform. The frequencies increased proportional to the square root of the mass ratio for these first five symmetric modes. These results are shown in Figures 5.6 through 5.10. Again, the undeformed top face sheet is shown in dashed lines and the deformed values (solid lines) are superimposed.

Table 5.1: Frequency Values for Pinned Corner
Conditions (Symmetric Modes Only)

Mode Number	Unloaded (Weight = 1000 lb) [Hz]	Loaded (Weight = 23300 lb) [Hz]
1	6.13	1.27
2	16.9	3.49
3	31.6	6.55
4	37.0	7.65
5	53.9	11.2

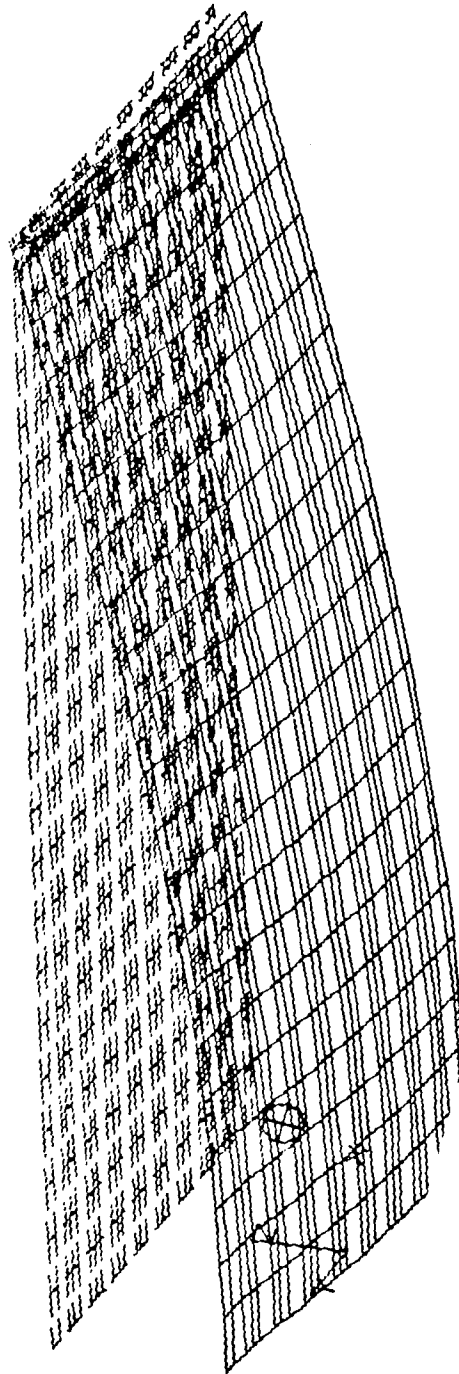


Figure 5.1. Mode 1, loaded platform.

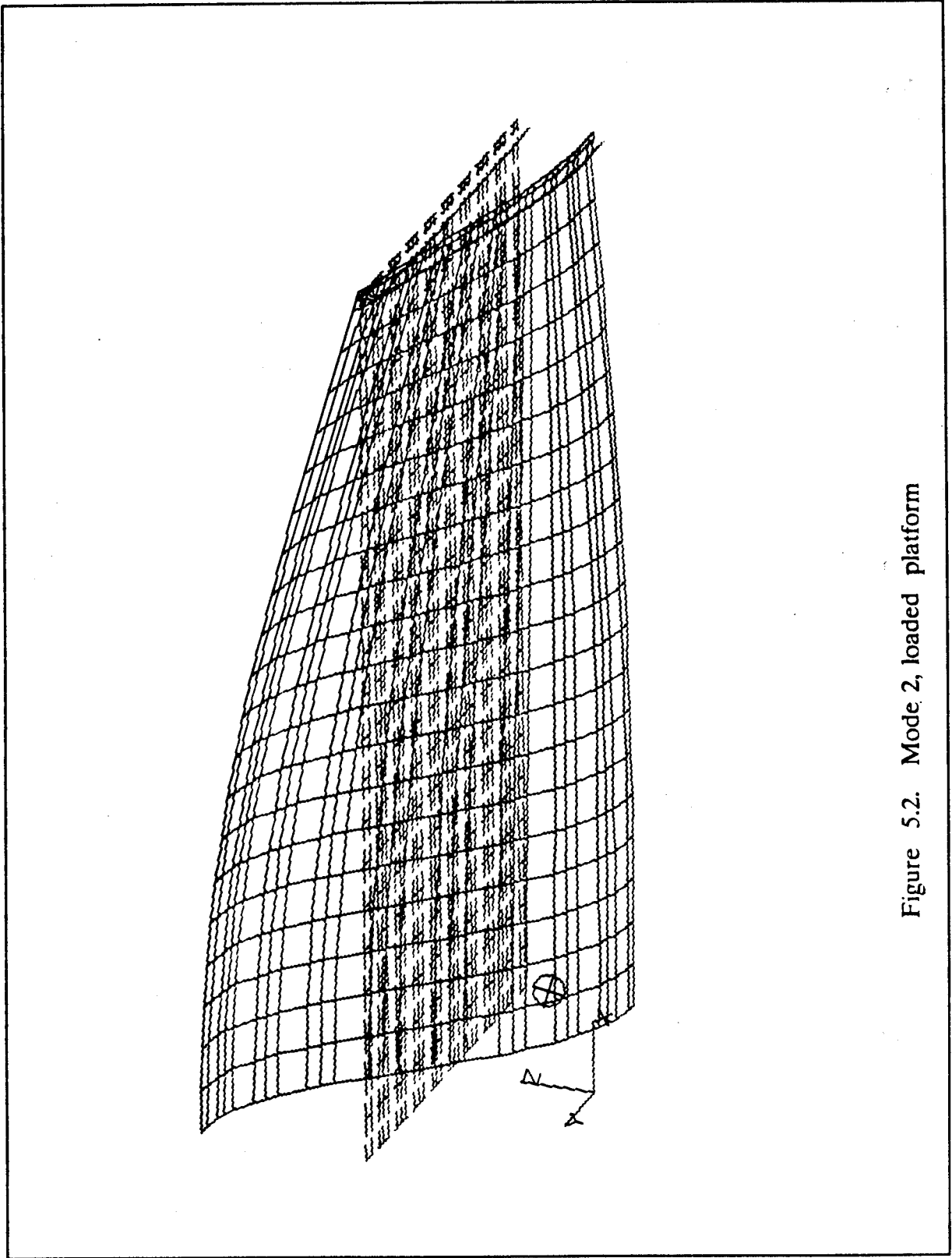


Figure 5.2. Mode 2, loaded platform

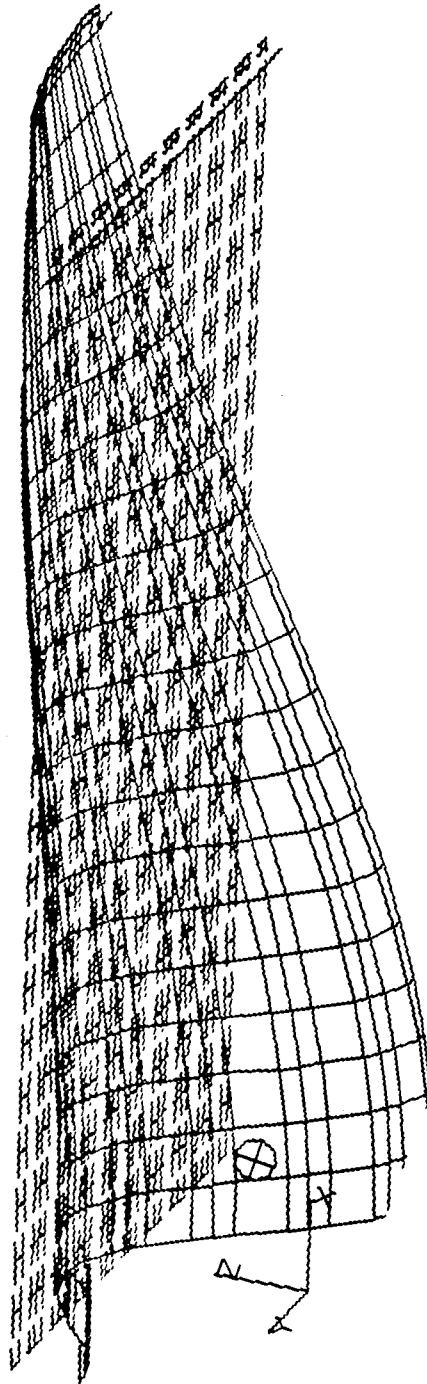


Figure 5.3. Mode 3, loaded platform

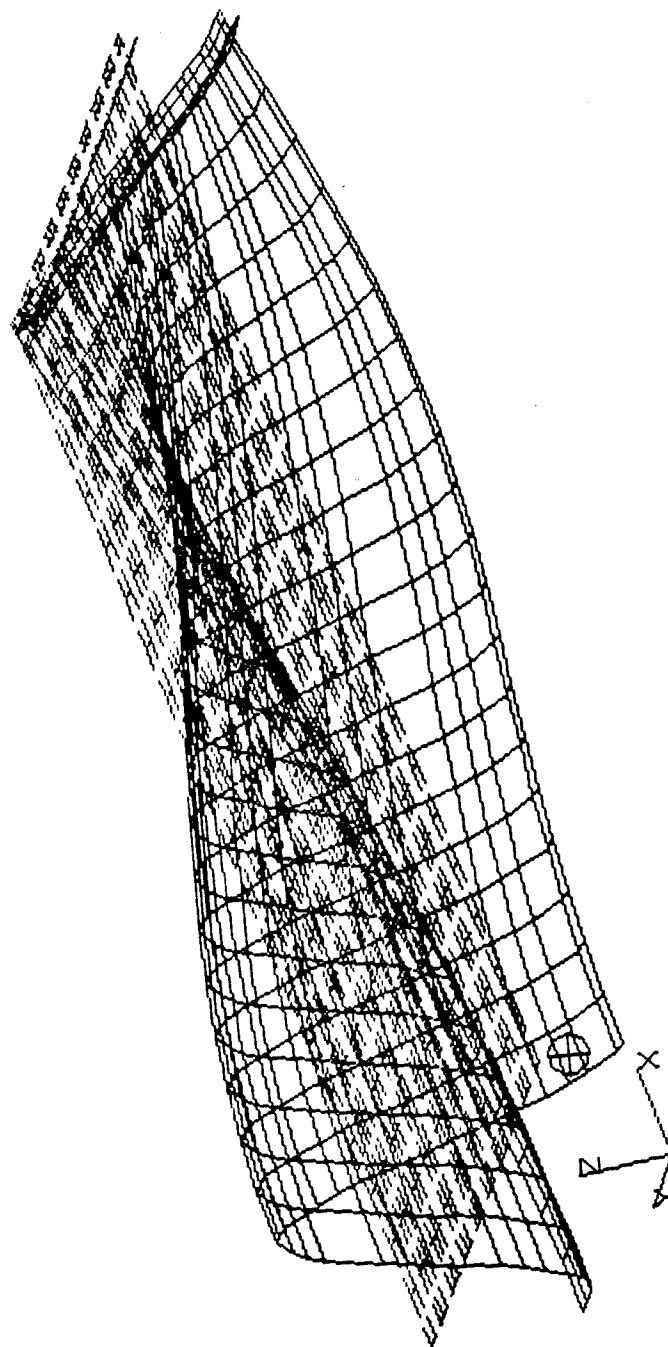


Figure 5.4. Mode 4, loaded platform

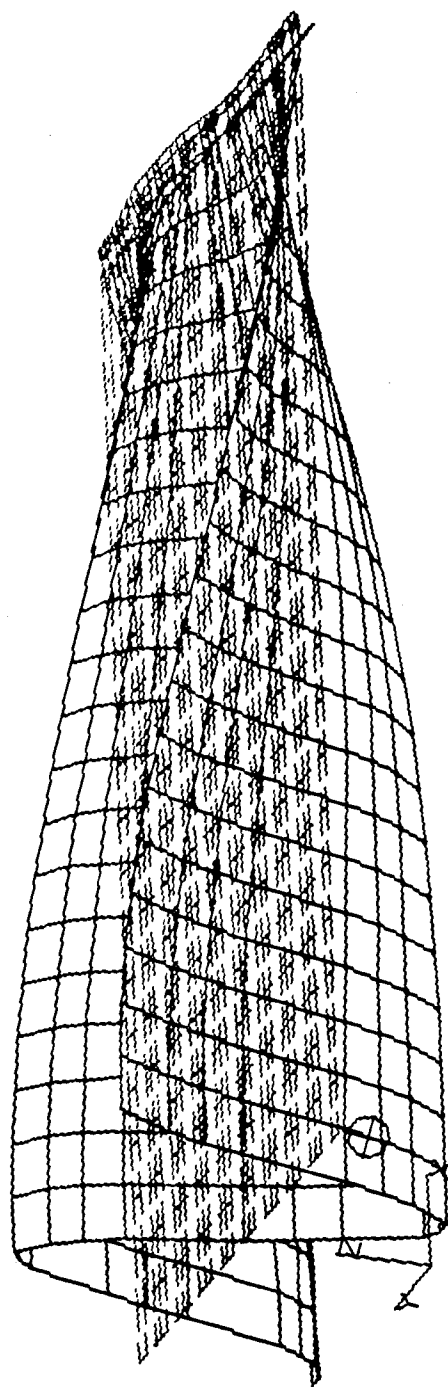


Figure 5.5. Mode 5, loaded platform

platform. The frequencies increased proportional to the square root of the mass ratio for these first five symmetric modes. These results are shown in Figures 5.6 through 5.10. Again, the undeformed top face sheet is shown in dashed lines and the deformed values (solid lines) are superimposed.

The analysis results obtained in Task 4 show the first bending frequency of the platform concept studied, under the loading conditions used, to be quite low. At this time, a minimum allowable frequency has not been specified. The main concern with a low bending frequency would be the potential for interaction between the platform and the parachute attachment cables, with this interaction causing resonance. If resonance occurred, large vertical oscillations could result, and possibly cause malfunctioning of the parachute. A complete study of the total system (platform, payload, attachment system, and parachute) would be required to fully evaluate this potential situation.

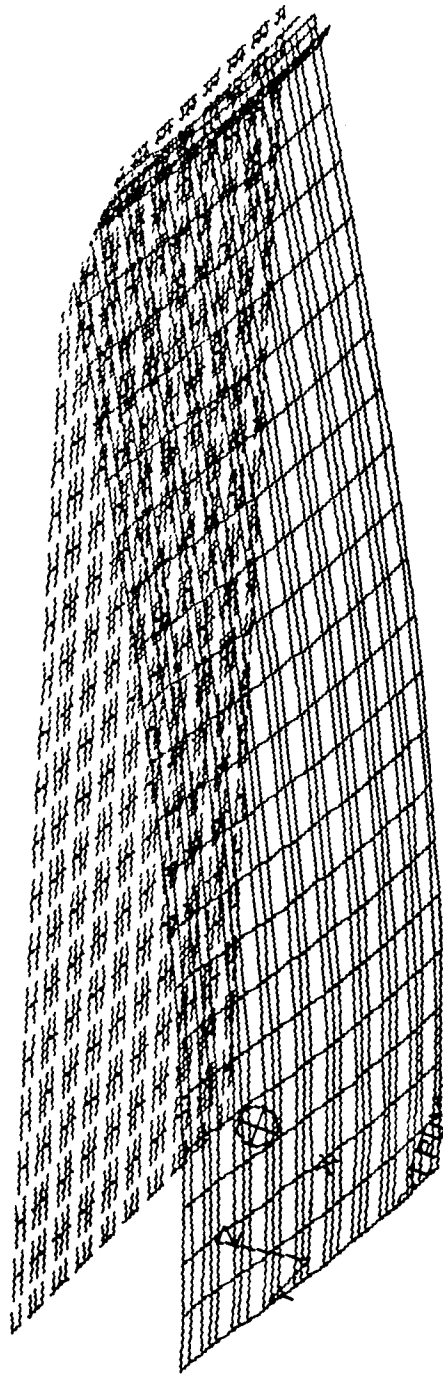


Figure 5.6. Mode 1, unloaded platform

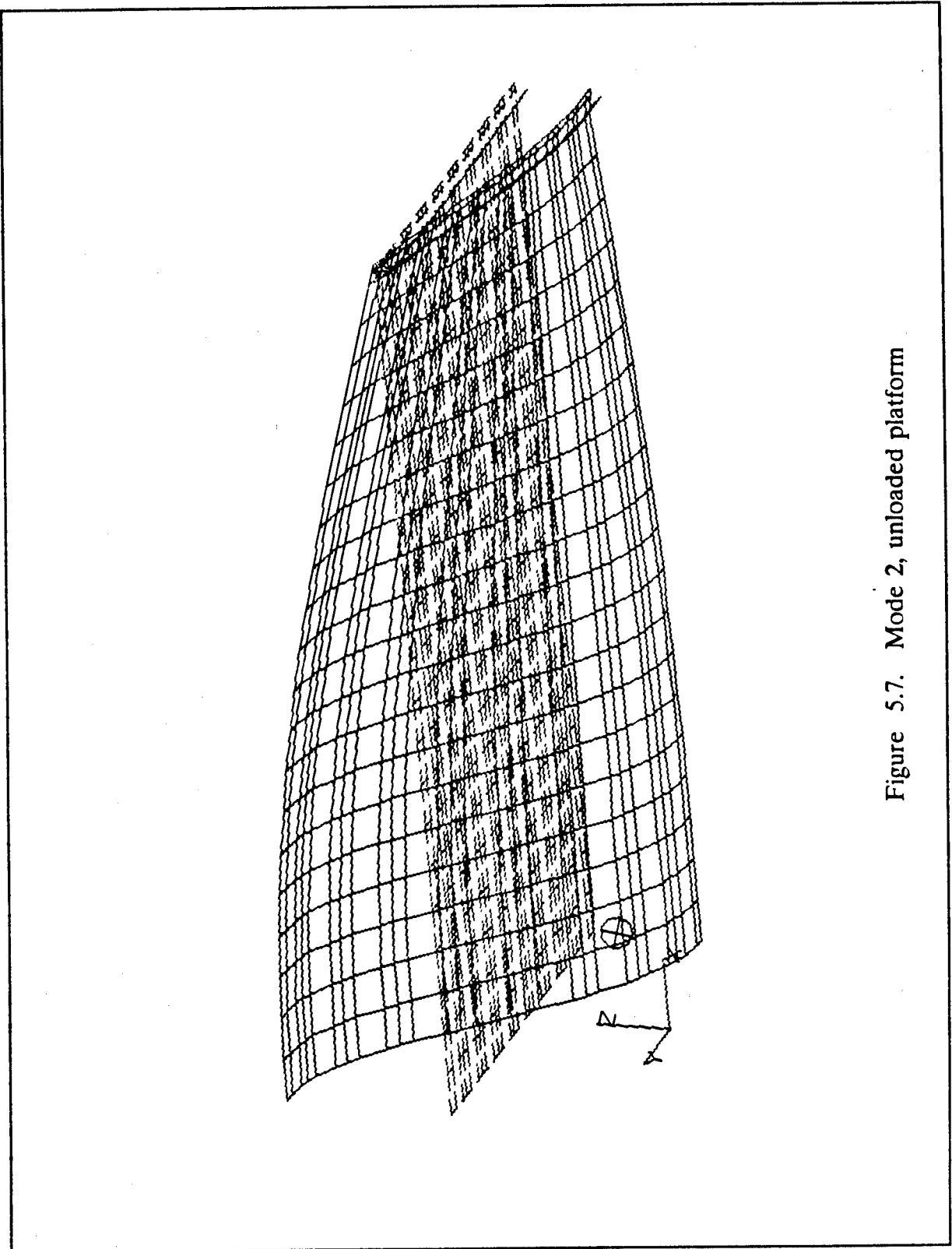


Figure 5.7. Mode 2, unloaded platform

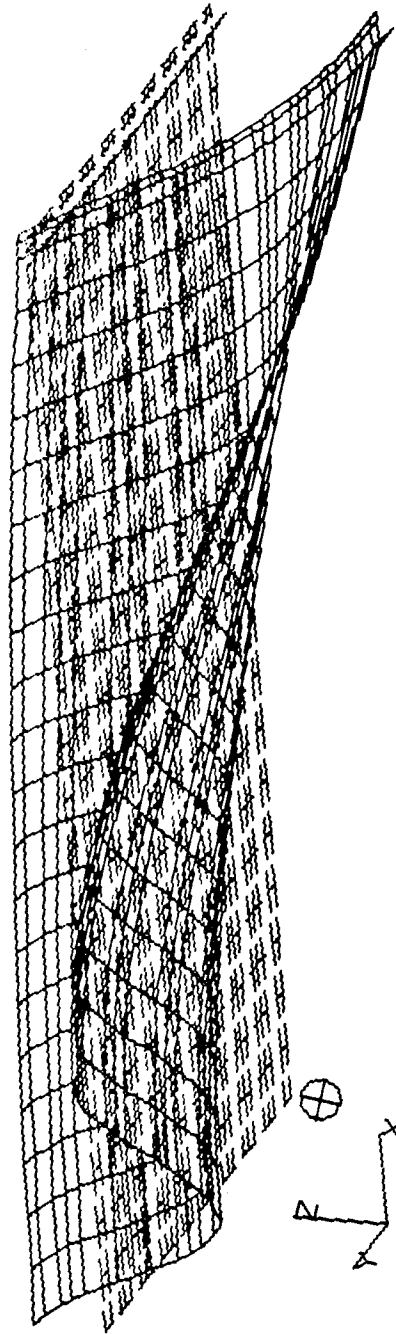


Figure 5.8. Mode 3, unloaded platform

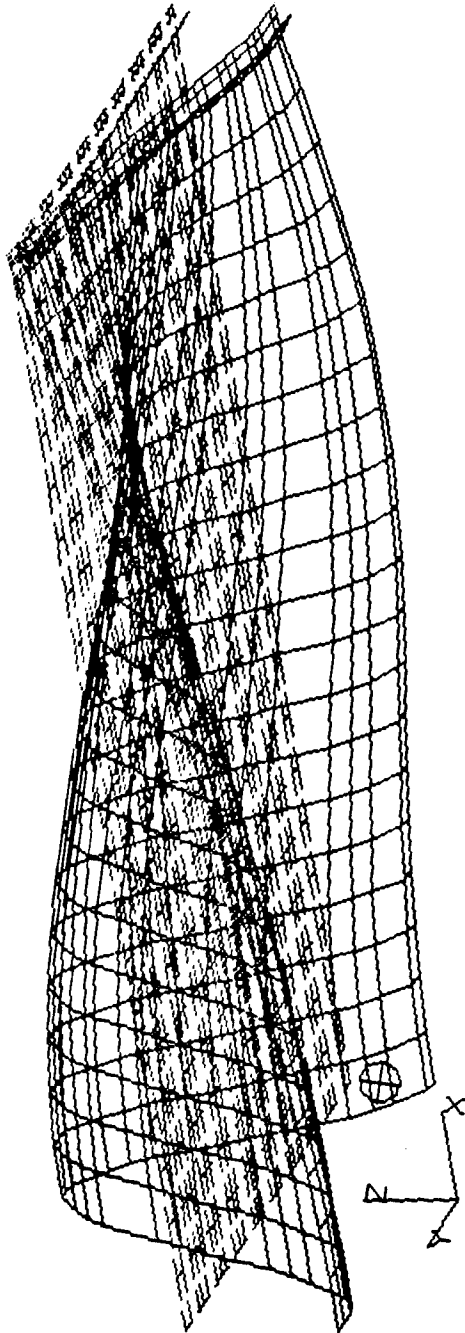


Figure 5.9. Mode 4, unloaded platform

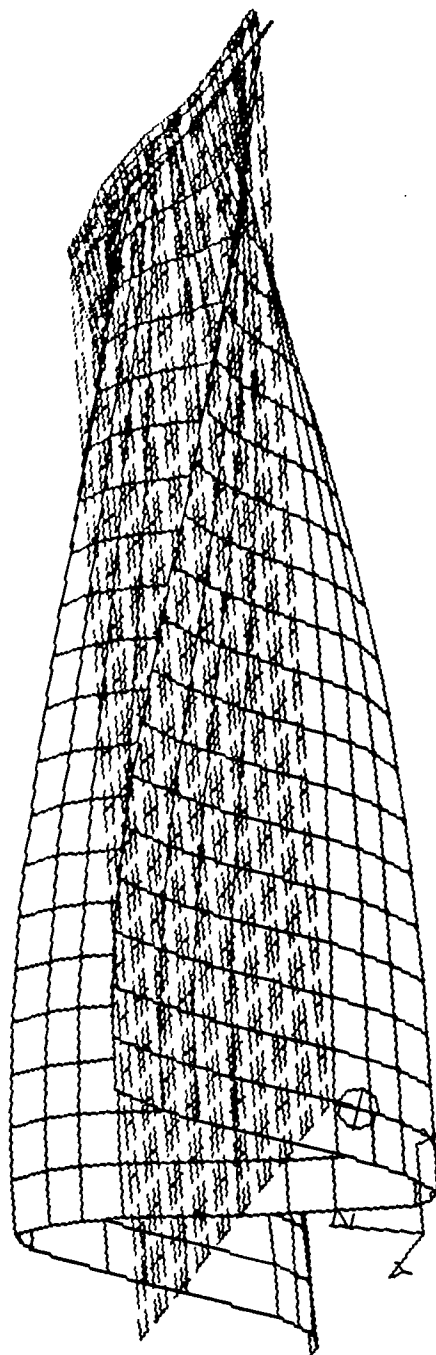


Figure 5.10. Mode 5, unloaded platform

The analysis results obtained in Task 4 show the first bending frequency of the platform concept studied, under the loading conditions used, to be quite low. At this time, a minimum allowable frequency has not been specified. The main concern with a low bending frequency would be the potential for interaction between the platform and the parachute attachment cables, with this interaction causing resonance. If resonance occurred, large vertical oscillations could result, and possibly cause malfunctioning of the parachute. A complete study of the total system (platform, payload, attachment system, and parachute) would be required to fully evaluate this potential situation.

6. CONCLUSIONS AND RECOMMENDATIONS

6.1 CONCLUSIONS

At the end of Phase I, the program conclusion was that in comparison with the Type V platform, a better performing and lighter weight advanced composite platform was possible for roughly comparable initial costs. During the Phase II effort, this conclusion was reinforced by further analysis and development. A concept consisting of S-glass/epoxy face sheets on an E-glass/epoxy I-beam core was found to have the best potential for development and deployment. Full development and design of an advanced composite airdrop platform has not been performed, but sufficient work has been done to indicate that an advanced composite airdrop platform does offer a good potential for lighter weight, better performance, and a lower lifetime cost.

6.2 RECOMMENDATIONS

In further development of advanced composite airdrop platforms, several areas are recommended for more detailed study than was possible during the early exploratory work of this program. As briefly mentioned earlier, the possibility of using hybrid face sheets is of interest because of the potential for further weight savings and performance improvements. During the Phase II effort, in discussions with composite (pultruded) beam manufacturers, a different type of pultruded beam was discussed. This type beam consisted of unidirectional material in the webs with the flanges composed of a long longitude directionally strengthened, fiber layup, resulting in an anisotropic beam rather than the isotropic beams studied so far. Along with a potential for increased performance, this type beam had definite potential for a cost savings, and is therefore of special interest. A possible area where performance problems might be encountered was briefly mentioned in Section 5, covering the dynamic analysis. This area has not been examined in depth, and further analysis is recommended. The final recommendation included here is that, in any further program effort which examines an aluminum material redesign of the airdrop platforms, portions of the Phase I effort should be referenced. During this effort, aluminum was considered as a potential material for use in a composite structure platform, and as a platform element material in a partially aluminum, partially composite material platform.

7. REFERENCES

1. SAP86: Users' Manual, "A Finite Element Program for Static and Dynamic Analysis of Linear Structural Systems," Release 3.0, August 1987, Number Cruncher Micro System, Inc., 1455 Hayes Street, San Francisco, California 94117.
2. ADINA: Users' Manual, "Automatic Incremental Nonlinear Analysis," Report ARD 87-1, December 1987, Adina R & D, Inc.
3. GENLAM: "Composites Design Fourth Edition, Section 25," Stephen W. Tsai, 1988, Think Composites, PO Box 581, Dayton, Ohio, 45419. GENLAM is a through-the-thickness point stress analysis computer program for composite laminates that computes the stiffness and strength of unsymmetric hybrid laminates subjected to complex, in-plane loads and bending moments applied to the edges of the plate.
4. "Final Report: Phase I of the Advanced Composites in Airdrop Program," ORNL Staff, January 1990. Oak Ridge National Laboratory, Oak Ridge, Tennessee 37931
5. "MSC/NASTRAN Users' Manual, Version 66A by The MacNeal Schwendler Corporation, dated November 1989, ISSN0741-8019 (MSC Part Number NA/2/000/UMA
6. PATRAN: Users' Manual, "PATRAN Plus, Volume I," Release 24, January 1990. PDA Engineering, PATRAN Division, 2975 Redhill Avenue, Costa Mesa, California 92626